POLITECNICO
MILANO 1863

SCUOLA DI INGEGNERIA INDUSTRIALE
E DELL'INFORMAZIONE

Thermodynamic Modelling of 6-stroke engines

TESI DI LAUREA MAGISTRALE IN
MECHANICAL ENGINEERING
INGEGNERIA MECCANICA

Author: **Dhruv Narayan Kaushik**

Student ID: 873428
Advisor: Gianluca D'Errico
Academic Year: 2020-21

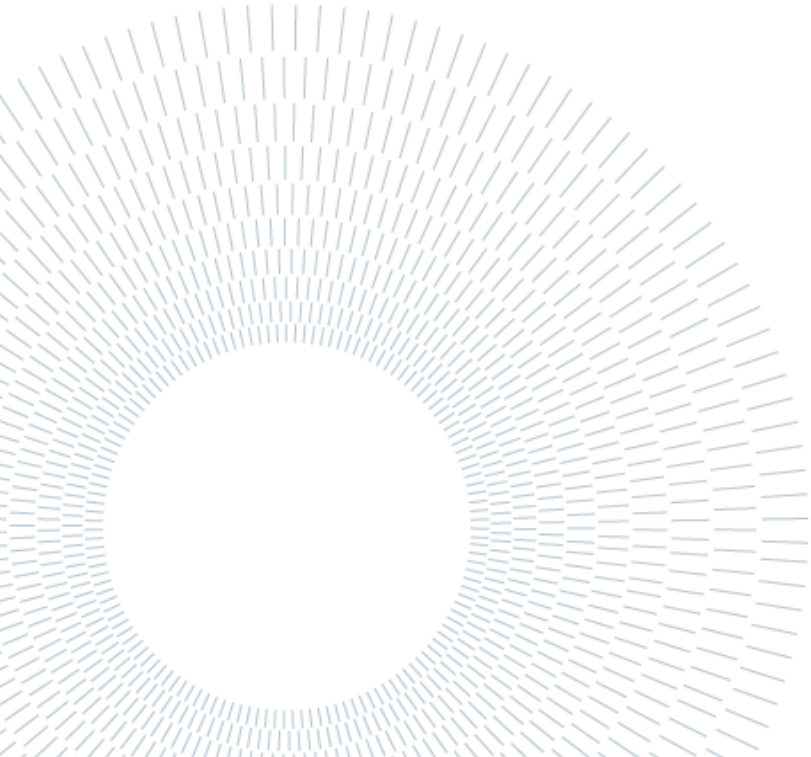

Abstract

This thesis consists of two parts. The first part, deals with the presentation of various design concepts of Six-Stroke engines. Their potentialities and limits are discussed. We conclude the first part of the thesis with an Ideal cycle analysis of the aforementioned Six-Stroke engine concepts and comparison with a conventional Four-Stroke SI engine Ideal Cycle. In the second part, we develop a simplified thermodynamic model of a conventional Four-Stroke SI engine for its simulation and then modify said model to simulate the theoretical working cycle of a Six-Stroke engine.

The first part focuses on providing an overview and the motivation for studying the different Six-Stroke engine designs. As the need for better thermal efficiency of the engines increase, we need to look at all the available methods and the ways to implement them. Six-Stroke engines can help achieve higher thermal efficiency by using:

- Water injection to recover heat from the exhaust gases and having a second power stroke.
- Opposed piston configuration, with one piston working on two-stroke cycle and the other on four-stroke cycle, to simulate the Atkinson cycle i.e. having a longer expansion stroke compared to the compression stroke.
- Different fuels such as Methanol, which can help reduce soot emissions and can be burnt in the second combustion process since it requires less oxygen to burn. Splitting the combustion process and allowing us to extract more work per cycle.

The second part focuses on developing the MATLAB code for simulation of the conventional SI engine. A detailed thermodynamic model for each process and sub process that occurs in SI engine operation have been formulated. This model was then modified to simulate the Six-stroke engine cycle.

Keywords: Six Stroke Engines; Engine Modelling; Engine Simulation.

Astratto

Questa tesi si compone di due parti. La prima parte, si occupa della presentazione di vari concetti di design dei motori a sei tempi. Vengono discusse le loro potenzialità e limiti. Concludiamo la prima parte della tesi con un'analisi del ciclo Ideale dei suddetti concetti di motore a sei tempi e confronto con un ciclo ideale di motore a quattro tempi convenzionale SI. Nella seconda parte, sviluppiamo un modello termodinamico semplificato di un motore SI a quattro tempi convenzionale per la sua simulazione e quindi modifichiamo detto modello per simulare il ciclo di lavoro teorico di un motore a sei tempi.

La prima parte si concentra sul fornire una panoramica e la motivazione per studiare i diversi progetti di motori a sei tempi. Con l'aumento della necessità di una migliore efficienza termica dei motori, è necessario esaminare tutti i metodi disponibili e le modalità per implementarli. I motori a sei tempi possono aiutare a raggiungere una maggiore efficienza termica utilizzando:

- Iniezione d'acqua per recuperare calore dai gas di scarico e avere una seconda corsa di potenza.
- Configurazione a pistoni contrapposti, con un pistone che lavora su ciclo a due tempi e l'altro su ciclo a quattro tempi, per simulare il ciclo Atkinson, cioè avere una corsa di espansione più lunga rispetto alla corsa di compressione.
- Diversi combustibili come il metanolo, che possono aiutare a ridurre le emissioni di fuliggine e possono essere bruciati nel secondo processo di combustione poiché richiede meno ossigeno per bruciare. Dividere il processo di combustione e permetterci di estrarre più lavoro per ciclo.

La seconda parte si concentra sullo sviluppo del codice MATLAB per la simulazione del motore SI convenzionale. È stato formulato un modello termodinamico dettagliato per ogni processo e sottoprocesso che si verifica nel funzionamento del motore SI. Questo modello è stato poi modificato per simulare il ciclo del motore a sei tempi.

Parole chiave: motori a sei tempi; modellazione motori; simulazione motori.

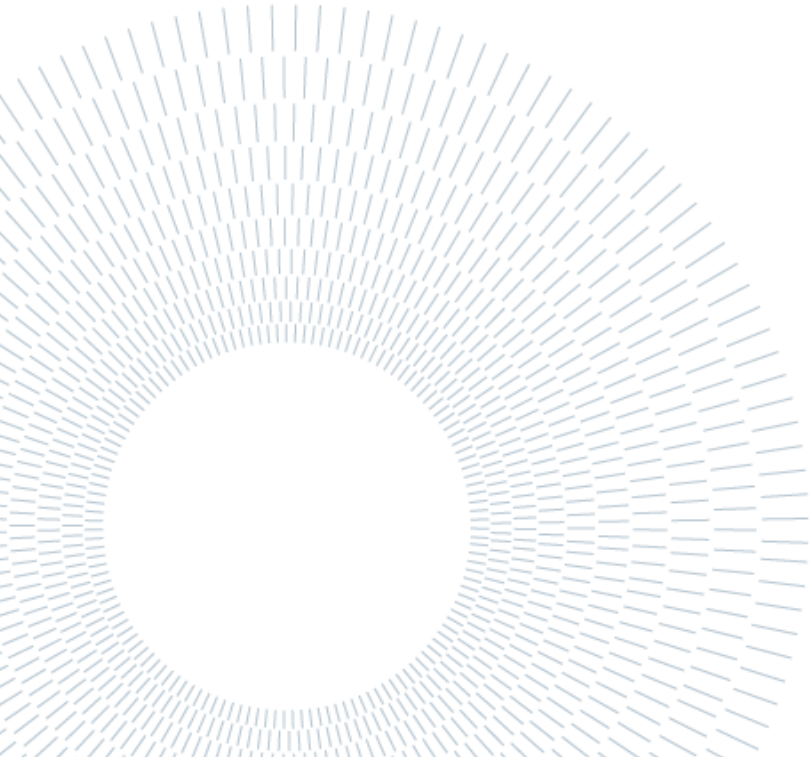

Table of Contents

List of Figures

List of Tables

Acknowledgements

Engines have always fascinated me. Their invention and subsequent use has quite literally driven the world. This thesis work is a result of my sincere efforts to accomplish the objectives of understanding and hopefully contributing to the world of Engines.

First of all, I wish to extend my sincere gratitude to Professor Gianluca D'Errico for offering me the opportunity to work under his guidance.

I would also like to take this opportunity to thank my friends and family for supporting my work at every step.

Nomenclature

- A - Surface Area (m^2)
- B - Bore (m)
- BDC – Bottom Dead Center
- C_p, C_v - Specific heat capacity under constant pressure or volume (J/kg/K)
- D_v - valve inner seat diameter (m)
- EVC – Exhaust Valve Closing
- EVO – Exhaust Valve Opening
- f – Residual gas mass fraction
- h – Specific Enthalpy (J/kg)
- IMEP – Indicated Mean Effective Pressure (Pa)
- IVC – Inlet Valve Closing
- IVO – Inlet Valve Opening
- LHV – Lower Heating Value
- L_v - valve lift (m)
- M - Mass (kg)
- MM - molar mass (kg/kmol)
- n - Number of moles (mole)
- N engine speed (rev/s)
- P - Pressure (Pa)
- Q - Heat (J)
- R - Gas constant for each species (J/kg/K)
- rc - compression ratio
- SI – Spark Ignition
- T – Temperature (K)
- t – time (seconds)

- TDC – Top Dead Center
- V - Cylinder volume (m^3)
- V_d - displacement volume (m^3)
- x_b – Burnt Mass Fraction
- y_b – Burnt Volume Fraction
- γ - Ratio of specific heats [C_p/C_v]
- η – Efficiency
- θ - Crank angle (°)
- ϱ - Gas density (kg/m^3)
- Φ – Fuel-air equivalence ratio
- ω_{eng} – Engine Speed (rad/sec)

Indices/Exponents:

- b – Burnt Gases
- d – Displacement
- e – Exhaust
- i - Inlet
- u – Unburned gases

1 Introduction

1.1 Background and Motivation

1.1.1 Internal Combustion Engines

Internal combustion engines is defined as the heat engine that converts chemical energy into mechanical energy [23]. Engines have been the major source of propulsion in automobiles through the 20th century, due to their high power density and reliable fuel supply [24]. Among the various types of internal combustion engines available, the four-stroke spark ignited reciprocating engine has become the most common.

However, at this point in time, fully electric and hybrid cars are becoming the frontrunners for general mobility, it may seem misguided to pursue improvements in the internal combustion engines. But there are still many applications for which the piston engine is indispensable and will remain so for some time. Furthermore, it seems prudent to keep working on making the current technology more efficient by using alternate fuels and novel engine designs, since we already have a vast knowledge base of its working and repurposing of current designs is cheaper.

With a typical thermodynamic efficiency of only around 25%, there seems to be tremendous room for improvement in increasing specific power and efficiency while reducing fuel consumption and in turn, emissions. [25]

For example, the Stratified Charge engine, which is similar to the standard internal combustion engine except that the fuel-to-air mixture in the combustion chamber is

much richer near the spark plug than elsewhere due to direct injection of gasoline in the cylinder. This stoichiometric mixture near the spark plug is easier to ignite and allows to have a leaner overall combustion. Which permits lower peak temperatures, higher compression ratios, and complete combustion. Resulting in increased fuel economy and reduced emission levels.

Lean burn combustion is one of the most promising technologies that can improve the performance and emission of an internal combustion engine.

1.1.2 Internal Combustion Engine Usage Restrictions

Carbon dioxide (a greenhouse gas) emissions from transport application make up about 23% of the total CO_2 production and the world-wide regulation on fuel economy is becoming more stringent than ever [24]. This phase in regulation is resulted by the depletion of fossil fuels, concerns over energy security and environmental concerns.

The regulations in EU requires CO2 emission to be reduced to 130 g/km, and 95 g/km by 2015 and 2021 respectively [27], [24]. Recently announced regulations in US requires passenger vehicles to satisfy fuel economies of 35.5 mpg and 54.5 mpg by 2016, and 2025 respectively. The goal in 2025 is a 53.5% improvement from that in 2016, which requires approximately 4.9% improvement annually. The CO2 regulations in other nations have similar tendency as in EU and US.

As the SI engines comprise the larger market share, it is crucial to improve the fuel economy of the systems equipped with SI engines [24]. Modern SI engines are mostly equipped with gasoline direct injection (GDI) system, which has the positive effect in fuel economy enhancement but may also increase particulate emission.

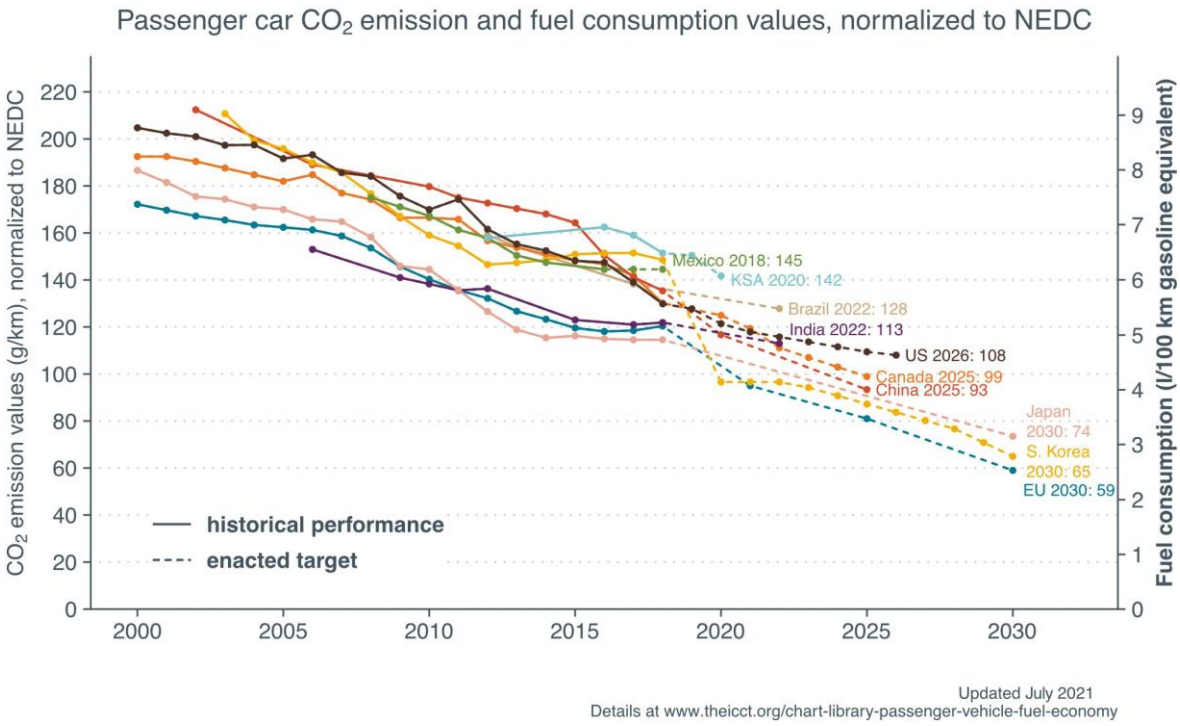

Figure 1 PASSENGER CAR CO2 EMISSIONS AND FUEL CONSUMPTION [27]

1.1.3 SI Engines Efficiency Factors and Improvement Methods

Analysis of energy flow in the engine shows that only about 25 % of the chemical energy of the fuel released, is used for propulsion and rest of the energy is used to overcome friction or is lost due to heat transfer and with exhaust enthalpy. [24]

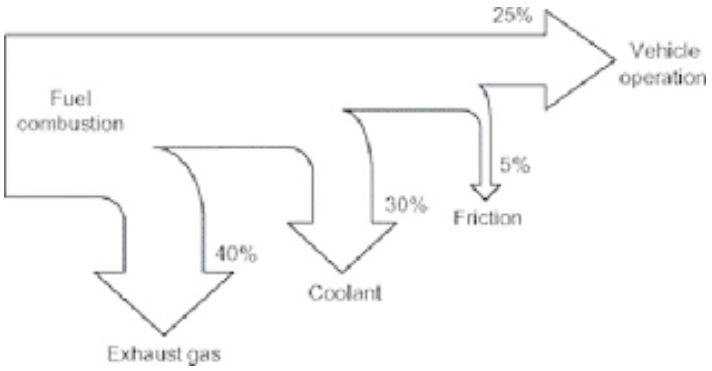

Figure 2 ENERGY PLOW OF AN INTERNAL COMBUSTION ENGINE [28]

The theoretical thermodynamic cycle of a SI engine is described by the Otto cycle. Therefore, the Otto cycle gives the ideal thermal efficiency for a SI engine. The efficiency can be expressed as:

$$\eta_{th} = 1 - \frac{1}{r_c^{\gamma-1}}$$

From this we can infer that compression ratio and specific heat ratio are major factors affecting thermal efficiency.

However, increasing the compression ratio is limited to avoid engine knock. Engine Knock is caused by auto-ignition of the air-fuel mixture before it is burnt by the propogating flame.

Specific heat ratio depends on the gas species present in the combustion chamber and the temperature of the mixture [24]. Adopting exhaust gas recirculation system (EGR) can reduce the temperature during combustion, but also results in change of gas species composition, which can lower the specific heat ratio.

From Figure 2, we can see that one of the major components is the heat loss to the wall (Coolant). The Otto cycle assumes the expansion stage to be an adiabatic process, but it is not so in reality. Cooling of the combustion chamber is done to avoid overheating and therefore, a significant amount of heat is transferred to the engine coolant, which cannot be used to extract work.

Finally, we have the “Pumping Loss”. Load control in SI engines is achieved using Throttle. At lower load, throttle opening is small and therefore the intake pressure is lower than the exhaust pressure [24]. This leads to negative work done by the piston.

One of the most difficult challenges in the engine technology is the need to increase thermal efficiency. A lot of different solutions corresponding to different engine parameters have been suggested, they can be distinguished into two broad categories [24],

1. Variable Mechanism
    - Variable valve timing (VVT) enables us to adjust the valave opening and closing timing, within a certain range. Using this we can control the amount of fresh mixture inducted and the amount of residual gas in the cylinder at different engine load and speed. Thus, helping us reduce the pumping loss. [29-31]
    - Variable Valve Lift (VVL) enables us to restrict the amount of fresh charge inducted by changing the valve profile. Thus helping us control the effective compression ratio. [34]

    The combination of of VVT and VVL systems are simply termed as Variable Valve Actuation (VVA). [32-33]

    - Cylinder Deactivation is another mechanism to reduce pumping losses. By deactivating some of the cylinders under a certain operating condition, makes the active cylinders to perform more work. This causes a shift in the operating condition of the active cylinders to higher load. [35-37]
    - Variable Compression Ratio can be realized by altering connecting rod length, combustion head height, eccentric piston pin, or complex linkage system for crank shaft. This is done to control the compression ratio of a cylinder. Compression ratio can be higher in

conditions free of knock and lowered when knock is to be avoided. [38-39]

2. Combustion System
    - Gasoline Direct Injection (GDI) Process of fuel injection and then vapourization causes the in-cylinder temperature to decrease, improving the Knock tolerance and hence the compression ratio can be increased. Fuethermore, GDI system has the potential to achieve stratified combustion which reduce the dependence on throttle for load control, thus reducing the pumping losses. [41-43]
    - Engine Downsizing is a concept of reducing engine displacement to shift the operating conditions to higher loads where the efficiency is higher. [44]
    - Dual fuel combustion is a method for increasing the compression ratio. It is achieved with the dual injection system where the fuel with higher octane rating, such as ethanol, is used in addition to gasoline when knock mitigation is needed. [40]

All of these methods have their own merits and limitations. In this study, we focus on novel engine design concepts to take advantage of the above mentioned solutions to improve thermal efficiency.

The engine design concepts are grouped together under the umbrella of six-stroke engines, but as we will see later in Chapter 2, different designs try to increase the thermal efficiency using distinct methods.

For example,

- Six-Stroke engine with Water Injection, uses injection of water to recover heat from the exhaust gases and have a second power stroke. In addition to extracting more power, the additional stroke cools the engine and removes the need for a cooling system, making the engine lighter.
- M4+2 engine, uses the opposed piston design of the engine to have variable compression ratios depending on the load on the engine. It also has a longer expansion stroke compared to the compression stroke, allowing us to extract more work.
- Dual Fuel engines use different fuel, such as Methanol, for a second combustion process. Splitting the combustion process allows us to extract more work per cycle.

Since it would be almost impossible to conduct optimization of the different six-stroke engine design concepts by means of experiments, we use simulation tools to keep the Cost and Time minimal.

The modelling of six-stroke engine designs are based on the four-stroke SI engine mathematical model. Their description, simulation and results are shown in Chapter 3.

1.1.4 Simulation Tools

There has been a continuous effort to understand the physics of the engine. The mechanics, vibrational dynamics, structures and thermodynamics of the engine were identified and understood to possess the ability to predict the behaviour of charge inside the cylinder and the flows in the intake and exhaust tracts.

With the application of Computational Fluid Dynamics (CFD) we attempt to create models that can predict the performance of the engine with its intake and exhaust systems before it is built. However, as in all of science and engineering, there are trade-offs.

The use of computational models in the development and optimization processes of engines offer fundamental contributions, such as: [14]

- Reduced time and cost, when compared to the use of experimental tests
- Allows predictions of the effect produced by single parameters, that cannot be easily varied in experimental tests, without altering other connected quantities
- Consents the individuation of key variables of the examined processes, helping in its rational analysis and in development of better understanding
- Permits the variation of a large number of design and operation parameters, assessing each for their produced effect
- Offers the chance of deepening the basic knowledge of the examined process, allowing a detailed and rigorous analysis of their development

In order to obtain these advantages different types of models, able to analyse the actual processes occurring in the engines, have been developed. However, in any phase of modelling developments the approximations introduced always had the aim of obtaining an acceptable balance between the accuracy of required predictions and model complexity, with resulting times and computation costs.

To predict the processes that govern engine performance, several types of models are available, that can be classified on the basis of their main characteristics such as: nature of used equations and details in space and time computed.

Referring to the used equations, distinction can be made between:

1. Semi empirical or phenomenological models, which describe processes by means of approximate assumptions and relations derived from empirical observations of phenomena, rather than from mathematical equations given by the fundamental theory;
2. Thermodynamic models, whose essential structure is based on energy conservation equation (expressed by the first law of thermodynamics) and mass balance only, written for a gaseous system usually assumed uniform in composition and state;
3. Gas dynamic models, which solve the full set of differential equations, expressing the conservation of mass, momentum, species and energy, for a full analysis of fluid motions, which determine the development of subsequent processes;

From the point of view of predicted space details, the models can be classified as:

1. Zero-dimensional models, which give a simplified description of processes, since there is no modelling of fluid motions and all the physical quantities are assumed uniform in the considered volume;
2. Mono-dimensional models, which assume that systems show one prevailing dimension on the other two, so reducing the three space variables describing geometry to just one and consequently greatly decreasing the computing complexity;
3. Multidimensional models, which give a full space resolution of fluid motions and related physical and chemical quantities defining the system characteristics of each of its points.

In this study, we formulate and use a two zone zero-dimensional thermodynamic model, to describe the working of a 4 stroke SI engine. We then modify the model created to describe and simulate different 6 stroke engine designs.

1.2 Objectives and Structure

The objective is to contribute to the knowledge about the behaviour of an internal combustion engine working on a six-stroke engine cycle. The interest in this research is based on the growing need to design cleaner and more efficient engines that use alternate fuels or novel engine designs.

We want to compare the behaviour and performance parameters of a four-stroke engine with that of a six-stroke engine under similar boundary conditions and verify the parameters and performance reported in the limited literature available.

For this purpose a MATLAB code needs to be developed, which can predict the performance of a four-stroke SI engine under different operating conditions.

Selecting that as the base of the study, the developed code then needs to be modified to simulate, and predict the performance of the six-stroke engine design under different operating conditions.

Thesis outline

This Introduction Chapter has presented the contemporary context of a four-stroke SI engine design. A brief introduction on the growing need of improvement in performance and pollutant emissions. Different type of models available to predict the processes that govern the engine performance.

In the Second Chapter, a detailed review is presented. This review covers the different types of six-stroke engine design concepts. Their potentialities and limits. Ideal cycle analysis and comparison of four-stroke SI engine cycle with different six-stroke engine design concepts.

In the Third Chapter, a thermodynamic model for the four-stroke SI engine is described and used to simulate an engine working cycle. Modification to the model based on the six-stroke engine design concept is done and used to simulate the theoretical concepts provided in the second chapter.

2 Literature Review

Otto and Diesel air standard cycles gave us the basis of the modern internal combustion engine. All the research and development in engines have since been targeted to increase the thermal efficiency of engines working on these cycles, thus producing more power while consuming lesser amount of fuel and having cleaner combustion.

Now with higher prices of fuel and worsening of our atmosphere, the need for higher thermal efficiency of the engines is of great significance. Considering this we must reconsider six-stroke engines.

The concept of six-stroke engines have been around since 1883 when Samuel Griffin first developed a slide valve to have a single acting six-stroke engine. However the phrase six-stroke was first used in the Beare head six-stroke engine, this engine combined the 2-stroke engine top portion with the four-stroke engine bottom part giving birth to a different approach of 6 stroke engines. The ultimate aim of the different approaches of six-stroke engine is same, to increase the thermal efficiency.

We will go through both approaches of six-stroke engine and analyse their thermodynamic processes. Finally we will calculate the thermal efficiency for their air standard cycles and compare them to the 4 stroke cycle operating on similar displacement engines. This is done to analyse the effectiveness of the six-stroke engine and to check if it is a viable option for general use. We also study and discuss the drawbacks and hindrances to their use.

2.1 Different Approaches of Six-Stroke Engines

The term six-stroke engine describes two different approaches in the internal combustion engines.

In **first approach** also known as the Single piston design, the engine captures the waste heat from the four-stroke Otto or Diesel cycle and uses it to get an additional power stroke of the piston in the same or different cylinder in an attempt to improve fuel efficiency and/or assist with engine cooling.

Design uses steam, air or another fuel as the working fluid. The additional stroke, in addition to extracting power also cools the engine and removes the need for a cooling system thus making the engine lighter and more efficient. The piston goes up and down 6 times for each cycle.

Examples: - Bajulaz engine, Velozeta six-stroke engine, Griffin six-stroke engine, Dyer's six-stroke engine.

The **second approach** is determined by the interaction between 2 pistons. Pistons may be opposed in a single cylinder or reside in separate cylinders.

In an opposed piston design usually one piston moves at half the cyclical rate of the main cylinder, giving 6 piston movements per cycle. The second piston replaces the valve mechanism and helps increase the compression ratio by eliminating hot-spots

in the combustion chamber, it also reduces the mechanical complexity and pumping losses by avoiding the pressure drop across the valves. The second piston can also be used to increase the expansion ratio, thus increasing the thermal efficiency in a similar manner to Miller or Atkinson cycle.

Examples: - Beare head six-stroke engine, Piston charger engine, M4+2 engine.

2.1.1 Six-Stroke Engines Based on 1st Approach

These designs use a single piston per cylinder, like a conventional two- or four-stroke engine. A second, fluid is injected into the chamber, and the leftover heat from combustion causes it to expand for a second power stroke followed by a second exhaust stroke

Griffin six-stroke engine (1883)

This engine was developed by Samuel Griffin in 1883. He developed a slide valve to have a single acting six-stroke engine. [1]

Key principle of the "Griffin Simplex" was a heated exhaust jacketed external vaporizer, into which the fuel was sprayed. The temperature was held around 550° F (288 °C), sufficient to physically vaporize the oil but not to break it down chemically. This fractional distillation supported the use of heavy oil fuels, the unusable tars and asphalts separating out in the vaporizer.

Hot-bulb ignition was used termed 'catathermic igniter' used in a small isolated cavity connected to the combustion chamber. The spray injector had an adjustable inner nozzle for the air supply, surrounded by an annular casing for the oil, both

the oil and air entering at 20 psi (140 kPa) pressure and being regulated by a governor.

In early 1900's the company patented its 'Hydro system ', in which a fine mist of water was sprayed into the engine along with the fuel.

Dyer's 6 stroke engine (1915)

Water is injected in the cylinder after the exhaust stroke, which instantly turns to steam, this expansion forces the piston down for an additional power stroke. [2]

Waste heat that needed an additional system to discharge is captured and put to use driving the piston. The objective of this was:

- To improve the efficiency by recovering heat generated, by the expansion of the gases and converting such heat into work.
- To improve the scavenging of the engine
- To simplify the cooling

Bajulaz six-stroke engine (1989)

Similar to regular engine in design with some modifications in the cylinder head. Two supplementary fixed capacity chambers (a combustion chamber and an air preheating chamber) are added above each cylinder. [3]

The combustion chamber receives a charge of heated air from the cylinder, the injection of fuel begins a constant volume burn, which increases the thermal efficiency compared to the burn in the cylinder.

High pressure air from the air-preheating chamber is then transferred to the cylinder for another power stroke.

The claimed advantages of the engine include reduction in fuel consumption by at least 40%, two expansion strokes in six strokes, multiple-fuel usage capability, a dramatic reduction in pollution, and costs comparable to those of a four-stroke engine.

Velozeta six-stroke engine (2005)

In a Velozeta engine, fresh air is injected into the cylinder during the exhaust stroke, which expands due to exhaust heat and therefore forces the piston down for an additional stroke. The valve overlaps have been removed, and the two additional strokes using air injection provide for better gas scavenging. [17]

The engine seems to show 40% reduction in fuel consumption and dramatic reduction in air pollution. Its power-to-weight ratio is slightly less than that of a four-stroke gasoline engine. The engine can run on a variety of fuels, ranging from gasoline and diesel fuel to LPG. An altered engine shows a 65% reduction in carbon monoxide pollution when compared with the four-stroke engine from which it was developed.

Crower six-stroke engine (2006)

In a six-stroke engine prototyped in the United States by Bruce Crower, water is injected into the cylinder after the exhaust stroke and is instantly turned to steam, which expands and forces the piston down for an additional power stroke. Thus,

waste heat that requires an air or water cooling system to discharge in most engines is captured and put to use driving the piston. [17]

Crower estimated that his design would reduce fuel consumption by 40% by generating the same power output at a lower rotational speed. The weight associated with a cooling system could be eliminated, but that would be balanced by a need for a water tank in addition to the normal fuel tank.

2.1.2 Six-Stroke Engines Based on 2nd Approach

These designs use two pistons per cylinder operating at different rates, with combustion occurring between the pistons.

Beare Head six-stroke engine (1994)

This concept is a radical hybridization of 2 and 4 stroke engines. It combines a four-stroke engine bottom end with an opposed piston in the cylinder head working at half the cyclical rate of the bottom piston. Functionally the bottom piston replaces the valve mechanism of a conventional engine. [17]

Major drawbacks of conventional engines are the poppet valves, its basic problems being inertia, inhibition of flow of gases and hot-spots in the combustion chamber.

Claimed advantages of this engine over the overhead camshaft four-stroke engine are:

- Increased power and torque output
- Better fuel efficiency
- Cleaner burning of fuel

M4+2 engine (2002)

The design is very similar to Beare head engine, combining 2 opposed pistons in the same cylinder with one piston working at half the cyclical rate of the other. However, while in the Beare head engine the main function of the second piston is to replace the valve mechanism, in M4+2 engine the engine's work is based on the co-operation of both modules.

The air load change takes place in the 2-stroke section of the engine, the four-stroke piston is an air load exchange aiding system. [4]

Piston Charger engine (1998)

Similar to Beare head design, a 'Piston charger' replaces the valve system. The piston charger charges the main cylinder and simultaneously regulates the inlet and outlet aperture, leading to no loss of air and fuel in the exhaust.

In the main cylinder combustion takes place every turn as in a 2-stroke engine and lubrication as in a four-stroke engine. Fuel injection can take place in the piston charger, in the gas transfer channel or in the combustion chamber.

The combination of compact design for the combustion chamber together with no loss of air or fuel is claimed to give the engine more torque, power and better fuel economy. [5]

2.2 Engine Designs Examined in this Thesis

Out of the many six-stroke engine designs, three have been examined in this work. The choice has been made based on the details available for the designs.

2.2.1 Six-Stroke Engine With Water Injection for Exhaust Heat Recovery

James C. Conklin and James P. Szybist put forward the concept of adding two strokes to the Otto or Diesel engine cycle to increase fuel efficiency [8]. A 4 stoke Otto or Diesel cycle followed by a two-stroke heat recovery steam cycle, where a partial exhaust event coupled with water injection adds an additional power stroke. Thus the waste heat from two sources is effectively converted into usable work: engine coolant and exhaust gas.

In internal combustion engines, a significant amount of the fuel energy exits the engine in the form of thermal energy in the exhaust. Thus, an abundant amount of available energy present in the exhaust of a modern gasoline vehicle can be used to improve overall system efficiency if an effective means of energy recovery can be employed. The concept posed by them utilizes a portion of this previously wasted energy in the exhaust to provide additional shaft work that would otherwise be discarded.

The modified cycle proposed adds two additional strokes that increase the work extracted per unit input of fuel energy. These additional strokes involve trapping and recompression of some of the exhaust from the fourth piston stroke, followed by a water injection and expansion of the resulting steam/exhaust mixture.

The residual exhaust gas needed for the second expansion process is trapped in the cylinder by closing the exhaust valve earlier than usual, well before top dead center (TDC).

Energy from the trapped recompressed exhaust gases is transferred to the liquid water, causing it to vaporize and increase the pressure. This added pressure then produces more work from another expansion process. The steam–exhaust gas mixture is expelled to ambient pressure near the point of maximum expansion.

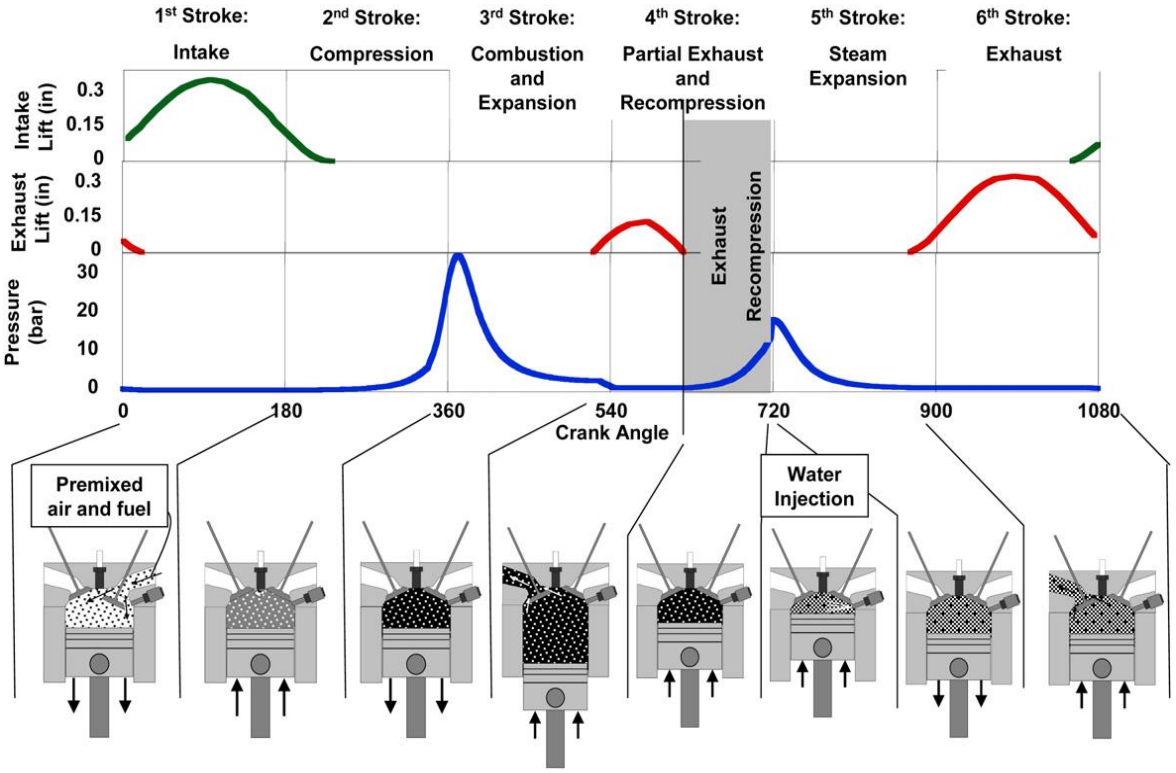

Figure 3 SIX STROKE ENGINE CYCLE PROCESSES [8]

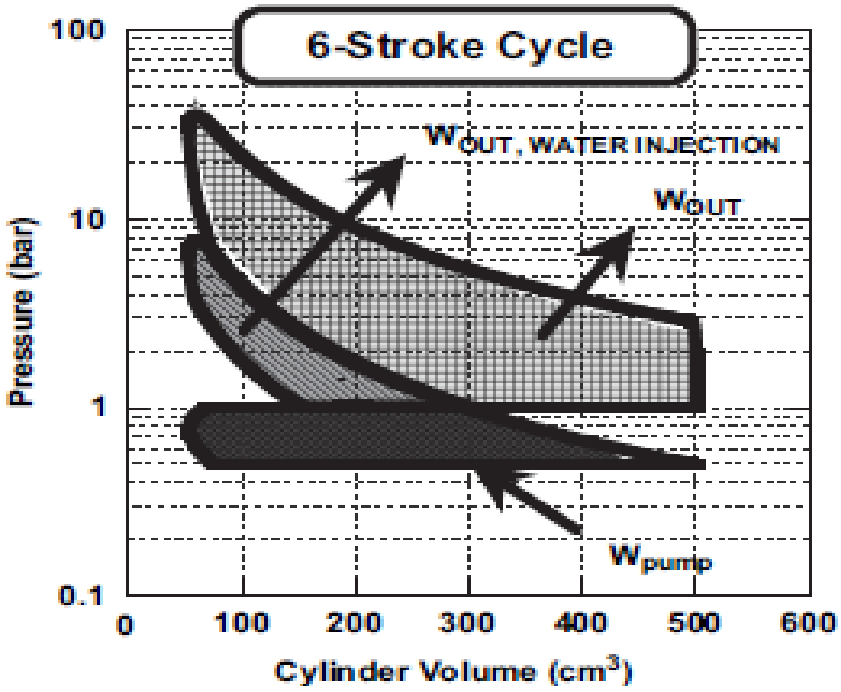

Figure 4 SIX STROKE ENGINE LOGLOG P-V PLOT [8]

The second power stroke produces additional output work from the engine without any additional fuel, thereby increasing the fuel efficiency of the engine.

2.2.2 M4+2 Engine

Piotr Mezyk and Adam Ciesiolkiewicz put forward the concept of M4+2 Double piston internal combustion engine [4].

The design of modern internal combustion engines, both four-stroke and two-stroke, although being constantly improved, still have many drawbacks. Analysing the properties of currently used internal combustion engines, we can come to the following conclusions:

- Improving the filling of the cylinder for a two-stroke engine would bring tangible benefits in the form of increased engine efficiency and reduced fuel consumption;
- Lengthening the engine's expansion curve will allow us to extract more energy from the expanding gas in the cylinder;

A proper design of the load exchange system would reduce the share of mechanical losses (friction and inertia forces of the timing system components) in the overall engine balance.

Structures in which the advantages of both types of engines can be gathered are double piston engines. A double-piston engine is an internal combustion engine in which cylinders have a common combustion chamber and in each cylinder two pistons move in opposite direction.

The 2 stroke combustion engine is characterised by a simple construction and system of air load change as well as bigger index of power output. Unfortunately its filling ratio is worse than that in four-stroke engine. The ecological index of the engine is also unfavourable, i.e. the combustion is incomplete. The system of valves are the disadvantage for four-stroke engine.

In M4+2 double piston engine, the cylinders of both modules have been joined along the axis with common cylinder head. The two pistons move at different speed (four-stroke crankshaft is rotated with twice the speed of the 2-stroke crankshaft) with appropriate stage displacement. The piston of the four-stroke engine is exchange aiding system which improves air load change. Filling process takes place at overpressure by the side inlet system and exhaust gases are removed as in the classical 2-stroke engine

The effective power output of the double piston engine is transferred by 2 crankshafts. These crankshafts are synchronised by a gear using which we can advance or retard one of the piston with respect to the other. This has another effect of changing the compression ratio. Thus we achieve the characteristic feature of this engine which is an opportunity of continuously changing the cubic capacity and compression ratio during engine work by changing the piston's location.

The 2 piston engine cycle can be compared to a four-stroke supercharged engine cycle. Similar nature of transformations are obtained but with less pressure at the end of the compression stroke and with one crankshaft revolution per engine cycle. Thus, we can conclude that the engine cycle uses the advantages of Miller and the Atkinson cycle.

The modified operation of the engines work is realized as a result of:

- The quotient of pistons strokes (k=S4/S2 in (1/2, 1)),
- The possibility of changing relative piston's position during the engine's work via automatic change of crankshaft's polar position (alfa = 40 ± 20 CAD).

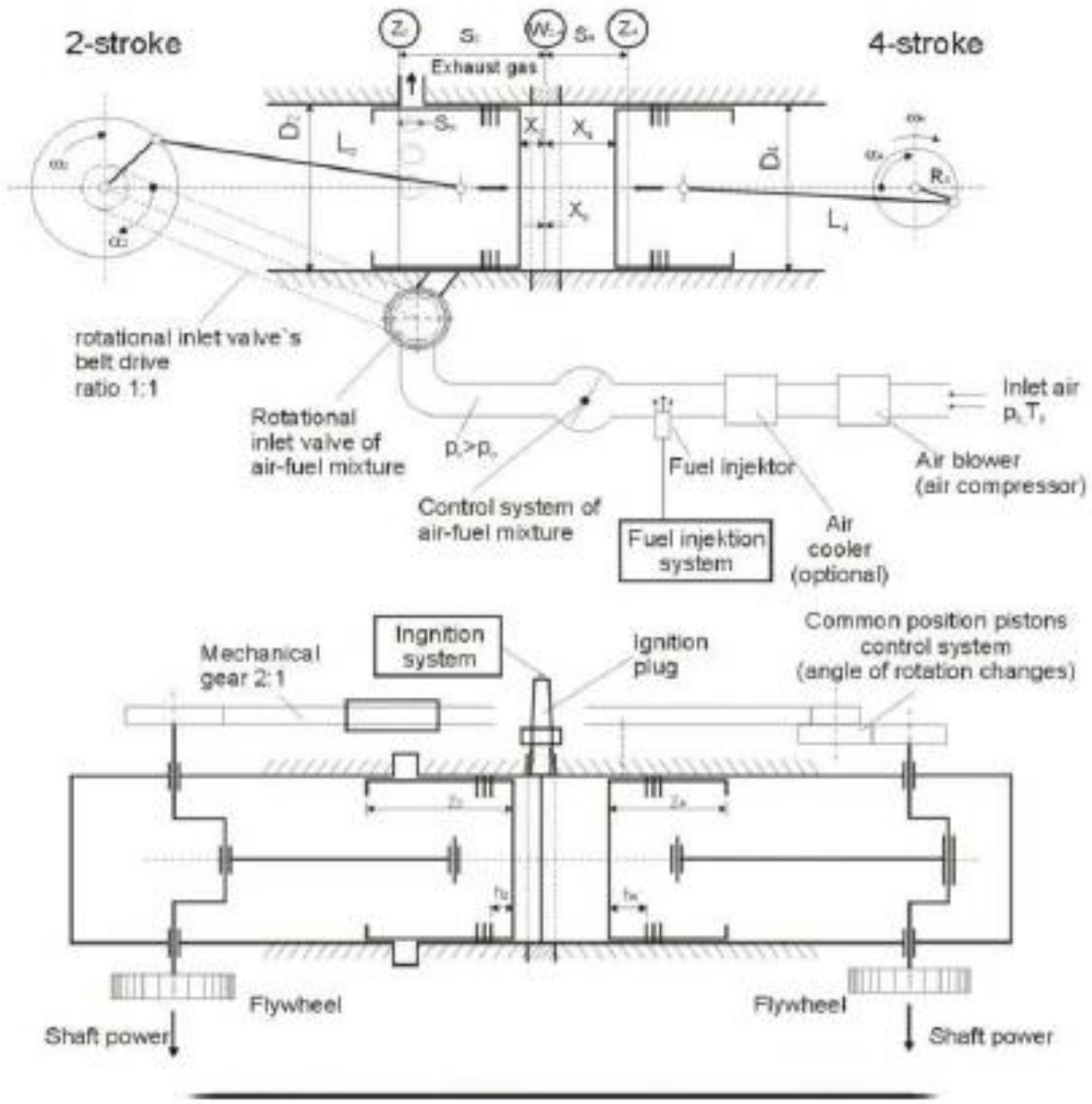

Figure 5 M4+2 ENGINE [4]

The engine is characterized by:

- Expanded gas expansion and limited exhaust gas temperature at the outlet,
- Variability of the compression ratio (from the low order of 6-7 to the high order of over 12),
- Possibility of changing the compression ratio during the engine's work depending on the temporary load,

- A beneficial changing of workspace during the mixture's compression,
- An almost constant increase of volume during the expansion stage at different piston position,
- Filling process of working space takes place at overpressure

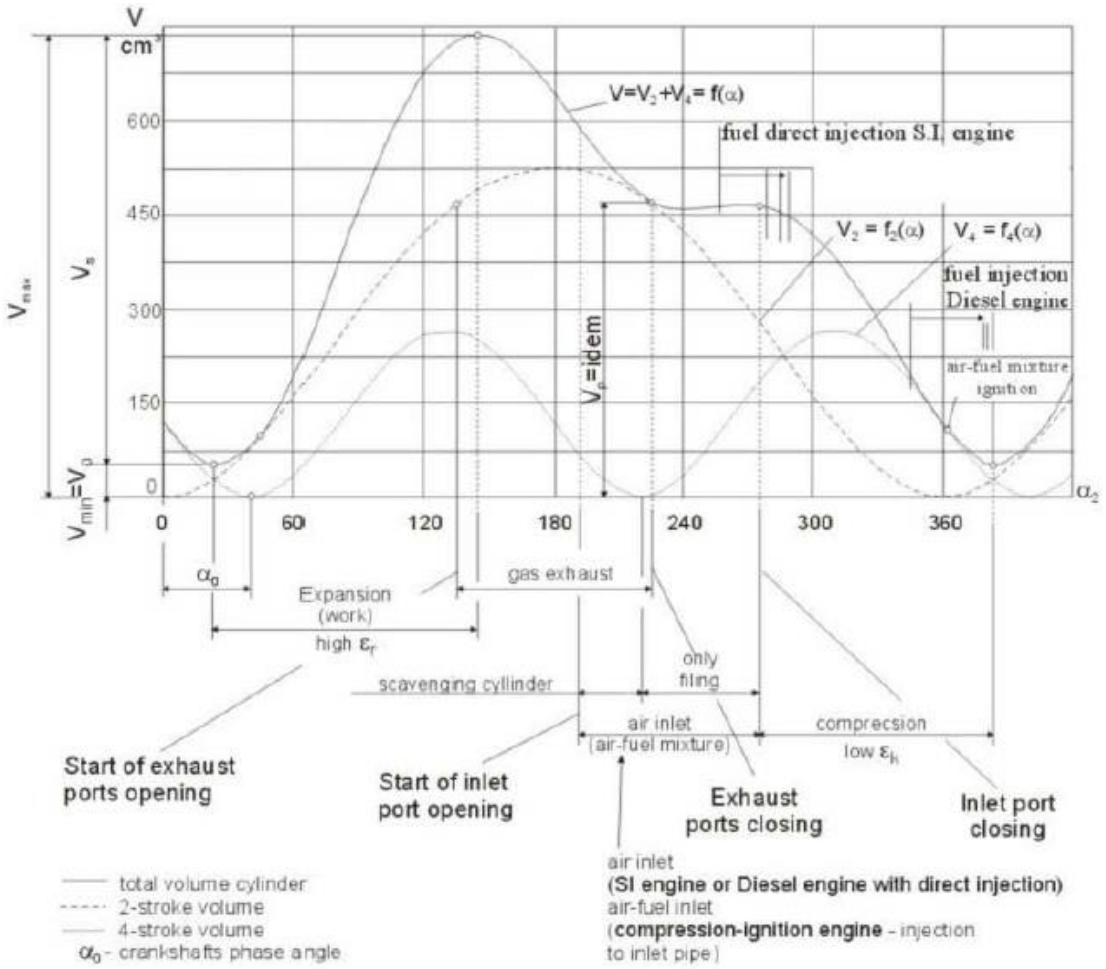

Figure 6 P-V PLOT FOR M4+2 ENGINE [4]

Preliminary research of this type of engine design shows,

- The increase of engine thermal efficiency (the mechanical efficiency is a little lower due to presence of 2 crankshafts),

- Higher total efficiency (more favourable at medium load). It is comparable with the diesel engine efficiency so the fuel consumption is relatively smaller,
- Higher torque and higher power output compared to the four-stroke SI engine with the same stroke volume.
- The engine has possibility of lean mixtures combustion (lambda>1)
- The properties and the possibility of compression ratio change during normal work forecast the possibility of different fuels combustion

2.2.3 Six-Stroke Direct Injection Engine Under Dual Fuel Operation

Tsunaki Hayasaki, Yuichirou Okamoto, Kenji Amagai and Masataka Arai in their paper suggested that a six-stroke direct injection diesel engine with second compression and combustion process could reduce the NO emissions. [9]

Furthermore, a reduction in the ignition delay of the second combustion process by a high temperature effect in the second compression stroke can be further utilised for ignition improvement of a fuel with low cetane number.

In the engine system reported through the paper, a conventional diesel fuel was supplied as the fuel for the first combustion process and in the second combustion process methanol was supplied.

Injection timing and injection flow rates for first combustion fuel (diesel) and the second combustion fuel (methanol) were varied independently based on the allocation ratio, this was done because the combustion heats of the two fuels are different.

Allocation ratio (α_H) is defined as the ratio of combustion heat supplied for the second combustion stroke to the total combustion heat supplied.

$$\alpha_H = \frac{Q_{II}}{Q_t} \tag{23}$$

where,

$$Q_t = Q_I + Q_{II}$$

The supplied combustion heat for the first combustion process is denoted by Q_I. The second combustion stroke is denoted by Q_{II}.

Methanol was used in this study as the fuel for second combustion process because the cetane number of methanol is low and it shows low ignitability, thus it is the optimum fuel to show the reduction in ignition delay due to rise in temperature after the first combustion process. Furthermore, methanol already contains oxygen which reduces the stoichiometric air fuel ratio resulting in complete combustion even with increased EGR effect in the second combustion process, it also forms an oxidizing radical (OH) during combustion, which has the potential to reduce the soot from the first combustion process

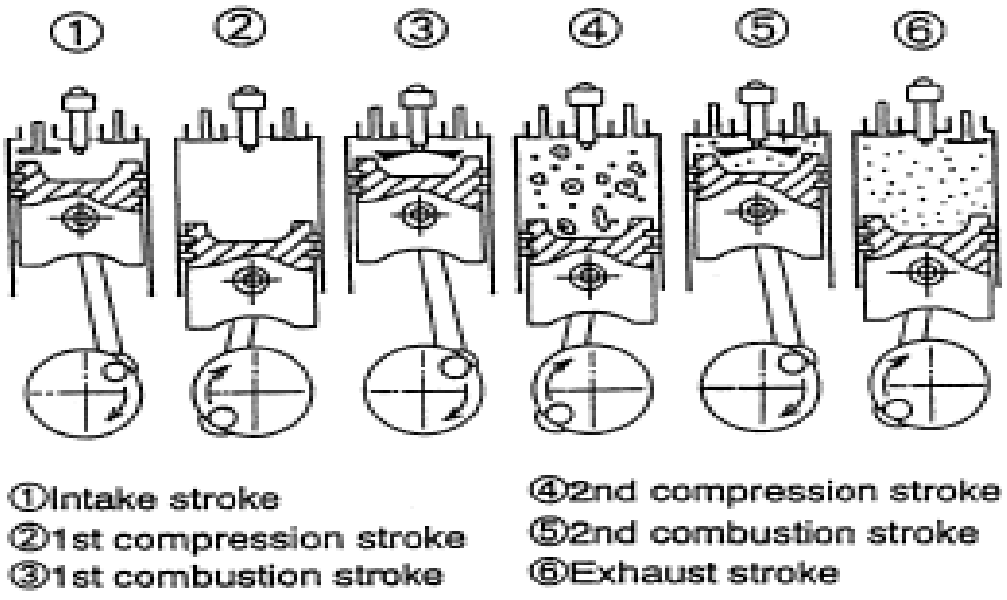

Figure 7 SIX STROKE ENGINE DUAL FUEL CYCLE PROCESSES [9]

The cycle of this engine consisted of six strokes: intake, first compression, first combustion, second compression, second combustion, and exhaust stroke. The combustion products from the first combustion stroke are re-compressed and utilized in the second combustion process before the exhaust stroke.

This second combustion process was the special feature of the proposed six stroke DI diesel engine.

Comparison with the four-stroke diesel engine - A four-stroke engine has one intake stroke for every two engine rotations. For the six-stroke engine, however, the intake stroke took place once for every three engine rotations. Therefore, in order to keep the combustion heat per unit time constant, the combustion heat supplied to one six-stroke cycle should be 3/2 times larger than that of the four-stroke engine.

Ideal cycle analysis of the above mentioned three engine designs will be carried out in the next section.

2.3 Ideal Cycle Analysis of Different Six-Stroke Engines

Internal combustion engine does not operate on a thermodynamic cycles as it involves an open system, that is, the working fluid enters the system at one set of conditions and leave at another. However, it is possible to analyse the open cycle as though it were a closed system by imagining one or two processes that would bring back the working fluid at exit back to the conditions of the starting point.

A theoretical tool, which is suitable for the demonstration of basic correlations through the application of basic thermodynamic equations, is the Ideal Cycle. The

working gas is considered as ideal gas with constant thermal capacities under constant pressure (C_p) and under constant volume (C_v) throughout the cycle. [16]

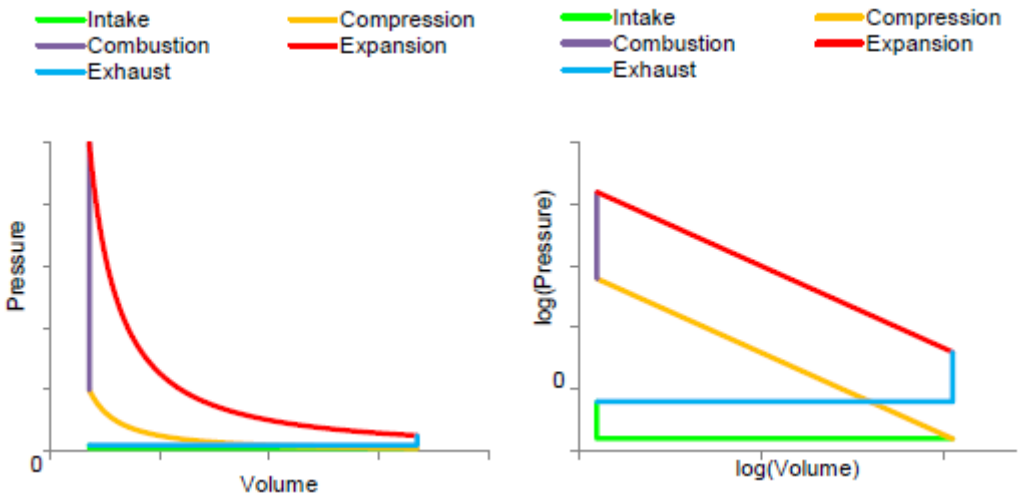

Figure 8 IDEAL CYCLE P-V DIAGRAM [16]

Analysis starts with the First law of thermodynamics for a control volume, which states that any change in the energy content of the system is the algebraic difference between heat supplied (Q) and the Work done by the system (W), during any change in state. [11]

$$dE = Q - W \quad (1)$$

Energy (E) may include many types like Kinetic, Potential etc. but from a thermodynamic point of view we only consider energies due to rise in temperature, denoted by "U" and called the internal energy.

Thus Eq. (1) can be written as:

$$dU = Q - W \quad (2)$$

The Eq. (2) holds for every stroke of the cycle and using it we can perform a thermodynamic analysis on the reference air-standard cycle.

Assumptions made for analysing the air-standard cycles are:

- Working medium is assumed to be a perfect gas and follow the Ideal gas law

$$pv = mRT \quad (3)$$

- There is no change in mass of the working fluid
- All processes in the cycle are reversible
- Heat is assumed to be supplied from a constant high temperature source and not from a chemical reaction during the cycle
- Heat is rejected to a constant low temperature sink during the cycle
- No heat is lost from the system to the surrounding
- Working medium has constant specific heats throughout the cycle

Due to these assumptions the analysis becomes oversimplified. The work output, peak pressure, peak temperature and the thermal efficiency based on air-standard cycles will be the maximum that can be reached.

According to the assumptions we take specific heats constant throughout the cycle. Moreover, we know that the specific heats of air are a function of temperature and as the temperature range of the engine cycle is large, we can safely assume that the specific heats and their ratios change during the cycle. Thus to get better results we take the values of specific heats and their ratio as [7]:

C_p = 1.108 kJ/kg-k

C_v = 0.821 kJ/kg-k

k = C_p/C_v=1.35

R = Cp-Cv=0.287 kJ/kg-k

Effect of dissociation is not considered here as the "Extent of dissociation" increases with increasing temperature and decreases with increasing pressure. Thus when the temperature increases after the combustion process which can potentially increase the extent of dissociation the pressure is also increased which reduced the extent of dissociation and as a result overall extent of dissociation increases only to a minor degree. [7]

At the end of each cycle there are some exhaust gases which remain in the cylinder and mix with the fresh air-fuel mixture, thus we have to consider a small mass of exhaust gases in the working fluid.

After considering above mentioned assumptions and values, we are now ready to analyse the thermodynamic cycle of the 6 stroke engines.

2.3.1 Exhaust Heat Recovery With Water Injection Based Six-Stroke Engine

A six-stroke cycle can be thought of as a four-stroke petrol or diesel cycle followed by a 2-stroke heat recovery steam cycle. A partial exhaust coupled with water injection adds an additional power stroke.

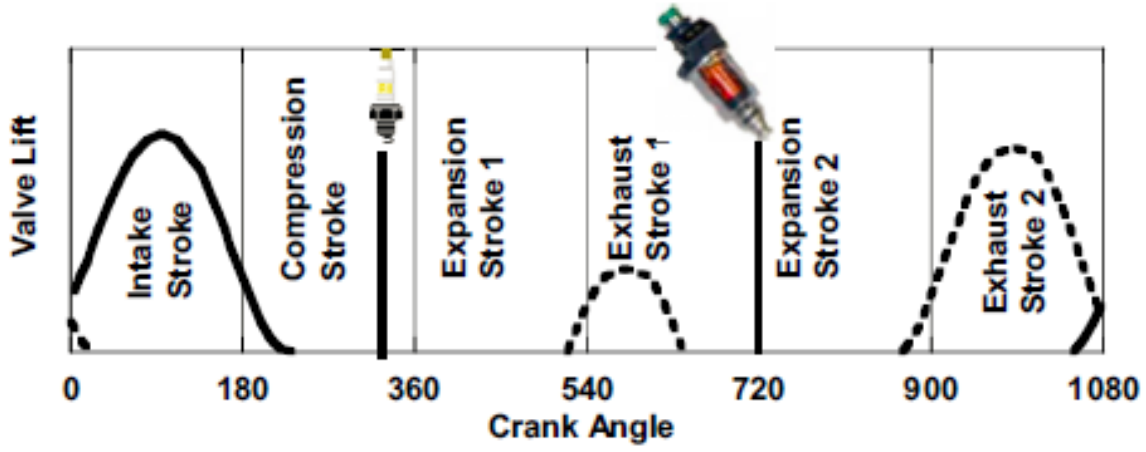

Figure 9 SIX STROKE ENGINE WITH WATER INJECTION VALVE ACTUATION [8]

To perform the thermodynamic analysis of the air-standard cycle for this engine we need to define all the processes occurring in the cycle.

- 0-1, Constant pressure intake
- 1-2, Isentropic compression
- 2-3, Constant volume heat addition
- 3-4, Isentropic expansion
- 4-5, Isentropic recompression (we assume no exhaust in the air-standard cycle)
- 5-6, Constant volume heat absorption increasing pressure (Water injection)
- 6-7, Second isentropic expansion
- 7-8, Constant volume heat rejection
- 8-9, Constant pressure exhaust stroke

First law analysis of all the processes in the air-standard cycle:

Process 0-1: Constant pressure intake stroke of air at atmospheric pressure (P_0)

- $P_1 = P_0$ (4.1)(Pressure at state 1 is same as atmospheric)
- $T_1 = 333\ K$ (4.2)(Temperature value assumed at the start)

- $w_{01} = P_0 * (v_1 - v_0)$ (4.3)(Specific work done)
- $q_{01} = 0$ (4.4)(No heat transfer)
- $v_1 = v_d + v_c$ (4.5)(Volume is sum of displacement and clearance)

Process 1-2: Isentropic compression stroke

- $T_2 = T_1 * \left(\frac{v_1}{v_2}\right)^{k-1}$ (5.1)(Rise in Temperature due to compression)
- $P_2 = P_1 * \left(\frac{v_1}{v_2}\right)^{k}$ (5.2)(Rise in Pressure due to the compression)
- $v_2 = v_c$ (5.3)(Volume at the end of the process)
- $q_{12} = 0$ (5.4)(No heat transfer during the process)
- $w_{12} = u_1 - u_2 = C_v * (T_1 - T_2)$ (5.5)(Specific work of the compression process)

Process 2-3: Constant volume heat addition stroke

- $v_3 = v_2$ (6.1)(Constant volume)
- $q_{23} = Q_{in} \rightarrow C_v * (T_3 - T_2) = m_f * Q_{HV} * \eta_c$ (6.2)(we can calculate T_3)
- $P_3 = P_2 * (T_3/T_2)$ (6.3)(P, T relation for constant Volume process)
- $w_{23} = 0$ (6.4)

Process 3-4: Isentropic Power or expansion stroke

- $T_4 = T_3 * \left(\frac{v_3}{v_4}\right)^{k-1}$ (7.1)(Change in Temperature)
- $P_4 = P_3 * \left(\frac{v_3}{v_4}\right)^{k}$ (7.2)(Change in Pressure)
- $w_{34} = u_3 - u_4 = C_v * (T_3 - T_4)$ (7.3)(Specific work)
- $q_{34} = 0$ (7.4)
- $v_4 = v_{BDC}$ (7.5)

Process 4-5: Recompression Stroke

- $T_5 = T_4 * \left(\frac{v_4}{v_5}\right)^{k-1}$ (8.1)(Change in temperature)
- $P_5 = P_4 * \left(\frac{v_4}{v_5}\right)^{k}$ (8.2)(Change in Pressure)
- $w_{45} = u_4 - u_5 = C_v * (T_4 - T_5)$ (8.3)(Specific work done)
- $q_{45} = 0$ (8.4)
- $v_5 = v_c$ (8.5)

Process 5-6: Constant volume heat absorption

We know the Latent heat of vaporization of water (Q_v) = -2260kJ/kg

- $v_5 = v_6$ (9.1)
- $w_{56} = 0$ (9.2)
- $q_{56} = m_{water} * Q_v = C_v * (T_6 - T_5)$ (9.3)
- $P_6 = P_5 * (T_6/T_5)$ (9.4)

Heat absorbed is mass of water multiplied by latent heat of vaporization of water, which is equal to the change in internal energy.

Process 6-7: Second expansion stroke

- $q_{67} = 0$ (10.1)
- $T_7 = T_6 * \left(\frac{v_6}{v_7}\right)^{k-1}$ (10.2)
- $P_7 = P_6 * \left(\frac{v_6}{v_7}\right)^{k}$ (10.3)
- $w_{67} = u_6 - u_7 = C_v * (T_6 - T_7)$ (10.4)
- $v_7 = v_{BDC}$ (10.5)

Process 7-8: Constant volume heat rejection stroke (Exhaust Blowdown)

- $v_7 = v_8$ (11.1)

- $w_{78} = 0$ (11.2)
- $q_{78} = Q_{out} = C_v * (T_8 - T_7)$ (11.3)
- $P_8 = P_1 = P_0$ (11.4)

Process 8-9: Constant pressure exhaust stroke

- $P_8 = P_9 = P_0$ (12.1)
- $w_{89} = P_0 * (v_9 - v_8)$ (12.2)

From this we can calculate the thermal efficiency of the cycle:

$$\eta_{thermal} = \frac{W_{net}}{Q_{in}} \quad (13)$$

where,

$$W_{net} = W_{12} + W_{23} + W_{34} + W_{45} + W_{56} + W_{67} + W_{78}$$

2.3.2 M4+2 Engine

To perform the thermodynamic analysis of the air-standard cycle for M4+2 engine we need to define all the processes occurring in the cycle.

From the figure below, we can see the principle of operation of the engine design and thereby can find out the processes involved.

1) Process 2-3, Constant volume heat addition
2) Process 3-4, Constant pressure heat addition
3) Process 4-5, Isentropic expansion
4) Process 5-6, Constant volume heat rejection
5) Process 6-7, Constant pressure scavenging process
6) Process 7-1, Constant volume filling process at overpressure
7) Process 1-2, Isentropic Compression

We see here that the engine is a combination of Dual cycle (or Limited Pressure cycle) and Miller cycle. The process of heat addition is divided in 2 part at constant volume and at constant pressure, as in the case of Dual cycle. Thus we divide the total input heat in 2 parts for addition over two processes.

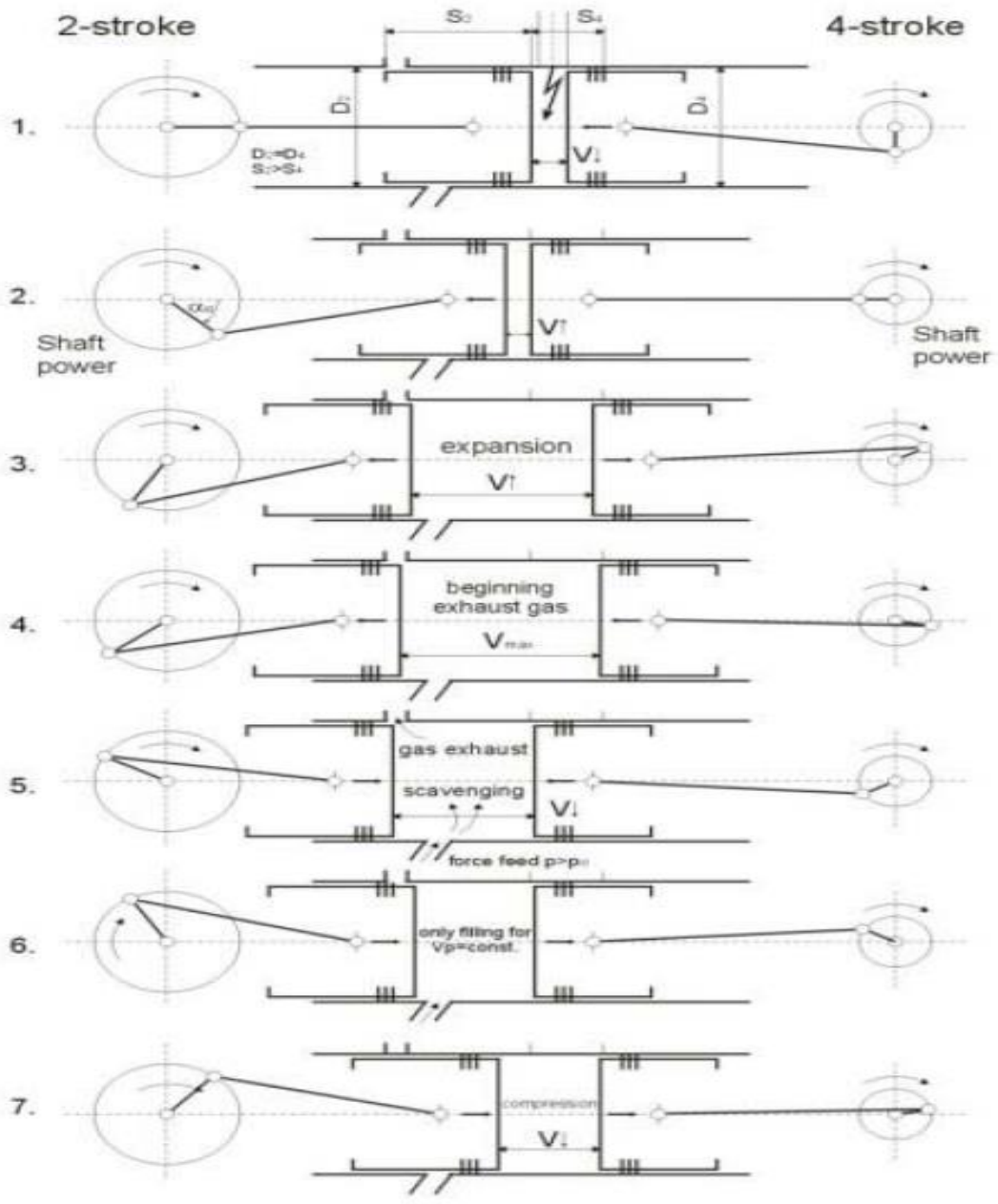

Figure 10 M4+2 ENGINE PROCESSES [4]

First law analysis of all the processes in the air-standard cycle:

Process 1-2: Isentropic compression stroke

- $T_2 = T_1 * \left(\frac{v_1}{v_2}\right)^{k-1}$ (14.1)(Rise in Temperature due to compression)
- $P_2 = P_1 * \left(\frac{v_1}{v_2}\right)^{k}$ (14.2)(Rise in Pressure due to the compression)
- $v_2 = v_{min}$ (14.3)(Volume at the end of the process)
- $q_{12} = 0$ (14.4)(No heat transfer during the process)
- $w_{12} = u_1 - u_2 = C_v * (T_1 - T_2)$ (14.5)(Work done of the compression process)

Compression ratio here is lower than the expansion ratio, as in the case of Miller cycle.

Process 2-3: Constant volume heat addition (first part of combustion)

- $v_3 = v_2$ (15.1)(Constant volume process)
- $q_{23} = C_v * (T_3 - T_2) = u_3 - u_2$ (15.2)(we can calculate T_3)
- $P_3 = P_2 * (T_3/T_2)$ (15.3)(P-T relation)
- $w_{23} = 0$ (15.4)

Process 3-4: Constant pressure heat addition (second part of combustion)

- $P_4 = P_3$ (16.1)(Constant Pressure process)
- $v_4 = v_3 * (T_4/T_3)$ (16.2)
- $q_{34} = C_p * (T_4 - T_3) = h_4 - h_3$ (16.3)
- $w_{34} = q_{34} - (u_4 - u_3) = P_3 * (v_4 - v_3)$ (16.4)

Total heat input is, $Q_{in} = Q_{23} + Q_{34} = (u_3 - u_2) + (h_4 - h_3)$ (17)

Process 4-5: Isentropic expansion stroke

- $T_5 = T_4 * \left(\frac{v_4}{v_5}\right)^{k-1}$ (18.1)(Change in Temperature)
- $P_5 = P_4 * \left(\frac{v_4}{v_5}\right)^{k}$ (18.2)(Change in Pressure)
- $v_5 = v_d + v_{min}$ (18.3)
- $w_{45} = u_4 - u_5 = C_v * (T_4 - T_5)$ (18.4)(Specific work)
- $q_{45} = 0$ (18.5)

Process 5-6: Constant volume heat rejection stroke (Exhaust Blowdown)

- $v_6 = v_5$ (19.1)
- $w_{56} = 0$ (19.2)
- $P_6 = P_0$ (19.3)
- $q_{56} = Q_{out} = C_v * (T_6 - T_5) = (u_6 - u_5)$ (19.4)

Process 6-7: Constant Pressure scavenging process

- $P_6 = P_7 = P_0$ (20.1)
- $w_{67} = P_0 * (v_7 - v_6)$ (20.2)

Process 7-1: Constant volume filling process under overpressure

- $v_7 = v_1$ (21.1)
- $q_{71} = C_v * (T_1 - T_7)$ (21.2)
- $w_{71} = 0$ (21.3)

From this we can calculate the thermal efficiency of the cycle:

$$\eta_{thermal} = \frac{W_{net}}{Q_{in}} \quad (22)$$

where,

$$W_{net} = W_{12} + W_{23} + W_{34} + W_{45} + W_{56} + W_{67} + W_{71}$$

2.3.3 Six-Stroke Direct Injection Dual Fuel Engine

Taking into account the positive effects of the proposed engine on emissions, it becomes important to study its thermodynamic processes, which can be defined as follows: -

I. Process 0-1, Constant pressure intake of air
II. Process 1-2, Isentropic compression
III. Process 2-3, Constant pressure heat addition
IV. Process 3-4, Isentropic expansion
V. Process 4-5, Second compression stroke
VI. Process 5-6, Second constant pressure heat addition
VII. Process 6-7, Second expansion
VIII. Process 7-8, Constant volume heat rejection
IX. Process 8-9, Constant pressure exhaust

Heat supplied in the two constant pressure heat addition process is divided by the allocation ratio.

First law analysis of all the processes in the air-standard cycle:

Process 0-1: Constant pressure intake stroke of air at atmospheric pressure (P_0)

- $P_1 = P_0$ (24.1)(Pressure at state 1 same as atmospheric)
- $T_1 = 333\ K$ (24.2)
- $v_1 = v_{BDC}$ (24.3)(Piston at Bottom dead center)
- $w_{01} = P_0 * (v_1 - v_0)$ (24.4)(Specific work done)
- $q_{01} = 0$ (24.5)

Process 1-2: Isentropic compression stroke

- $T_2 = T_1 * \left(\frac{v_1}{v_2}\right)^{k-1}$ (25.1)(Rise in Temperature due to compression)
- $P_2 = P_1 * \left(\frac{v_1}{v_2}\right)^{k}$ (25.2)(Rise in Pressure due to the compression)
- $v_2 = v_c$ (25.3)(Volume at the end of the process)
- $q_{12} = 0$ (25.4)(No heat transfer during the process)
- $w_{12} = u_1 - u_2 = C_v * (T_1 - T_2)$ (25.5)(Specific work done)

Process 2-3: Constant pressure heat addition stroke (First combustion process)

- $P_3 = P_2$ (26.1)(Constant pressure process)
- $q_{23} = Q_I \rightarrow C_P * (T_3 - T_2)$ (26.2)(we can calculate T_3)
- $v_3 = v_2 * (T_3/T_2)$ (26.3)(P- T Relation)
- $w_{23} = q_{23} - (u_3 - u_2) = P_2 * (v_3 - v_2)$ (26.4)(specific work done)

Process 3-4: Isentropic Power or expansion stroke

- $T_4 = T_3 * \left(\frac{v_3}{v_4}\right)^{k-1}$ (27.1)(Change in Temperature)
- $P_4 = P_3 * \left(\frac{v_3}{v_4}\right)^{k}$ (27.2)(Change in Pressure)
- $v_4 = v_{BDC}$ (27.3)
- $w_{34} = u_3 - u_4 = C_v * (T_3 - T_4)$ (27.4)(Specific work)
- $q_{34} = 0$ (27.5)

Process 4-5: Recompression Stroke

- $T_5 = T_4 * \left(\frac{v_4}{v_5}\right)^{k-1}$ (28.1)(Change in temperature)
- $P_5 = P_4 * \left(\frac{v_4}{v_5}\right)^{k}$ (28.2)(Change in Pressure)
- $v_5 = v_c$ (28.3)
- $w_{45} = u_4 - u_5 = C_v * (T_4 - T_5)$ (28.4)(Specific work done)
- $q_{45} = 0$ (28.5)

Process 5-6: Constant pressure heat addition stroke (Second combustion process)

- $P_6 = P_5$ (29.1)(Constant pressure process)
- $q_{56} = Q_{II} \rightarrow C_P * (T_6 - T_5)$ (29.2)(we can calculate T_6)
- $v_6 = v_5 * (T_6/T_5)$ (29.3)(P-T relation)
- $w_{56} = q_{56} - (u_6 - u_5) = P_5 * (v_6 - v_5)$ (29.4)

Process 6-7: Second expansion stroke

- $q_{67} = 0$ (30.1)(No heat exchange)
- $T_7 = T_6 * \left(\frac{v_6}{v_7}\right)^{k-1}$ (30.2)(Temperature at end of expansion)
- $P_7 = P_6 * \left(\frac{v_6}{v_7}\right)^{k}$ (30.3)(Pressure at end of expansion)
- $w_{67} = u_6 - u_7 = C_v * (T_6 - T_7)$ (30.4)(specific work done)
- $v_7 = v_{BDC}$ (30.5)

Process 7-8: Constant volume heat rejection stroke (Exhaust Blowdown)

- $v_7 = v_8$ (31.1)
- $w_{78} = 0$ (31.2)
- $P_8 = P_0$ (31.3)
- $T_8 = T_7 * (P_8/P_7)$ (31.4)
- $q_{78} = Q_{out} = C_v * (T_8 - T_7) = (u_8 - u_7)$ (31.5)

Process 8-9: Constant pressure exhaust stroke

- $P_8 = P_9 = P_0$ (32.1)
- $v_9 = v_c$ (32.2)
- $w_{89} = P_0 * (v_9 - v_8)$ (32.3)

From this we can calculate the thermal efficiency of the cycle:

$$\eta_{thermal} = \frac{W_{net}}{Q_{in}} \quad (33)$$

where,

$$W_{net} = W_{12} + W_{23} + W_{34} + W_{45} + W_{56} + W_{67} + W_{78}$$

Constant pressure Intake work and Exhaust work cancel each other out

2.4 Results and Conclusions for Ideal Cycle Analysis

To understand the effectiveness of the six-stroke engines, we must compare them to the four-stroke engine operating under similar conditions of displacement, compression ratio, Air-Fuel ratio, heat supplied, EGR effect and intake pressure, volume and temperature conditions. Then we calculate and compare the thermal efficiency, peak temperature and pressure reached and the indicated mean effective pressure of the air-standard cycles.

For this purpose we use a MATLAB script to perform First law analysis of the different processes in the air-standard cycle. We calculate the work done by the system and using the heat supplied find the thermal efficiency, we also calculate the state of the system after each process to find the maximum temperature and pressure and finally plot the P-V indicator diagram.

2.4.1 Exhaust Heat Recovery With Water Injection Based Six-Stroke Engine

The 6 stroke engine cycle suggested by James C. Conklin and James P. Szybist in their paper [8] is a modification of the Otto cycle thus the comparison is also with a four-stroke Otto cycle.

The script as an input takes the specifications of the engine that is the volume, compression ratio and number of cylinders. Furthermore, we assume the intake pressure and temperature constant at 1 bar (100 kPa) and 60˚C (333 K) respectively for all the air standard cycles unless specified otherwise to keep the conditions as similar as possible.

From the intake pressure and temperature values assumed and displacement volume calculated from the input, we can find the thermodynamic state at point 1 of the air-standard cycle. From the Eqs. (4-13) we can calculate the thermodynamic state at each point of the air-standard cycle and also calculate the work done and heat transfer of each process. Using these values we can easily calculate the thermal efficiency of the cycle and plot the P-V indicator diagram.

	4- stroke cycle	**six-stroke cycle (0.3g water injection)**	**six-stroke cycle (0.2g water injection)**
Thermal efficiency [%]	51.7	35.6	40.97

Peak Temperature [K]	4239	4239	4239
Peak Pressure [kPa]	10186	10186	10186
Temp. before Exhaust [K]	2047	899.7	1077
Thermal Efficiency based on Heat rejected* [%]	51.7	66.7	61.72

Table 1 SIX STROKE ENGINE WATER INJECTION IDEAL CYCLE ANALYSIS RESULTS

* Calculation of thermal efficiency based on Heat Rejected = $(\frac{Q_{supplied}-Q_{rejected}}{Q_{supplied}})$

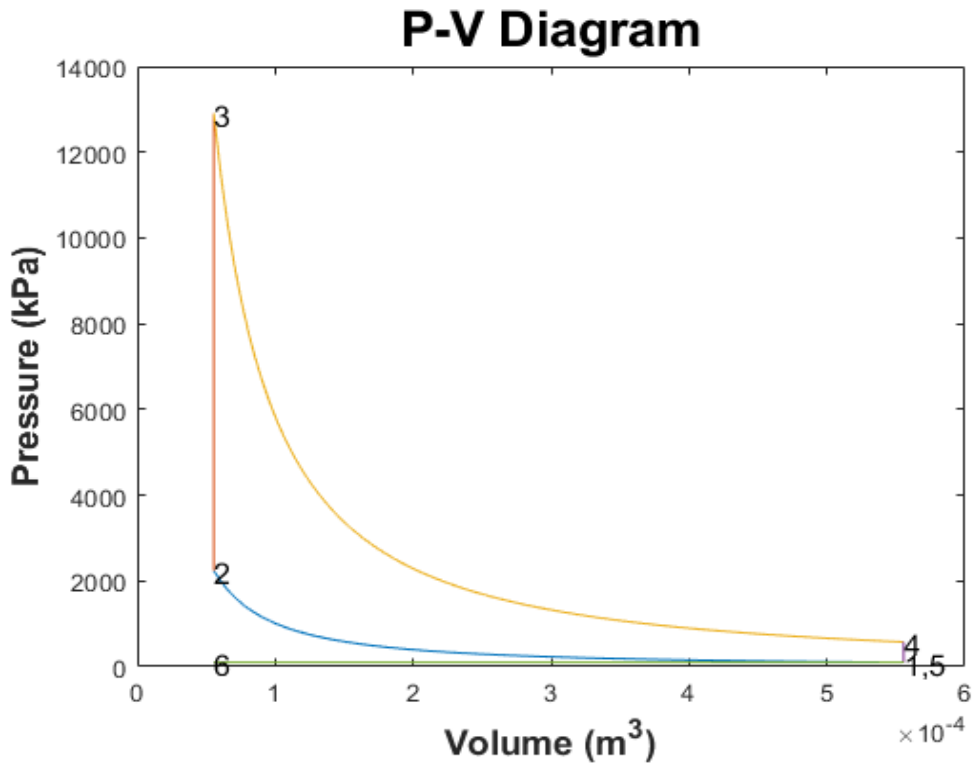

Figure 11 FOUR-STROKE SI ENGINE IDEAL CYCLE P-V DIAGRAM

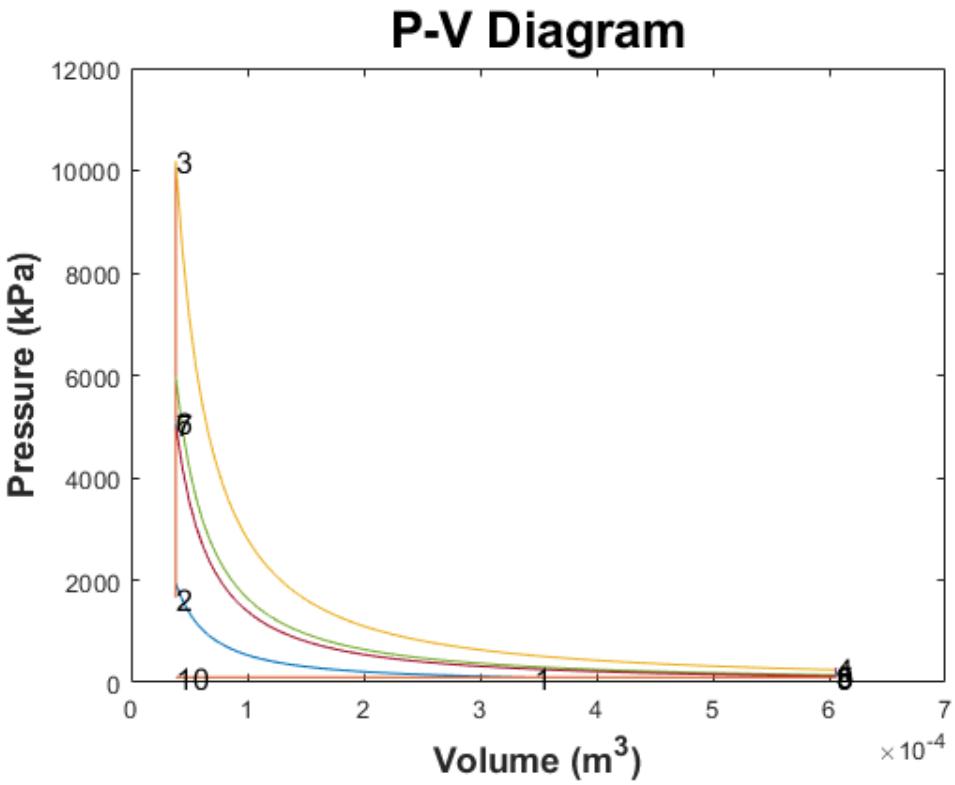

Figure 12 SIX-STROKE WATER INJECTION IDEAL CYCLE P-V DIAGRAM

It is clear from the results shown that the thermal efficiency calculated from dividing net work done throughout the cycle by the heat input, is lower than that for the four-stroke engine since in the six-stroke cycle we have a recompression process at higher temperature whereas the expansion stroke is at lower temperature due to heat absorption by injected water. As a result net work is lower for the same heat input causing lower thermal efficiency of the air-standard cycle.

However, if we calculate the thermal efficiency as the ratio of heat utilised to produce work and the total heat supplied, we see that the six-stroke cycle is more efficient (There is a disparity in the thermal efficiency because we cannot take into account the heat absorbed by water in our calculation of indicated work). The same can also be seen from the temperature at exhaust which is much lower for six-stroke

cycle compared to four-stroke cycle. The peak pressure and temperature is same as the constant volume heat addition process is same for both cycles.

Moreover, when we reduce the amount of water injected we see that the amount of heat rejected through exhaust increases causing the thermal efficiency to reduce, whereas the increase in the temperature for the second expansion causes an increase in the work done.

Theoretically we can increase the amount of water injected to absorb more amount of heat from exhaust gases thus improving the efficiency, however that is not possible practically because we need to have complete vaporization of water to avoid any equipment damage due to droplet erosion and to avoid reduction of temperature during expansion below the dew point temperature causing condensation, which would result in decreased specific volume and thus reduced expansion work. Moreover we must have enough temperature of exhaust gases for optimum operation of exhaust purification system.

In conclusion we can say that the efficiency gain will come with a power density penalty due to reduced net work done, but the net power that can be approximated is at an increased fuel efficiency due to the additional power stroke achieved by water injection to utilise the exhaust heat of the combustion cycle.

2.4.2 M4+2 Double Piston Engine

The proposed engine can be seen as the combination of two cycles, Atkinson cycle and Miller cycle. As a result the heat addition process is divided in two parts, constant volume and constant pressure similar to dual cycle, it has a prolonged expansion process similar to Atkinson cycle and possibility of different compression and expansion ratios similar to Miller cycle. It also eliminates the disadvantages of

these cycles, complete decompression in case of Atkinson and worse filling in case of Miller cycle.

We have the displacement volume from the input taken at the start of the script, using the expansion ratio we can calculate the minimum volume of the cycle. Multiplying the minimum volume with the compression ratio we get the volume at point 1. Pressure at point 1 is taken as 140 kPa due to the overpressure provided by the compressor [5]. Temperature is assumed to be 333 K. Now we have the thermodynamic state at point 1 and using equations (14-22) we can calculate the state of all the points of the air-standard cycle and from that the thermal efficiency and the P-V indicator diagram.

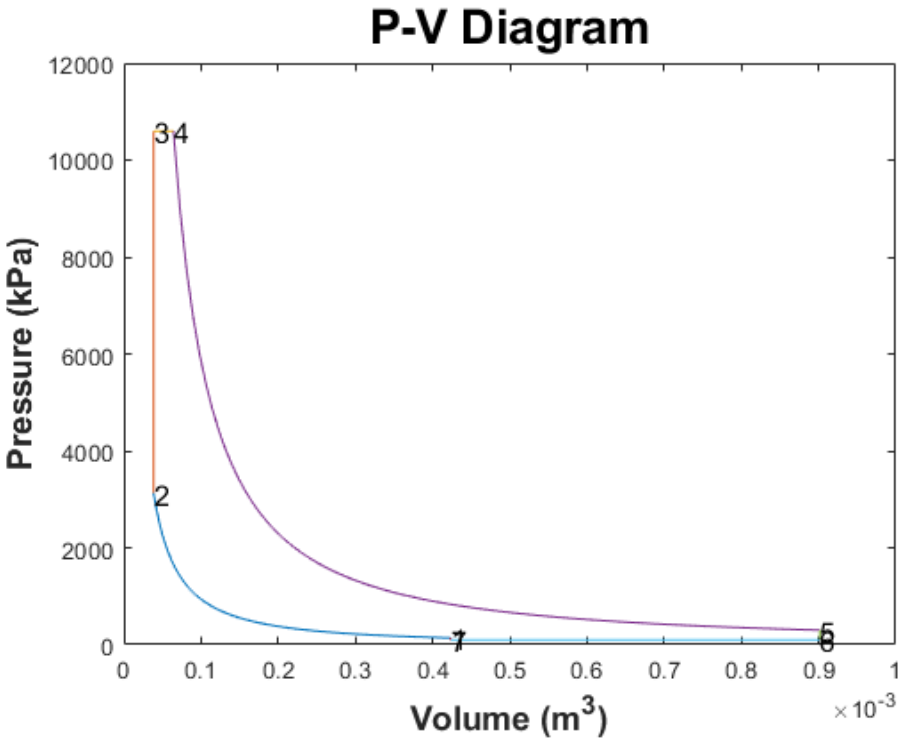

Figure 13 M4+2 ENGINE IDEAL CYCLE ANALYSIS P-V DIAGRAM

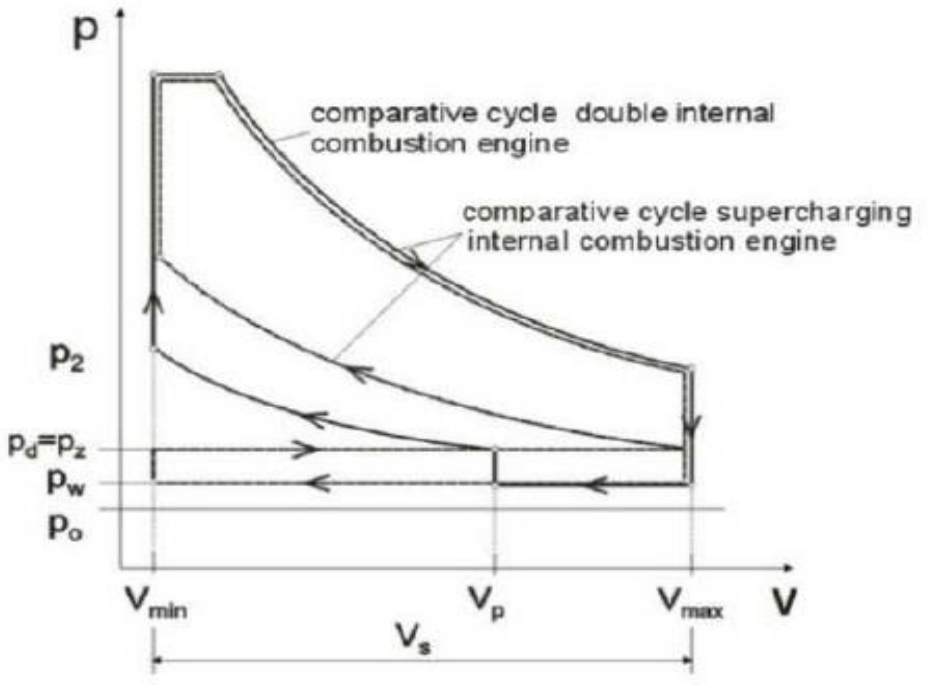

Figure 14 THEORETICAL IDEAL CYCLE P-V DIAGRAM FOR M4+2 ENGINE [4]

The above 2 figures show the Ideal P-V graph calculated and the Ideal P-V graph for the engine design as assumed by the inventor of the M4+2 engine design.

	Four-Stroke cycle	**M4+2 cycle**
Thermal efficiency [%]	51.7	65.7
Peak Temperature [K]	4239	3780
Peak Pressure [kPa]	10186	8289
Temperature before exhaust [K]	2047	1500

Indicated mean effective pressure [kPa]	1802	1944

Table 2 M4+2 ENGINE IDEAL CYCLE ANALYSIS RESULTS

From results shown above we can see that the thermal efficiency has increased for the M4+2 engine this is because of the larger expansion stroke compared to compression, similar to miller cycle. Due to which there is a need for a compressor to help provide stoichiometric air-fuel mixture in the combustion chamber.

Since the two pistons are synchronised, we can change the compression ratio while the engine is operating depending on the load thus having better thermal efficiency over a larger range of the engine operating load.

Furthermore, the engine speed could be increased as it is not limited by the operation of poppet valves in addition to increase in the net work done, thus we will have higher power and torque output. This can also be seen from increased indicated mean effective pressure for M4+2 double piston engine.

Due to separate scavenging and filling phase we have a very low amount of residual exhaust gases in the combustion chamber, which can be further optimised through the design of inlet port.

However, there is a reduction in mechanical efficiency due to the 2 crankshaft assembly which also results in problem involving the passage of power from both parts of the engine. There is also an issue regarding complete combustion of fuel due to gaps between inlet port and rotational valve, which can be solved by using a direct injection system.

Even considering above mentioned issues, the thermodynamic advantage of the M4+2 engine cannot be overlooked. The characteristic feature of providing a continuous change in cubic capacity and compression rate provides higher thermal efficiency and power output over a larger range of engine operating load.

2.4.3 Six-Stroke Direct Injection Engine Under Dual Fuel Operation

The proposed concept is an addition of a second compression and combustion process to a regular direct injection diesel engine. The ignition delay of the second combustion process can be reduced by the high temperature effect in the second compression stroke. This can be used to improve the ignitability of a fuel with low cetane number, for example methanol which is considered here.

We consider methanol also because it will form an oxidizing radical (OH) during combustion which has the potential to reduce soot produces in the first combustion process and since it already contains oxygen in its molecular formula, the stoichiometric air-fuel ratio is lower (6.47).

The engine presented is a modification of a regular four-stroke diesel engine cycle thus it is compared with the same. We consider the same displacement volume (V_d) as that of the 2 above mentioned engine concepts, however the values of compression ratio, Stroke to Bore ratio, Air-Fuel ratio, Heat supplied and EGR effect changes.

We consider the same conditions at the start of the cycles and the total heat input for both four-stroke diesel and six-stroke dual fuel is same. We use the allocation ratio to divide the amount of total heat supplied between the two combustion processes.

Considering the same displacement volume as before we calculate the clearance volume (V_c) using the typical compression ratio of a diesel engine. Adding the clearance volume and displacement volume we get the volume at point 1, temperature and pressure is considered same as before 333 K and 100 KPa. This gives us the thermodynamic state at point 1, now through equations (23-33) we can calculate the thermodynamic states at each point, change in internal energy after each process, thermal efficiency and P-V indicator diagram of the air-standard cycle. Comparison between the four-stroke and six-stroke cycle is provided in table and figure below.

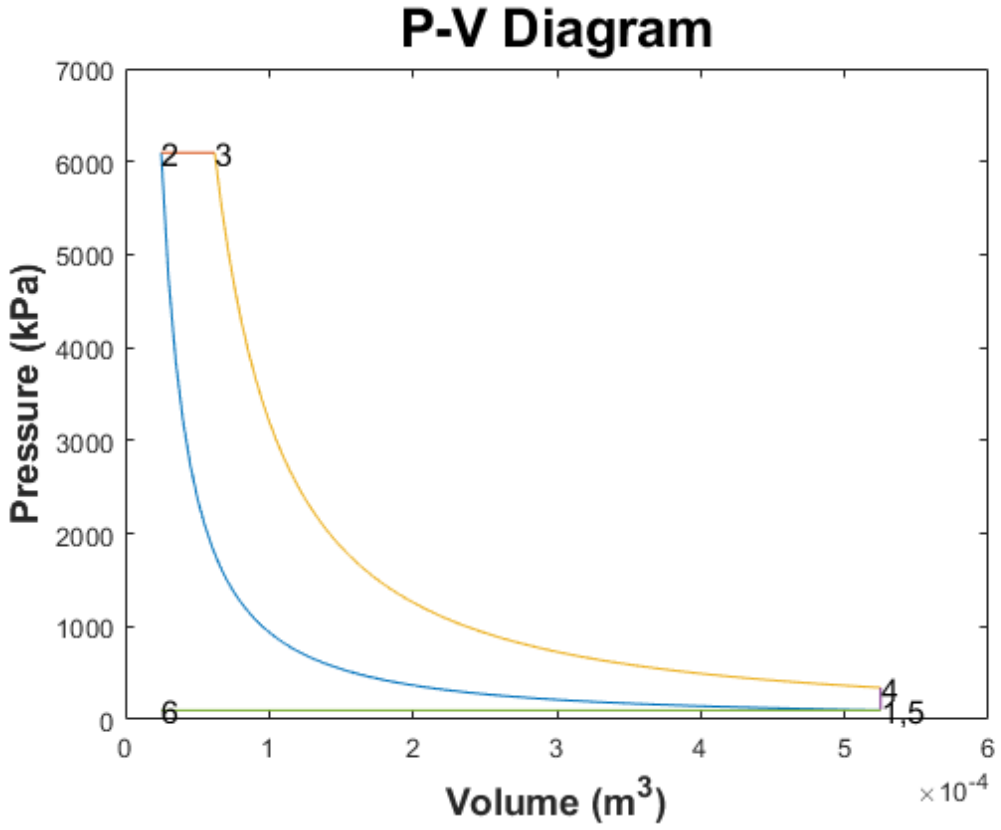

Figure 15 DIESEL ENGINE IDEAL CYCLE P-V DIAGRAM

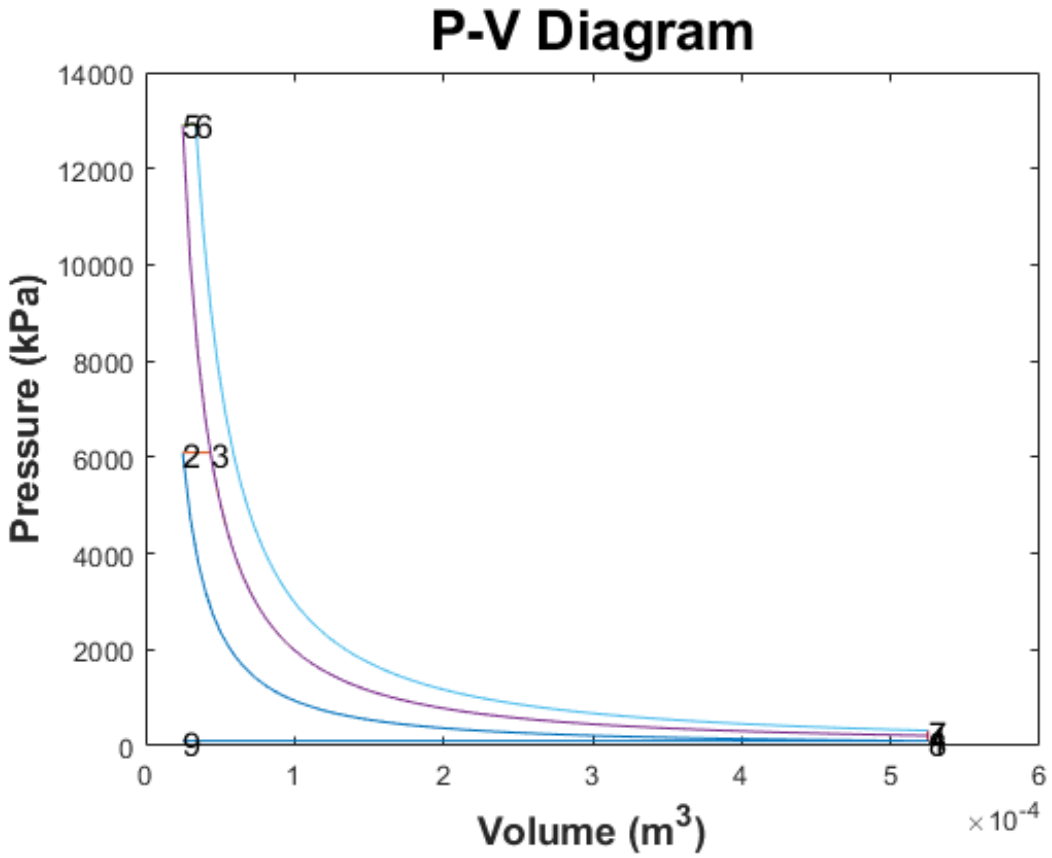

Figure 16 SIX-STROKE DUAL FUEL ENGINE IDEAL CYCLE P-V DIAGRAM

	four-stroke	six-stroke (Heat allocation ratio – 30%)	six-stroke (Heat allocation ratio – 70%)
Thermal efficiency [%]	58.4	61.5	62.4
Peak Temperature [K]	2403	2963	2596

Peak Pressure [kPa]	6095	15967	10028
Temperature before exhaust [K]	1139	1078	1061
Indicated mean effective pressure [kPa]	1022	1076	1091

Table 3 SIX-STROKE DUAL FUEL ENGINE CYCLE RESULTS

From the results shown, we can see that the thermal efficiency of the six-stroke dual fuel engine is more than that of the four-stroke diesel engine, as can be seen from the temperature of gases at exhaust which is lower for six-stroke cycle thus rejecting less heat. The torque and power output which can be approximated from the indicated mean effective pressure is almost same for four-stroke and six-stroke cycle.

The characteristic feature of the six-stroke dual fuel cycle is not thermal efficiency or power output, which is not considerable higher than the four-stroke cycle. The characteristic feature is the reduction in harmful emissions.

We can see from the table below that the temperature in the cylinder after the first combustion process for six-stroke dual fuel engine is lower than that for four-stroke engine and the second combustion process has a large EGR effect, thus the NO

concentration in the exhaust gases was decreased. Moreover, the soot formed in the first combustion process is oxidised in the second combustion process.

	four-stroke	**six-stroke (Heat allocation ratio – 30%)**	**six-stroke (Heat allocation ratio – 70%)**
Temperature after first combustion process [K]	2403	1972	1397

Table 4 SIX-STROKE DUAL FUEL ENGINE TEMPERATURE COMPARISON

However, there are some issues with the dual fuel six-stroke engine such as for the second combustion process, since the combustion heat of diesel and methanol is different, specific fuel consumption will be higher. The mechanical efficiency of the engine is lower due to the presence of extra nozzle and pump for methanol injection.

Therefore in conclusion, a six-stroke direct injection dual fuel engine has significant possibilities to improve combustion process because it is more controllable relative to four-stroke engine. Although it has a higher specific fuel consumption and lower mechanical efficiency, the advantage of lower emissions is much more important.

From the results of the thermodynamic analysis of different six-stroke engines shown above, it is clear that thermal efficiency of the six-stroke engine is better than that of four-stroke engine cycle so we can safely assume a better fuel economy. The indicated mean effective pressure of two of the three six-stroke engines shown

above is similar or higher than that for four-stroke engine, thus the thermal efficiency gain does not incur a power penalty.

In addition to which, engine characteristics like possibility to use different fuels, variable compression ratio, cleaner combustion and lower emissions is making quiet a strong case for further research and eventual largescale use of the six-stroke engines.

3 Real Cycle Simulation

From the Ideal cycle analysis, we can see the potential advantages of six-stroke engines over conventional four-stroke engines. Keeping that in mind we proceed to the real cycle analysis of the six-stroke engine designs.

The real cycle simulation is based on the assumptions and details provided by the researchers that came up with these designs. The aim was to come as close to the theoretical cycle predicted in the research. For this purpose a thermodynamic model for a 4 stroke Spark Ignited engine cycle was created and then used as the basis for the thermodynamic model of six-stroke engine designs.

3.1 Four-Stroke SI Engine Model Description, Simulation and Results

The 4 stroke SI engine is an internal combustion engine with spark-ignition, designed to run on gasoline (petrol) and similar volatile fuels.

In 1862, Alphonse Beau de Rochas gave the theory of an Ideal cycle for the internal combustion engine. This theory was applied in 1876 in Germany by German inventor Nikolaus August Otto, building the first 4 stroke SI engine. This is why sometimes a SI engine is also called an Otto engine. [16]

The power output is controlled by means of regulation of mixture mass flow. In the case of naturally aspirated engines (no supercharging or turbocharging) only a throttle valve controls the air quantity, which will enter the combustion chamber.

In most SI engines, the fuel and air are usually pre-mixed inside the intake duct before they enter the combustion chamber. The value of fuel/air equivalence ratio (Φ) is a way to express the relation between fuel and air masses (m) in the charge. When Φ > 1, the mixture is rich (fuel in excess) and when Φ < 1, the mixture is lean (air in excess).

$$\varphi = \frac{\left(\frac{F}{Air}\right)_{Act}}{\left(\frac{F}{Air}\right)_{st}}$$

Engine Processes:

- During the Intake stroke the piston moves from the Top Dead Center (TDC) to the Bottom Dead Center (BDC). The intake valves are open and permit the fuel/air mixture to enter the cylinder. For a tuned engine, the Intake Valve Opening (IVO) occurs before TDC (between 0-40 deg bTDC) and Inlet Valve Closing (IVC) after the BDC (~50 deg aBDC).

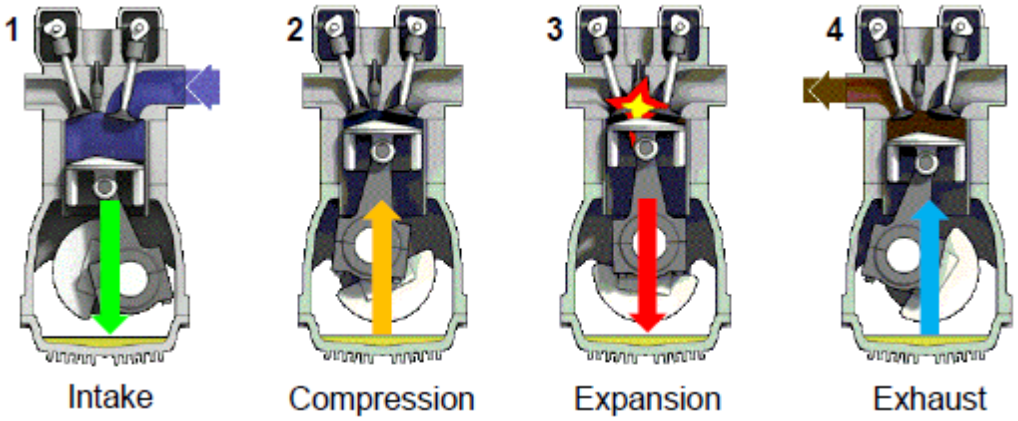

Figure 17 FOUR STROKE ENGINE STROKES [16]

- Compression stroke starts once the intake valves are closed. During this stroke, the chamber contains the premixed charge of fuel and air as well as the EGR. The piston moves from the BDC to the TDC and both cylinder pressure and temperature rise.

- In a typical naturally aspirated engine, ignition starts some crank angle degrees before the end of compression at TDC. Combustion process, which is deployed inside the compression and expansion strokes, takes place and the pressure and temperature rise even more.

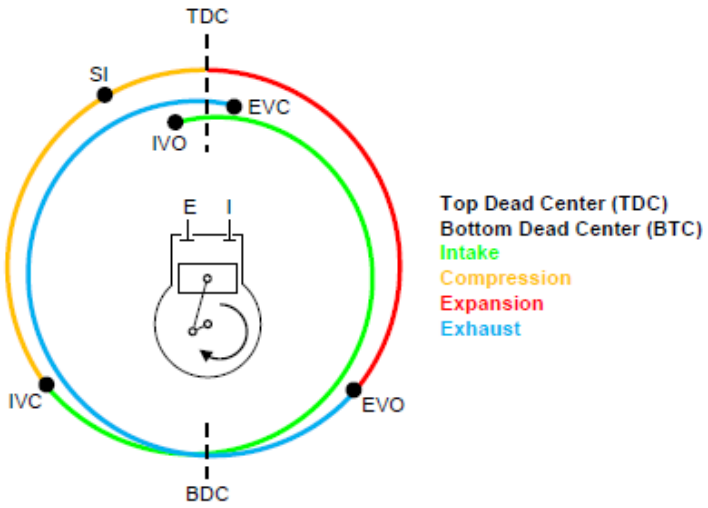

Figure 18 VALVE TIMING DIAGRAM [16]

- The Expansion stroke starts when the piston is at TDC. It finishes when the Exhaust Valve Opens (EVO). This stroke is also known as the Power stroke, as it offers useful work and takes advantage of the energy released by the combustion process. The chemical energy of the fuel is transformed into mechanical work by the exerted force on the piston.

- During the Exhaust Stroke, burnt gases exist in the chamber. The exhaust stroke starts when the Exhaust Valve Opens (EVO). This happens before the piston reaches BDC (typical value of 50 deg before BDC). The piston then moves from BDC to TDC, pushing the burnt gases to the exhaust valve. The four-stroke cycle ends when the piston reaches TDC.

There is an overlap period when both intake and exhaust valves are open. This overlap has been designed for the optimization of the engines gas exchange process.

A considerable effort has been spent to improve the performance of spark-ignition (SI) engines. Studies concerning internal combustion engines are grouped mainly as experimental and theoretical. Experimental studies provide actual results about the engine operation, design and manufacturing, however testing of new engines or new systems is expensive and requires more time than theoretical methods.

On the other hand, if a mathematical model of an engine cycle can be proposed with realistic assumptions and can be run as a computer code, the engine cycle and its performance can be predicted at the beginning of design or development project. For this reason, cycle simulation studies have had great interest to date.

Internal combustion engines consist of open thermodynamic systems such as cylinder, intake, and exhaust manifolds. These systems are open to the transfer of mass, enthalpy, and energy in the form of work and heat.

The aim of the simulation studies is to determine the thermodynamic state of the charge involved by the above mentioned systems. For this purpose a set of equations governing the fluid mechanic and thermodynamic behaviour of the

engine working fluid throughout the cycle is derived and then solved numerically on a computer.

Generally, mathematical cycle simulation models are divided into two main groups. The first is fluid dynamic based models and the second is thermodynamic based models.

Fluid dynamic based models are also called multidimensional models due to the fact that their formulation is based on the conservation of mass, chemical species, and energy at any location within the engine cylinder or manifolds at any time. Thus, spatial coordinates and time are the independent variables governing the partial differential equations.

Thermodynamic cycle models are based on the thermodynamic analysis of the cylinder contents during the engine operating cycle. In these models the First Law of Thermodynamics is applied to an open system composed of a fuel-air-residual gas charge within the engine manifolds and cylinders. Thermodynamic models are zero dimensional because the only independent variable is time. Thus the governing equations consist of ordinary differential equations instead of partial differential equations.

For theoretical investigation of a SI engine cycle, a mathematical model must be established for the calculation of cylinder charge state at each engine process.

3.1.1 Mathematical Model

The SI engine cycle consists of 4 consecutive processes: intake, compression, combustion-expansion, and exhaust. In general, for investigating the changes in the thermodynamic state of the cylinder contents, expressions for the time rates of the charge temperature and pressure must be established. The in-cylinder pressure is

uniform across the combustion chamber space, but obviously varies with crank-angle

By using the First Law of Thermodynamics and ideal gas laws, the following equations for the time rates of pressure and temperature of an open system have been derived [15], [20]:

$$\dot{T} = \frac{B'}{A'}\left[\frac{\dot{m}}{m}\left(1-\frac{h}{B'}\right)-\frac{\dot{V}}{V}-\frac{C'}{B'}\dot{\phi}+\frac{1}{B'm}\left(\sum_j \dot{m}_j h_j+\dot{Q}_w\right)\right] \quad (1)$$

where:

$$\begin{cases} A' = \frac{\partial h}{\partial T}+\frac{\frac{\partial \rho}{\partial T}}{\frac{\partial \rho}{\partial P}}\left(\frac{1}{\rho}-\frac{\partial h}{\partial P}\right) \\ B' = \frac{1-\rho(\partial h/\partial P)}{\partial \rho/\partial P} \\ C' = \frac{\partial h}{\partial \phi}+\frac{\partial P/\partial \phi}{\partial \rho/\partial p}\left(\frac{1}{\rho}-\frac{\partial h}{\partial P}\right) \end{cases}$$

In the above equation, 'm' represents the mass in the control volume. When Equation (1) is solved to calculate bulk cylinder temperature during compression and combustion, 'm' is a constant as no mass transfer occurs when intake and exhaust valves are shut. In Equation (1), 'V' represents control volume, 'h' represents specific enthalpy of gas in the control volume, 'φ' represents equivalence ratio, ' $\sum j\ \dot{m}_j h_j$ ' represents total enthalpy transfer rate and '$\dot{Q}_w$' represents heat transfer rate into the control volume.

The density derivatives used in equations above [19]:

$$\left(\frac{d\rho}{dp}\right)_T = \frac{1}{RT}$$

$$\left(\frac{d\rho}{dT}\right)_p = -\left(\frac{p}{RT^2}\right) = -\left(\frac{\rho}{T}\right)$$

The enthalpy derivatives used in equations above [19]:

$$\left(\frac{dh}{dT}\right)_p = C_p$$

$$\left(\frac{dh}{dp}\right)_T = \left(\frac{C_p}{\rho R}\right) * \left[1 - \left(\frac{p}{\rho}\right)\frac{d\rho}{dp}\right] = 0$$

Using the enthalpy and density derivatives, we can find out the values of A′, B′ and C′ used in the equation for calculating the time rate of Temperature during different engine processes. [20]

$$A' = C_p - \frac{p}{\rho T}, \text{ B′ = RT, C′ = 0}$$

During the cycle, these equation (1) must be rearranged with reasonable assumptions for each process due to different physical and chemical events in the engine processes.

<u>Intake Process:</u>

$$\dot{m} = \dot{m}_i - \dot{m}_e$$

$$\dot{T} = \frac{B}{A}\left[\frac{\dot{m}}{m}\left(1 - \frac{h}{B}\right) - \frac{\dot{V}}{V} + \frac{1}{Bm}(\dot{m}_\iota h_\iota - \dot{m}_e h_e - \dot{Q}_w)\right]$$

Where, m is the mass of gas in the cylinder, m_i and m_e are the mass flow rates through the inlet valve and the exhaust valve. The subscripts "i" and "e" denote properties of the flow through the intake and exhaust valves, respectively. The thermodynamic properties for these flows are the values upstream of the valves and therefore depend on whether the flow is into or out of the cylinder. [20]

Compression Process:

The mass consisting of air-fuel-residual gases, contained in the engine cylinder inducted during the intake process is compressed. [20]

$$\dot{m} = 0$$

$$\dot{T} = \frac{B}{A}\left[-\frac{\dot{V}}{V} + \frac{\dot{1}}{Bm}(-\dot{Q}_w)\right]$$

Combustion Process:

The compressed fuel-air-residual gas mixture within the combustion chamber is ignited by a spark discharge starting the process. In this study, we assume that two distinct zones separated by a thin spherical flame that has a negligible volume are formed during combustion.

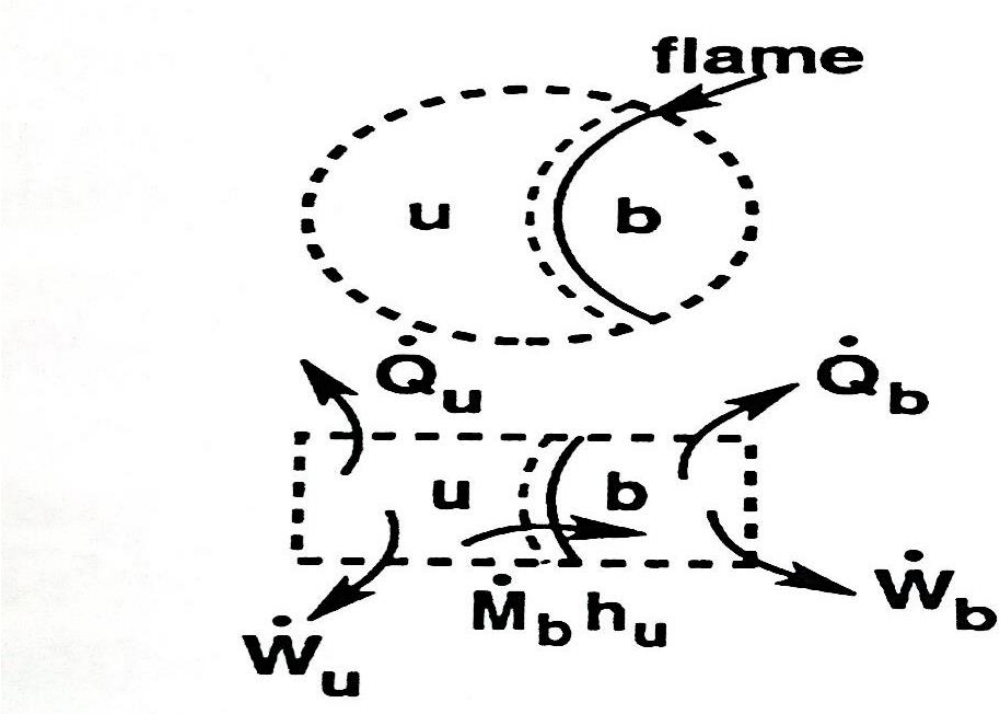

Figure 19 COMBUSTION PROCESS HEAT AND WORK EXCHANGE BETWEEN ZONES [15]

The governing equations must be solved separately for each zone. [20]

$$\dot{m} = 0$$

$$\dot{T}_i = \left(\frac{B}{A}\right)_i \left[\left(\frac{\dot{m}}{m}\right)_i \left(1 - \frac{h_i}{B_i}\right) - \left(\frac{\dot{V}}{V}\right)_i + \frac{1}{(Bm)_i}(-\dot{Q}_{wi} + \dot{m}_i h_u)\right]$$

Here, for the unburned mixture ($i = u$) and for the burned mixture ($i = b$). From the conservation of mass it is obvious that $\dot{m}_b = -\dot{m}_u$.

Expansion Process:

After burning of the entire charge within the cylinder, the expansion process starts. During the expansion the cylinder charge consists of fully burned gases and the total mass is constant. [20]

$$\dot{m} = 0$$

$$\dot{T}_b = \left(\frac{B}{A}\right)_b \left[-\frac{\dot{V}}{V} + \frac{-\dot{Q}_{wb}}{(Bm)_b}\right]$$

Exhaust Process:

The process starts when the Exhaust valve opens and the burned gases are then pushed from the engine cylinder. [20]

$$\dot{m} = -\dot{m}_e$$

$$\dot{T} = \frac{B}{A}\left[-\frac{\dot{m}_e}{m}\left(1 - \frac{h}{B}\right) - \frac{\dot{V}}{V} + \frac{1}{Bm}\left(-\dot{m}_e h_e - \dot{Q}_w\right)\right]$$

3.1.2 Sub Models

Solving the governing equation for each process requires: [21]

- The initial conditions at the start of compression, at intake valve closing (IVC); the pressure at IVC, the fresh mass of air and fuel (and EGR if applicable), the residual gas fraction and the equivalence ratio. The trapped conditions can result from calculation of the intake stroke (gas dynamics).

- The cylinder volume as a function of crank angle and the rate of change of cylinder volume. These are functions of the engine geometry: bore, stroke, connecting rod length and compression ratio.
- Gas properties (C_p, C_v, R and h) of the unburned and burned gases as a function of Temperature using JANAF tables.
- Heat transfer between the cylinder walls and the gases has to be modelled. Several empirical correlations have been developed for the calculation of the instantaneous heat transfer coefficient. The formula developed by Woschini has been used here.
- Burn mass fraction calculation using Wiebe function.

Gas Exchange:

In thermodynamic models the sole interest in simulating the intake and exhaust processes is to determine the instantaneous mass flow rates through the intake and exhaust valves in order to calculate the trapped mass of gases within the combustion chamber. [18]

The mass flows through the valves can be approximated by a steady flow through an adiabatic nozzle. The flows can either be subsonic or sonic.

The subsonic flow rates are given by:

$$\dot{m} = A_t p_u \sqrt{\frac{2}{RT_u}\left(\frac{p_t}{p_u}\right)^{2/\gamma} \frac{\gamma}{(\gamma-1)}\left[1-\left(\frac{p_t}{p_u}\right)^{(\gamma-1)/\gamma}\right]}$$

where, A_t is the actual open flow area, p_u is the upstream pressure, R is the specific gas constant, T_u is the upstream gas temperature, p_t is the throat (or downstream) pressure, and γ is the ratio of specific heats.

The sonic or choked flow rates are given by:

$$\dot{m} = A_t p_u \sqrt{\frac{\gamma}{RT_u}\left(\frac{2}{\gamma+1}\right)^{(\gamma+1)/(\gamma-1)}}$$

The actual open flow area (A_t) is based on a "curtain" area definition at the valve opening,

$$A_t = C_D \pi D_v L(\theta)$$

where,

- D_v is the valve diameter,
- $L(\theta)$ is the instantaneous valve lift.

Since the valve lift profiles are not necessarily known, a standard assumption has been used for the valve lift based on the maximum lift and the valve open duration, and using a sinusoidal shape.

$$L(\theta) = L_{max} \sin\left(\pi \frac{\theta - \theta_{vo}}{\theta_{dur}}\right)$$

The formulation used in the cycle simulation includes the capability for "reverse" flows. Thus allowing to calculate the residual mass fraction in the cylinder.

Kinematics:

The key geometrical items of a conventional reciprocating engine is shown in the figure. Bore and stroke are denoted as "*B*" and "*S*." The piston travels between "top

dead center" (TDC) and "bottom dead center" (BDC). The volume above the TDC position is the clearance volume (V_c), the volume between BDC and TDC is the displaced volume (V_d), and the sum of V_c and V_d is the total cylinder volume (V_{tot}). [18]

The cylinder volume at any crank angle is given by,

$$V = V_c + \frac{\pi B^2}{4}(\ell + a - s)$$

From the triangular relationship, an expression for "s" (which is the distance from the crank center to the end of the connecting rod and is a function of crank angle) is given by,

$$s = a\cos\theta + (\ell^2 - a^2\sin^2\theta)^{1/2}$$

Rate of change of cylinder volume is given by,

$$\dot{V} = \frac{\pi B^2}{4} a\sin\theta\left[1 + \frac{a\cos\theta}{\left(\ell^2 - a^2\sin^2\theta\right)^{1/2}}\right]$$

The compression ratio can be calculated as,

$$CR = \frac{V_{tot}}{V_c} = \frac{V_c + V_d}{V_c} = 1 - \frac{V_d}{V_c}$$

The crank radius "a", is related to the stroke as, S = 2a. The connecting rod length is given by the symbol "l".

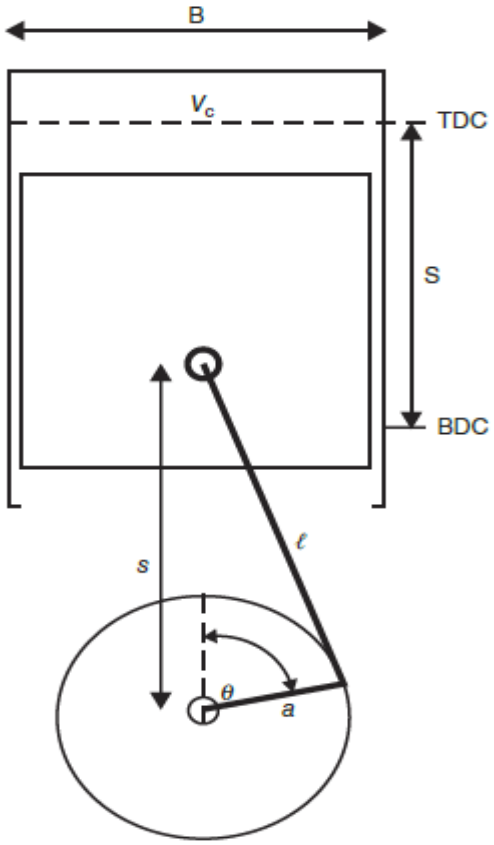

Figure 20 ENGINE CYLINDER GEOMETRY [18]

Gas Properties:

The thermodynamic properties needed for solving the first law relations include the internal energy, enthalpy, gas constant, molecular mass, and a number of property derivatives. These properties are needed as functions of time (crank angle) for the cylinder contents and for any material entering the cylinder. [18]

Depending on the specific processes during a cycle, the thermodynamic properties may be for mixtures of air, fuel vapour, and combustion products. The concentrations of the combustion products may be "frozen" for the lower temperatures, or these concentrations may be based on an instantaneous

determination of chemical equilibrium for higher temperatures. In general, the determination of the equilibrium composition of the products is somewhat complex and one of the computationally intensive aspects of cycle simulations.

- Unburned Mixture Composition:

  The unburned mixture during the compression stroke prior to combustion consists of the inlet mixture of air and fuel, and the residual cylinder contents of combustion products from the preceding cycle.

  The determination of the species in the burned gas fraction is a major part of determining the unburned mixture properties. For a simple hydrocarbon fuel (CHy), the reaction may be represented (for *one mole of O2 reactant*) as

$$\varepsilon\phi C + 2(1-\varepsilon)\phi H_2 + O_2 + \psi N_2 \rightarrow$$
$$n_{CO_2} CO_2 + n_{H_2O} H_2O + n_{CO} CO + n_{H_2} H_2 + n_{O_2} O_2 + n_{N_2} N_2$$

  Where, ψ is the molar N/O ratio (= 3.7732 for pure air), y is the molar H/C ratio of the fuel, Φ is the fuel–air equivalence ratio, "n_i" is the moles of species "i" per mole of O2 reactant, and ε = 4 / (4 + y).

  n_i for the different species in the unburned mixture composition are calculated from,

For $\phi \le 1.0$ (stoichiometric and lean):	For $\phi > 1.0$ (rich):
$n_{fuel} = 4(1-x_b)(1+2\varepsilon)\phi / M_f$ $n_{CO_2} = x_b \varepsilon \phi$ $n_{H_2O} = 2x_b(1-\varepsilon)\phi$ $n_{CO} = 0$ $n_{H_2} = 0$ $n_{O_2} = 1-x_b\phi$ $n_{N_2} = \psi$	$n_{fuel} = 4(1-x_b)(1+2\varepsilon)\phi / M_f$ $n_{CO_2} = x_b(\varepsilon\phi - c)$ $n_{H_2O} = x_b[2(1-\varepsilon\phi)+c]$ $n_{CO} = x_b c$ $n_{H_2} = x_b[2(\phi-1)-c]$ $n_{O_2} = 1-x_b$ $n_{N_2} = \psi$
$n_u = (1-x_b)\left[\frac{4(1+2\varepsilon)\phi}{M_f} + 1 + \psi\right] + x_b n_b$	

Table 5 UNBURNED MIXTURE COMPOSITION [18]

The values in the table can be converted to mole fractions. For example, for oxygen,

$$y_{O2} = \text{mole fraction} = \frac{n_{O2}}{n_{tot}}$$

For oxygen containing fuels, we represent the fuel molecule as (CH_yO_z) and the balanced equation is,

$$\varsigma\,\varepsilon\phi C + 2\varsigma\,(1-\varepsilon)\phi H_2 + O_2 + \left(1-\frac{\varepsilon z}{2}\right)\varsigma\,\psi N_2 \rightarrow n_{CO_2}CO_2 + n_{H_2O}H_2O + n_{CO}CO + n_{H_2}H_2 + n_{O_2}O_2 + n_{N_2}N_2$$

Where,

$$\varsigma = \frac{2}{2-\varepsilon z(1-\phi)}$$

$$y = \frac{C}{H}$$
$$z = \frac{C}{O}$$
$$\varepsilon = \frac{4}{4+y}$$

As a result, we see have to change the following definitions as,

$$\phi^* = \varsigma\phi$$
$$\psi^* = \left(1-\frac{\varepsilon z}{2}\right)$$

The reactant reaction now becomes,

$$\phi^*\varepsilon C + 2\phi^*(1-\varepsilon)H_2 + O_2 + \psi^* N_2$$

Which is similar to the reactant expression for simple hydrocarbon and therefore we can use the same table to calculate the mixture composition mole fraction values.

- Burned Mixture Composition:

  For determining the frozen composition of the burned mixture, six major product species are considered. The general combustion equation for a fuel molecule of the form CHy with standard air for these six product species is,

$$\varepsilon\phi C + 2(1-\varepsilon)\phi H_2 + O_2 + \psi N_2 \rightarrow$$
$$n_{CO_2}CO_2 + n_{H_2O}H_2O + n_{CO}CO + n_{H_2}H_2 + n_{O_2}O_2 + n_{N_2}N_2$$

Where, ψ is the molar N/O ratio (= 3.7732 for pure air), y is the molar H/C ratio of the fuel, Φ is the fuel–air equivalence ratio, n_i is the moles of species i per mole of O2 reactant, and $\varepsilon = 4 / (4 + y)$.

The next step is to determine the composition (i.e., values for the n_i). The following assumptions are used:

1. For lean and stoichiometric mixtures, n_{CO} and n_{H2} are assumed zero.
2. For rich and stoichiometric mixtures, n_{O2} is assumed zero.
3. For rich mixtures, the "water gas" reaction is assumed to be sufficiently accurate to determine the n_{CO} and n_{H2}.

The "water gas" reaction is,

$$CO_2 + H_2 \rightarrow CO + H_2O$$

Typically the reaction is assumed to be in equilibrium, defined as,

$$K(T) = \frac{n_{H_2O}\, n_{CO}}{n_{CO_2}\, n_{H_2}}$$

The equilibrium constant K(T) equation is a curve fit of JANAF table data,

$$\ln K(T) = 2.743 - \frac{1.761}{t} - \frac{1.611}{t^2} - \frac{0.2803}{t^3} \quad \left(t = \frac{T}{1000}\right)$$

n_i for the burned mixture composition can be calculated from the table below,

For $\phi \leq 1.0$ (Stoichiometric and lean):	For $\phi > 1.0$ (rich):
(moles of species *i per mole of* O_2 *reactant*)	
$n_{CO_2} = \varepsilon\phi$	$n_{CO_2} = \varepsilon\phi - c$
$n_{H_2O} = 2(1-\varepsilon)\phi$	$n_{H_2O} = 2(1-\varepsilon\phi) + c$
$n_{CO} = 0$	$n_{CO} = c$
$n_{H_2} = 0$	$n_{H_2} = 2(\phi - 1) - c$
$n_{O_2} = 1 - \phi$	$n_{O_2} = 0$
$n_{N_2} = \psi$	$n_{N_2} = \psi$
$n_b = (1-\varepsilon)\phi + 1 + \psi$	$n_b = (2-\varepsilon)\phi + \psi$

Table 6 BURNED MIXTURE COMPOSITION [18]

The value of "c" in the expressions in above shown table is found from the solution of the quadratic equation from the water-gas reaction,

$$(K-1)c^2 - \{K[2(\phi-1)+\varepsilon\phi]+2(1-\varepsilon\phi)\}c + 2K\varepsilon\phi(\phi-1) = 0$$

"c" can be found as,

$$c = \frac{-b \pm \sqrt{b^2 - 4ad}}{2a}$$

where

$$a = K - 1$$

$$b = -\left(K\left(2(\phi-1)+\varepsilon\phi\right)+2(1-\varepsilon\phi)\right)$$

$$d = 2K\varepsilon\phi(\phi-1)$$

Cylinder Heat Transfer:

The overall convective heat transfer to the cylinder gases is given by,

$$\dot{Q}_w = h_c A(\theta)(T_{wall} - T)$$

Where, h_c is the instantaneous convective heat transfer coefficient, A(θ) is the instantaneous surface area, T_{wall} is the cylinder wall temperature, and T is the instantaneous gas temperature.

Instantaneous heat transfer coefficient (h_c) is given by Woschini correlation:

$$h_c = 3.26B^{-0.2}P^{0.8}T^{-0.55}v^{0.8}$$

Where,

$$v = C_1 c_m + C_2 \frac{V_d T_1}{p_1 V_1}\left(p - p_{mot}\right),$$

During the combustion process, the heat transfer is allocated to the various zones (but the total is still given by the above equation). The heat transfer is assumed to be proportional to the surface area of each zone. The appropriate surface area is assumed to be proportional to the volume raised to the 2/3 power. In addition, the heat transfer is proportional to the temperature difference. [18]

$$\dot{Q}_u = \left(\frac{V_u}{V_{total}}\right)^{2/3}\left(\frac{T_{wall} - T_u}{T_{wall} - T}\right)\dot{Q}_{total}$$

$$\dot{Q}_b = \dot{Q}_{total} - \dot{Q}_u$$

Mass Fraction Burned using Wiebe function:

The purpose of the function is to reproduce the typical S-shaped profile of the integrated heat release rate of SI engines. [18]

$$x_b(\theta) = 1 - \exp\left[-a\left(\frac{\theta - \theta_s}{\theta_d}\right)^n\right]$$

$$n = m+1$$

Where, the constant "*m*" defines the shape of the integrated heat release curve and "*a*" is derived from the perception that only a certain fraction of the injected fuel has been burned at the end of combustion. Values used here are a = 5.0 and m = 2.0, θ_d is the burn duration, θ_s is the start of combustion and θ is the current crank angle.

3.1.3 Simulation and Results

The model created requires some inputs to simulate the initial combustion chamber conditions from there the simulation progresses through three complete cycles.

The simulation starts at -180 CAD (BDC) at the end of Intake stroke, for the first cycle we assume that the pressure and temperature values are ambient. Then as the simulation progresses to the second cycle we have an idea of what the value of pressure and temperature would be at the end of Intake stroke based on the conditions provided.

ITEM	VALUE (a)	VALUE (b)	VALUE (c)	VALUE (d)
Displaced Volume [litre]	2	2	2	2

Number of Cylinders	4	4	4	4
Bore to Stroke ratio	1.2	1.2	1.2	1.2
Con rod to Crank rad ratio	3.3	3.3	3.3	3.3
Compression Ratio	8	10	10	10
Engine speed [RPM]	4000	4000	3000	3000
Equivalence ratio	0.9	0.9	0.9	0.9
Engine Load	0.9	0.9	0.9	0.7
Spark Advance	33	33	30	30
Fuel Used	Iso-Octane	Iso-Octane	Iso-Octane	Iso-Octane

Table 7 ENGINE SPECIFICATIONS

For the Wiebe combustion, we use the values as recommended by Heywood [15]: m = 2.0 and a = 5.0. The combustion duration was 60°CA. For the cylinder heat transfer, the correlation recommended by Woschni has been used.

Presentation of Results:

ITEM	**VALUE (a)**	**VALUE (b)**	**VALUE (c)**	**VALUE (d)**

Indicated Thermal Efficiency [%]	26.98	30.33	29.898	26.76
Indicated Power [kW]	9.78	11.01	8.00	5.42
IMEP [kPa]	586.7	660	640	433.8

Table 8 RESULTS

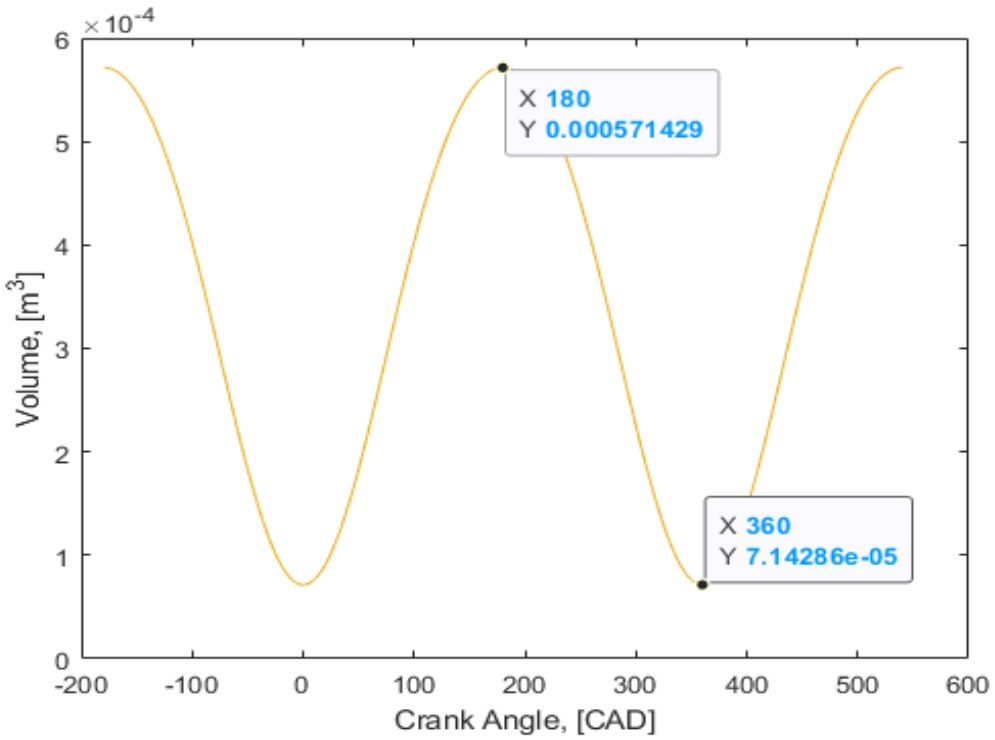

[Compression Ratio = 8]

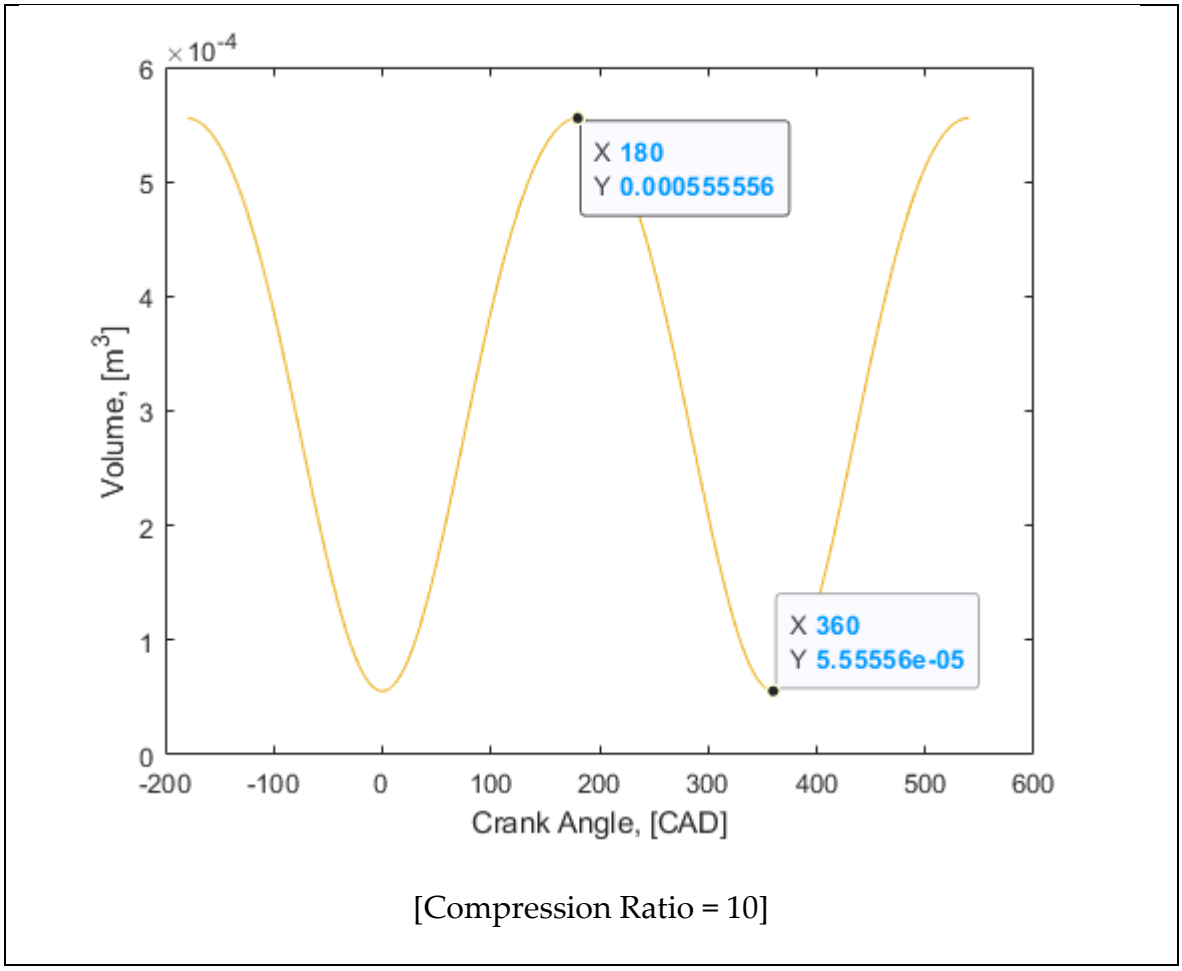

Figure 21 INSTANTANEOUS CYLINDER VOLUME AS A FUNCTION OF CRANK ANGLE

Figure 19 shows Instantaneous cylinder volume as a function of crank angle for one cylinder of the different engine specifications (specifically, Compression Ratio). The minimum and maximum volumes are the clearance and total volumes, respectively.

The cycle starts from BDC (-180 CAD) and ends after completing two revolutions at BDC (540 CAD) i.e. end of Intake Stroke.

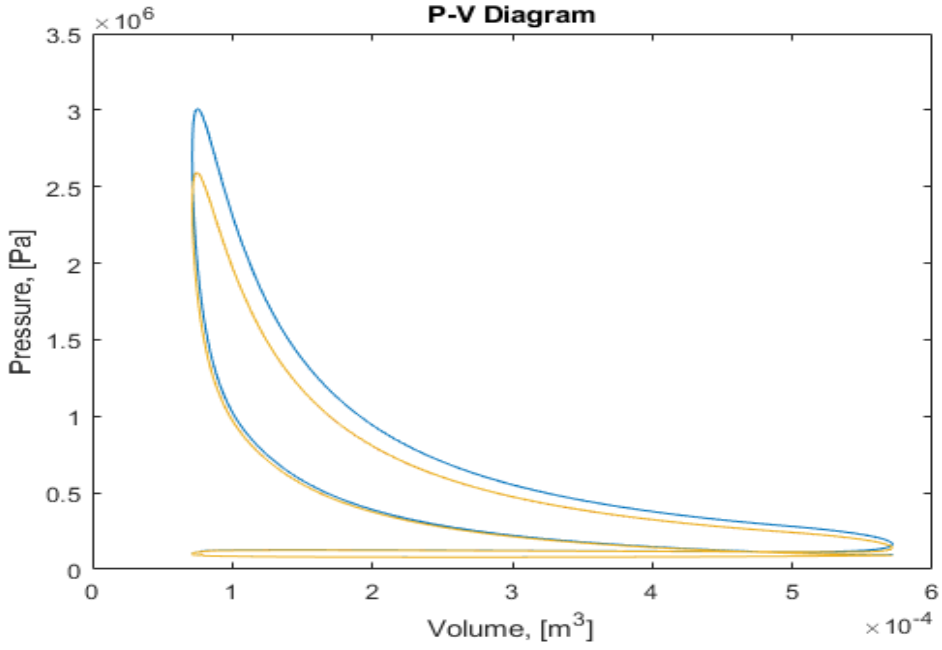
P-V Diagram
×10^6
3.5
3
2.5
2
1.5
1
0.5
0
Pressure, [Pa]
0
1
2
3
4
5
6
Volume, [m^3]
×10^-4

(a)

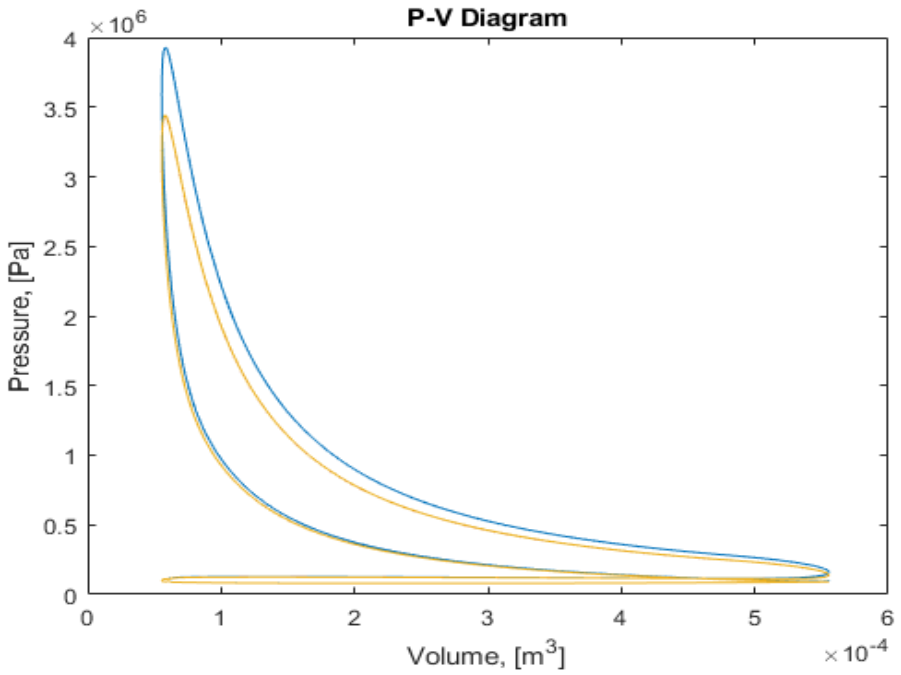
P-V Diagram
×10^6
4
3.5
3
2.5
2
1.5
1
0.5
0
Pressure, [Pa]
0
1
2
3
4
5
6
Volume, [m^3]
×10^-4

(b)

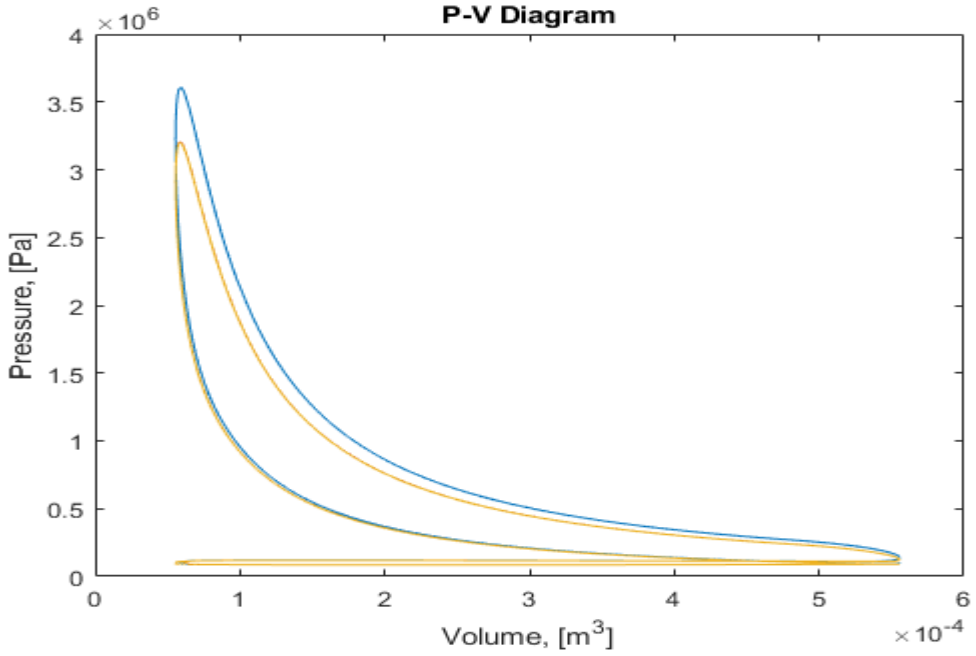

(c)

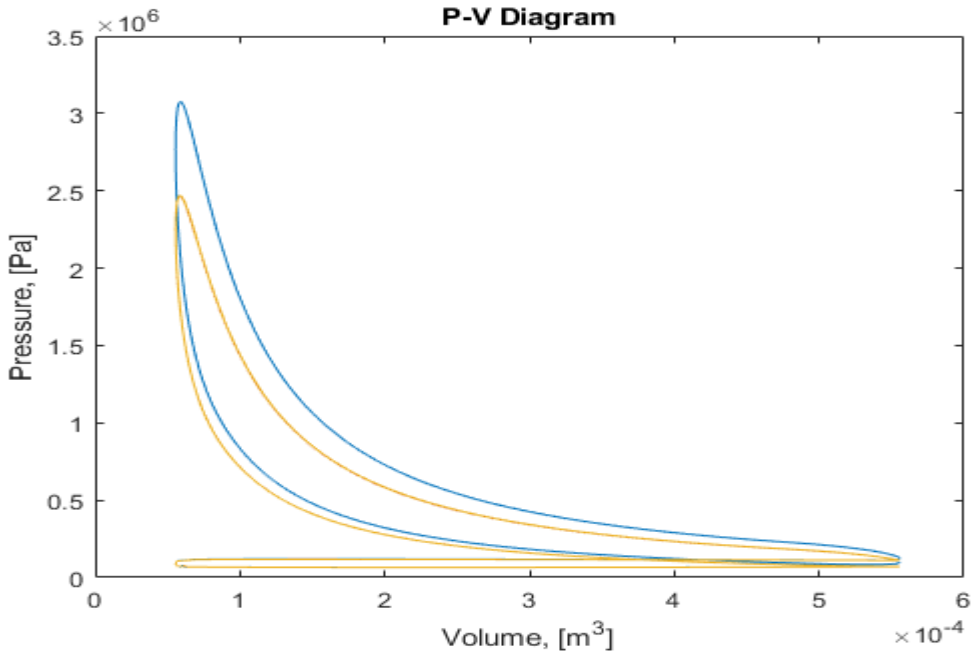

(d)

Figure 22 CYLINDER PRESSURE AS THE FUNCTION OF CYLINDER VOLUME

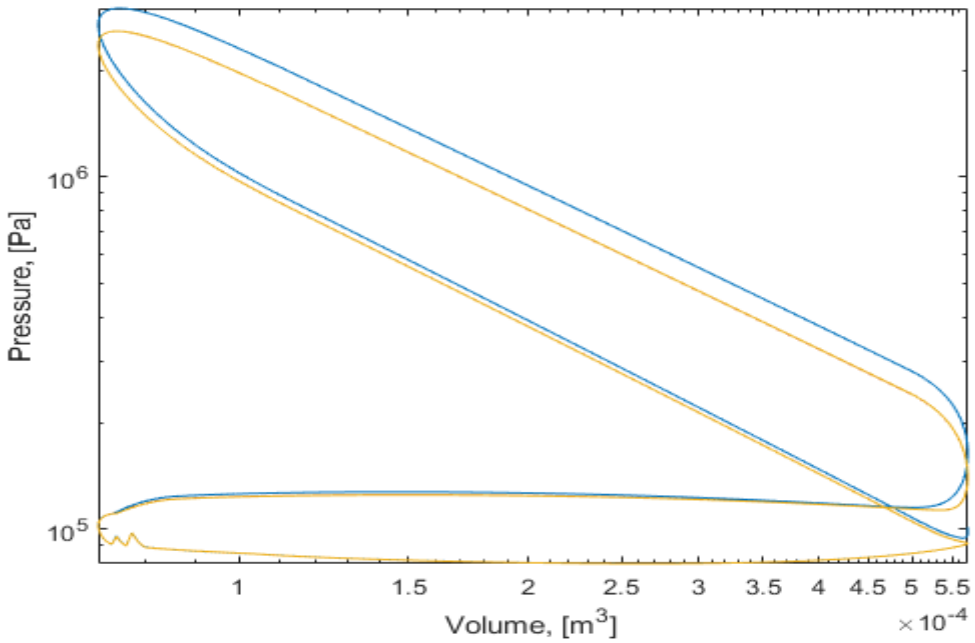
Pressure, [Pa]
10^6
10^5
1
1.5
2
2.5
3
3.5
4
4.5
5
5.5
Volume, [m^3]
$\times 10^{-4}$

(a)

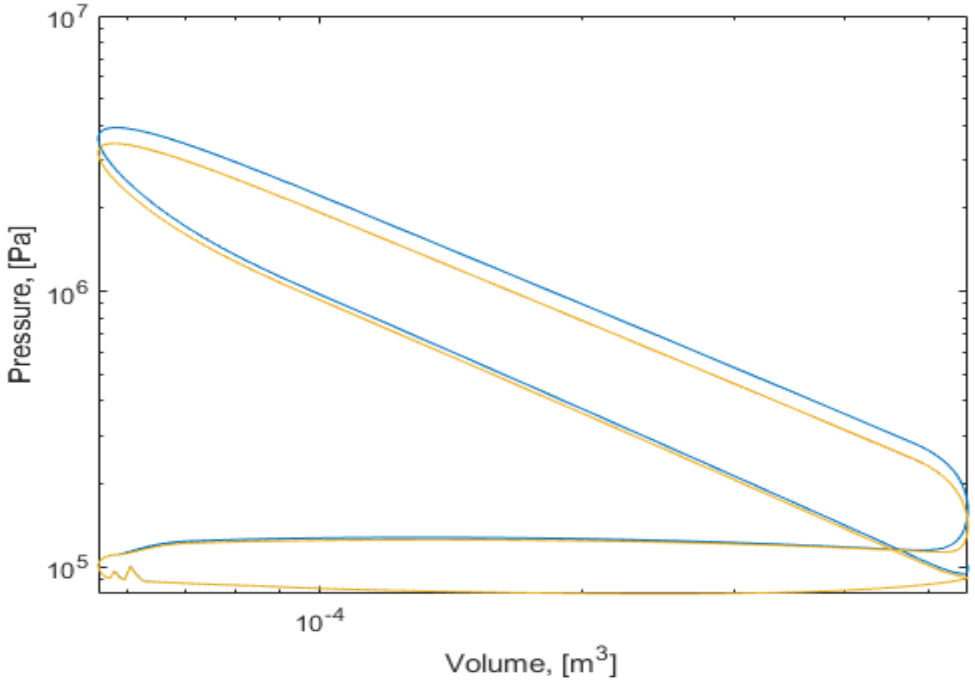
Pressure, [Pa]
10^7
10^6
10^5
10^{-4}
Volume, [m^3]

(b)

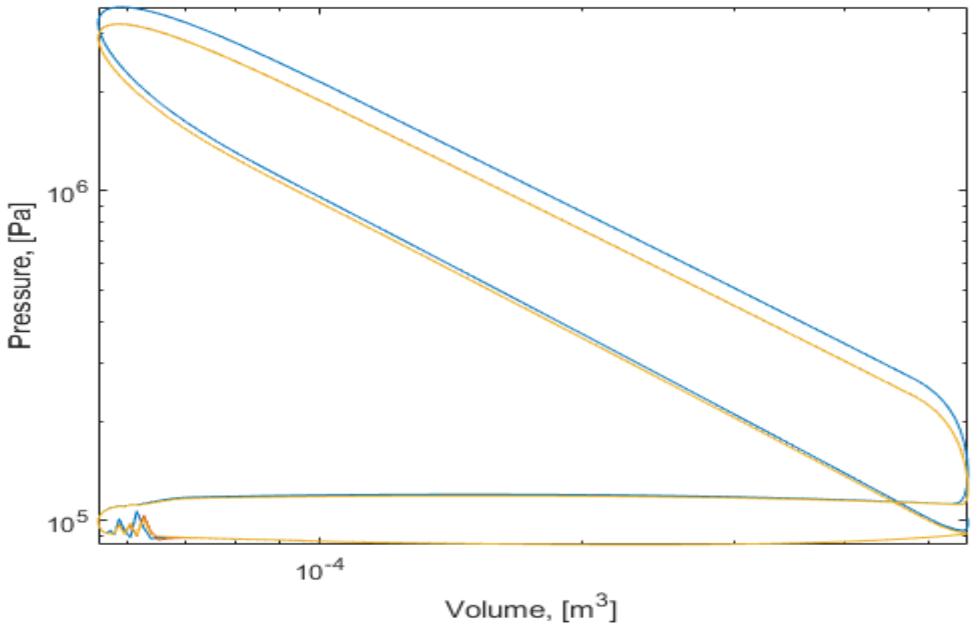

(c)

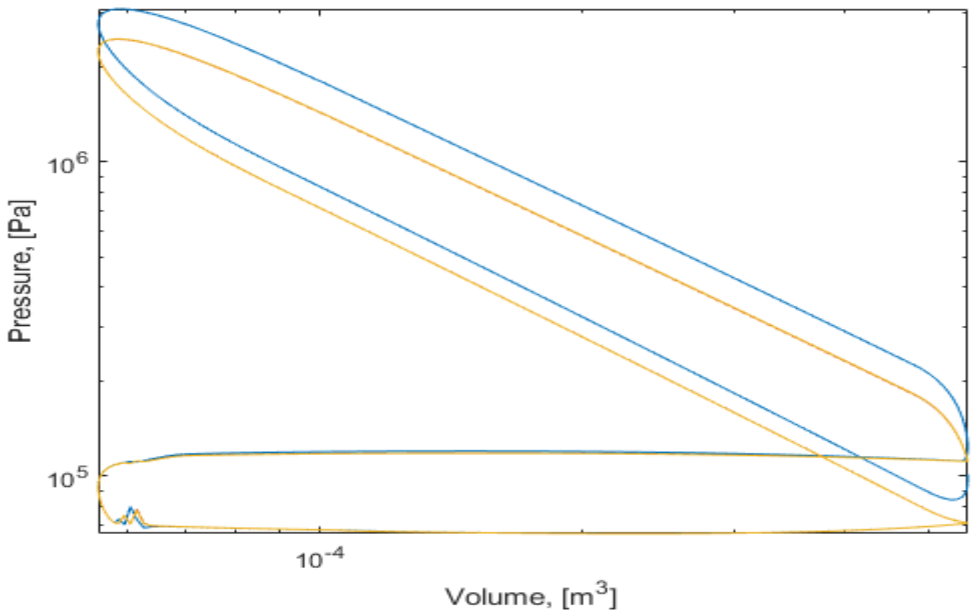

(d)

Figure 23 LOGLOG PLOTS OF CYLINDER PRESSURE AS A FUNCTION OF CYLINDER VOLUME

Figure 20 shows the Cylinder Pressure as the function of Cylinder Volume for the different combustion chamber simulation conditions. We can see from the difference in 20a and 20b, that for different compression ratios, while keeping the other values same, we have higher peak cylinder pressure and thermal efficiency (from Table 8) for the condition with higher compression ratio.

From 20c and 20d we see that the effect of Engine load on the peak cylinder pressure and thermal efficiency. The residual gas fraction increases as can be seen in Figure 25, which causes a reduction of fresh mixture inducted (Figure 24) and therefore less energy is released. We see the effect on all the parameters, Pressure (Figure 22), Temperature (Figure 23) and the specific enthalpy of the mixture inducted (Figure 28).

The Figure 21 shows the variation of cylinder pressure as a function of cylinder volume on a logrithmic scale. The log plot shows the "Pumping loop" in more detail. The nearly linear part of the loglog plot characterizes the polytropic process for compression and expansion, as in [18].

The plots shown in Figures 19-29 and even for the six-stroke engine simulation, all show three curves, the complete cycle (all four strokes) was run three times in the simulation to check for convergence. The plot of first cycle for which ambient conditions were assumed, is in Blue colour and as the simulation progresses through the second (plot in Orange) and third cycle (plot in Yellow), based on the conditions provided in Table 7, we can see the results converge.

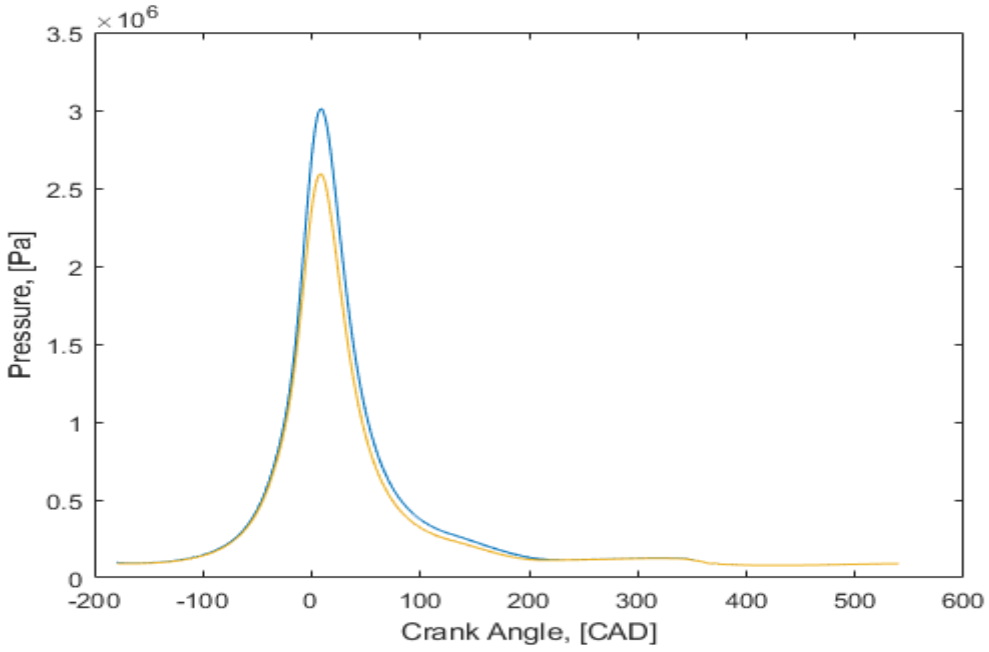
×10^6
3.5
3
2.5
2
1.5
1
0.5
0
Pressure, [Pa]
-200
-100
0
100
200
300
400
500
600
Crank Angle, [CAD]

(a)

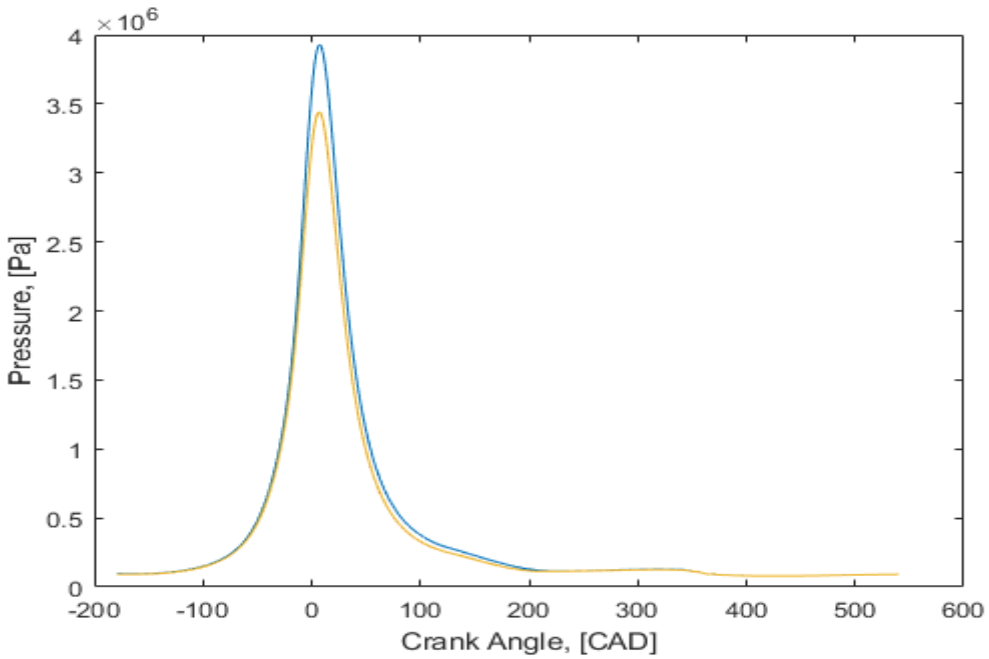
×10^6
4
3.5
3
2.5
2
1.5
1
0.5
0
Pressure, [Pa]
-200
-100
0
100
200
300
400
500
600
Crank Angle, [CAD]

(b)

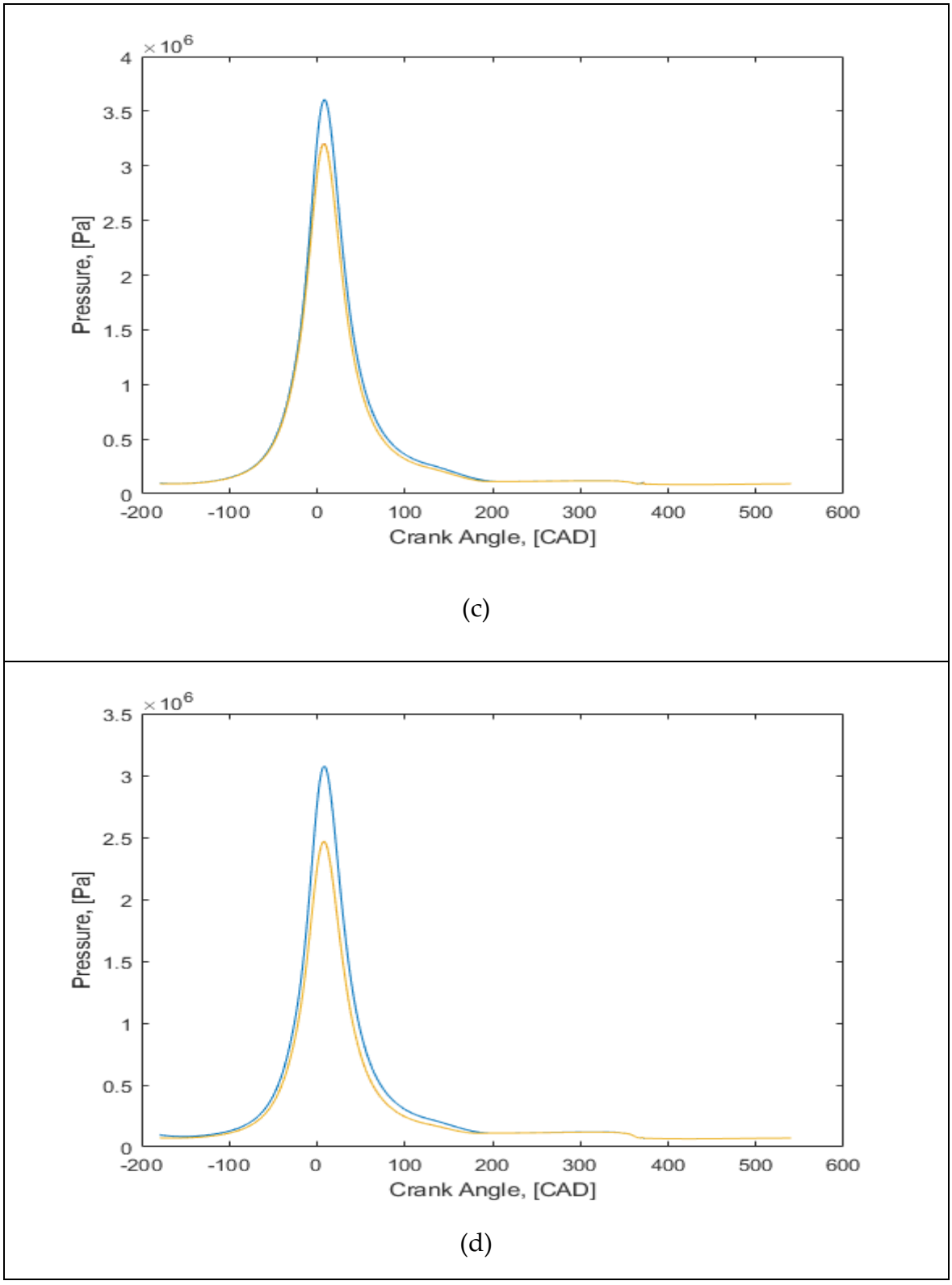

Figure 24 CYLINDER PRESSURE AS FUNCTION OF CRANK ANGLE

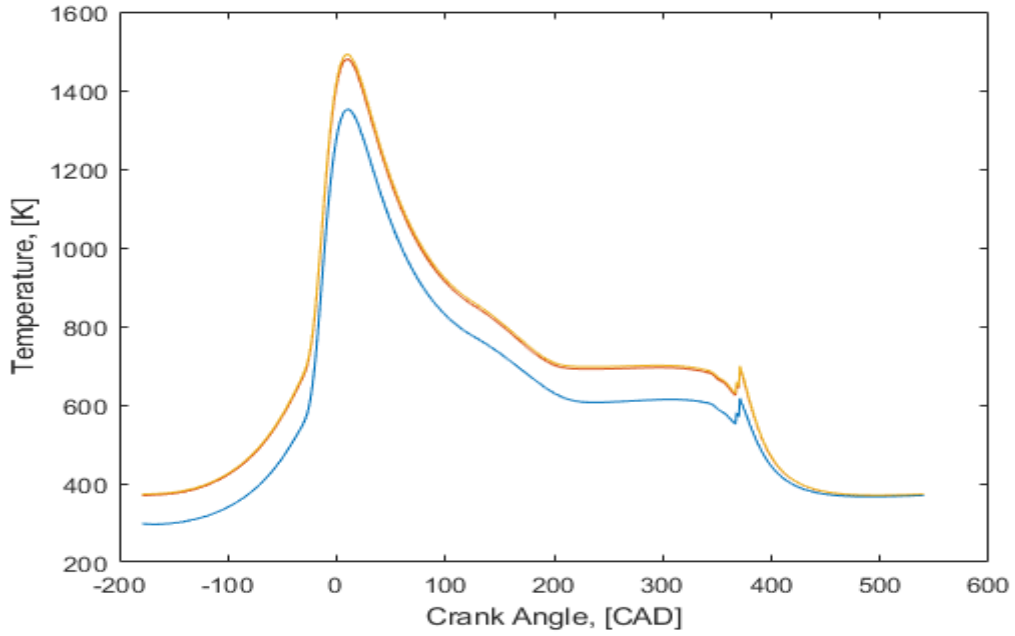
Temperature, [K]
Crank Angle, [CAD]
1600
1400
1200
1000
800
600
400
200
-200
-100
0
100
200
300
400
500
600

(a)

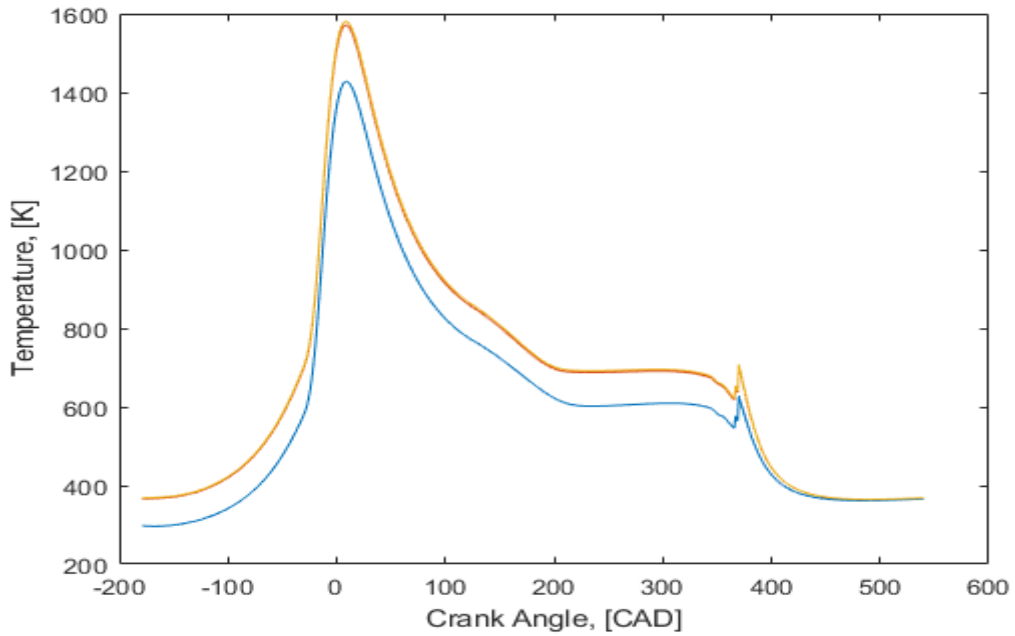
Temperature, [K]
Crank Angle, [CAD]
1600
1400
1200
1000
800
600
400
200
-200
-100
0
100
200
300
400
500
600

(b)

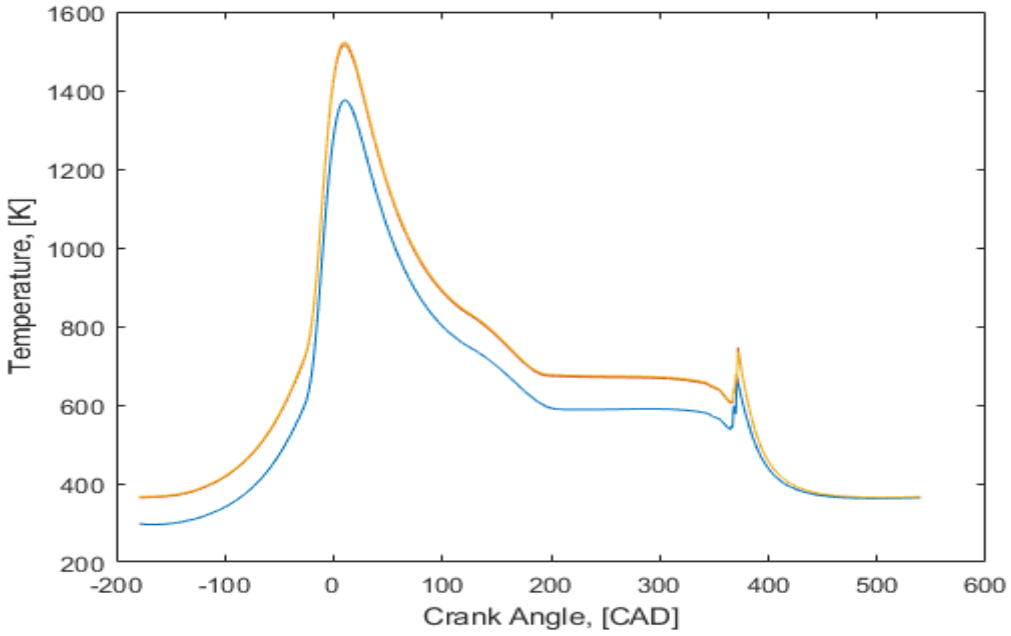

(c)

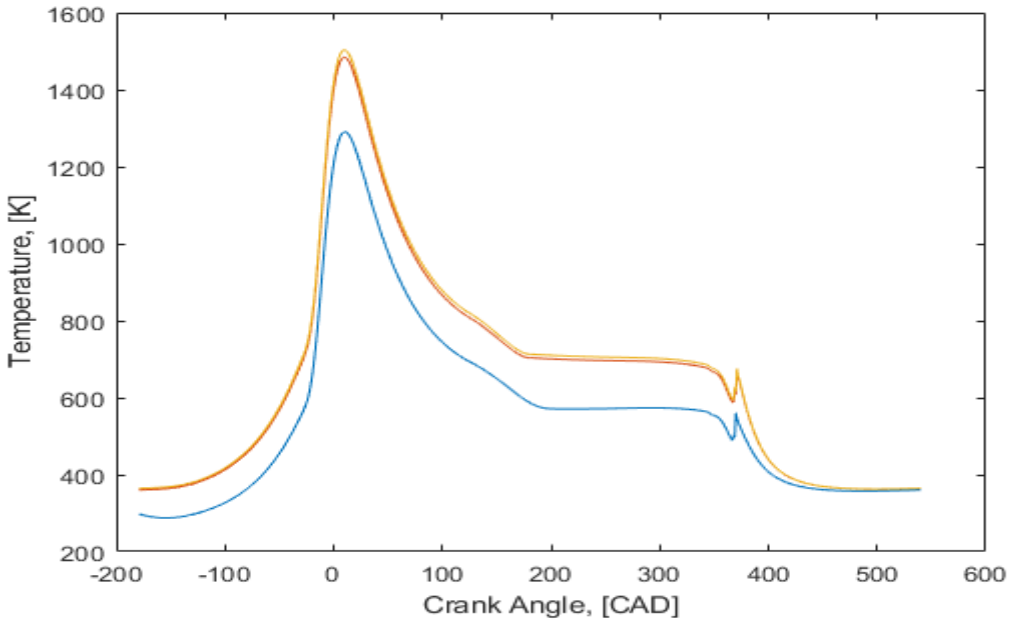

(d)

Figure 25 CYLINDER TEMPERATURE AS FUNCTION OF CRANK ANGLE

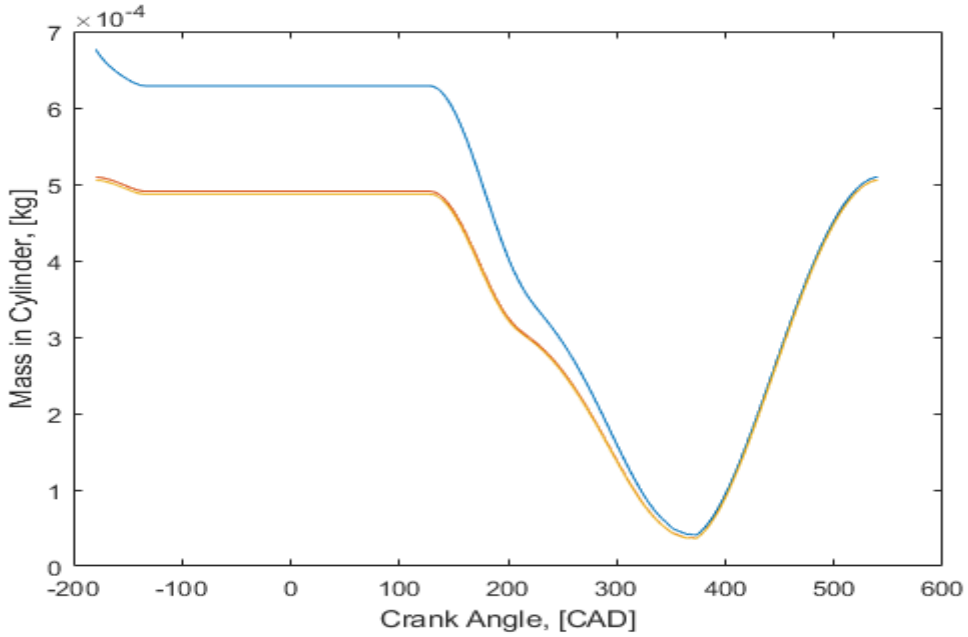
×10^-4
7
6
5
4
3
2
1
0
Mass in Cylinder, [kg]
-200
-100
0
100
200
300
400
500
600
Crank Angle, [CAD]

(a)

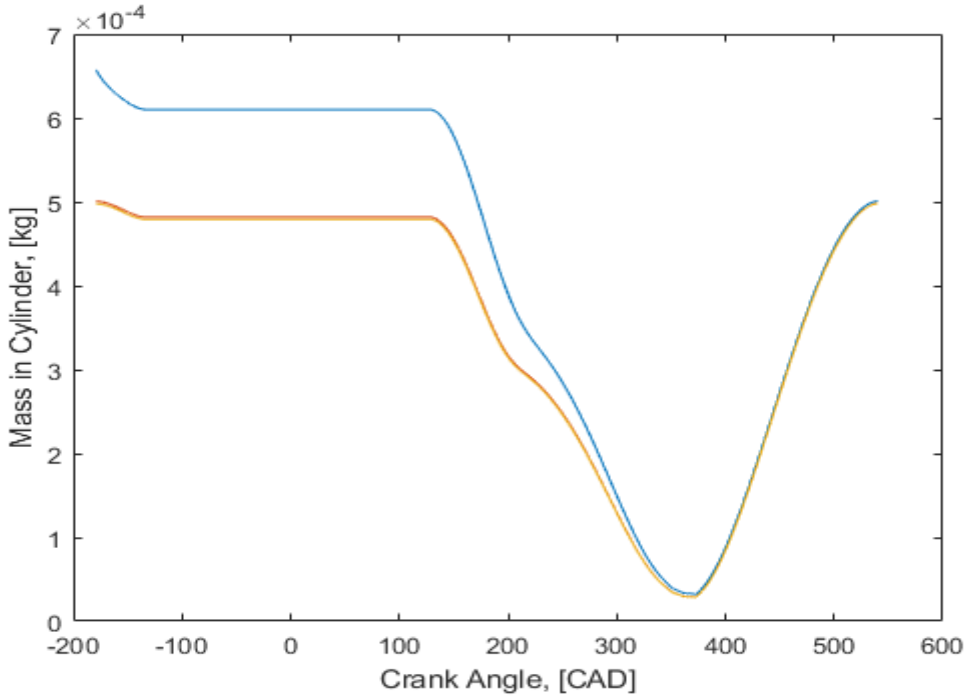
×10^-4
7
6
5
4
3
2
1
0
Mass in Cylinder, [kg]
-200
-100
0
100
200
300
400
500
600
Crank Angle, [CAD]

(b)

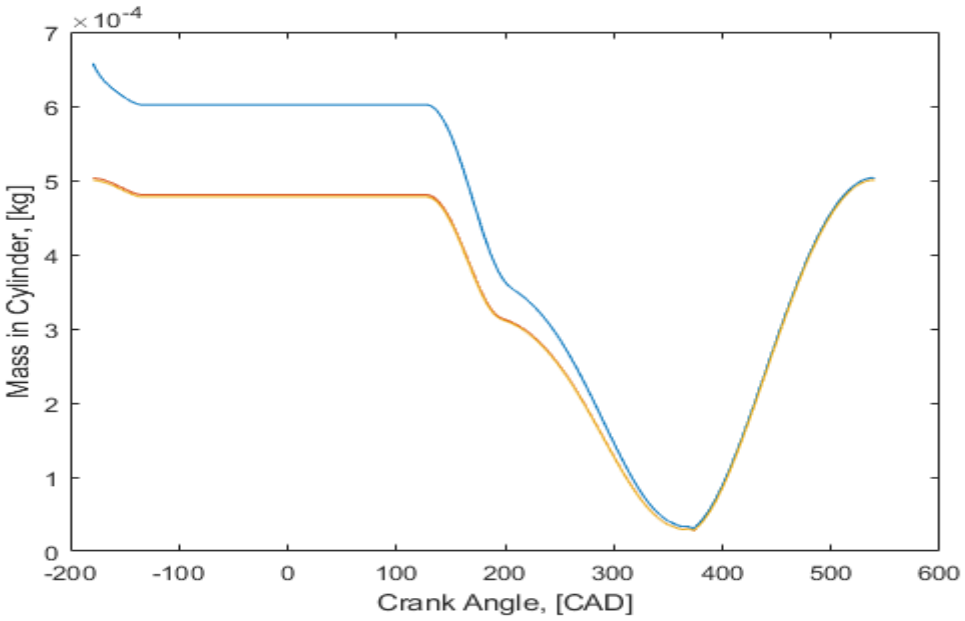

(c)

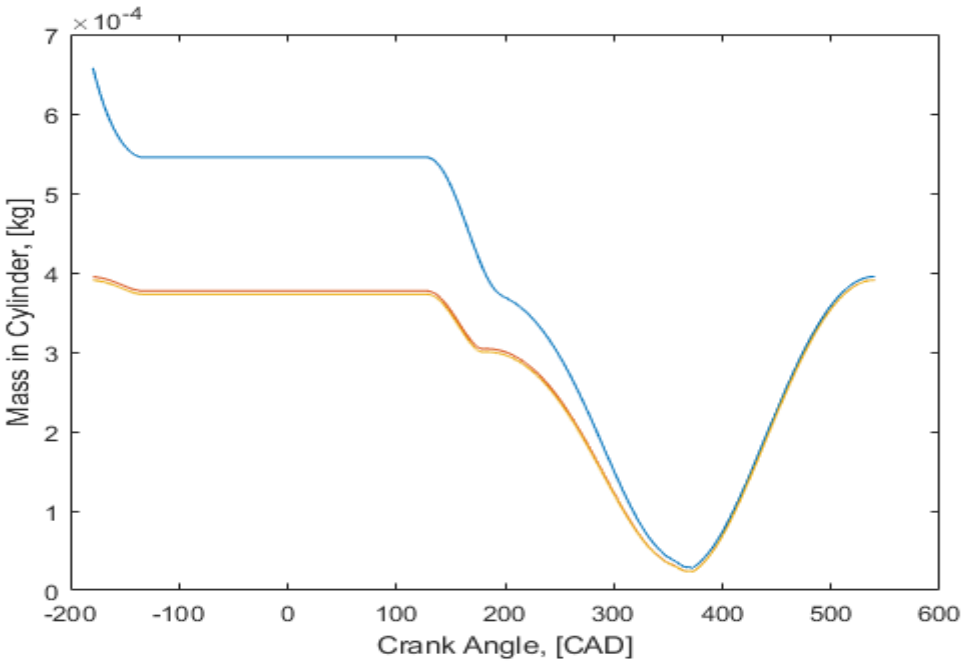

(d)

Figure 26 CYLINDER MASS AS FUNCTION OF CRANK ANGLE

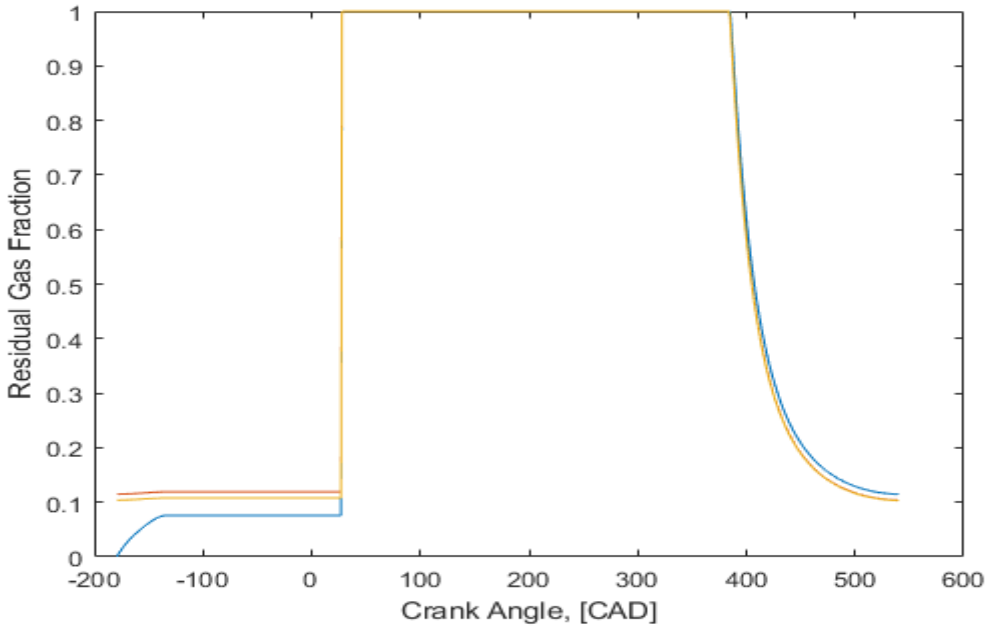
Residual Gas Fraction
Crank Angle, [CAD]
1
0.9
0.8
0.7
0.6
0.5
0.4
0.3
0.2
0.1
0
-200
-100
0
100
200
300
400
500
600

(a)

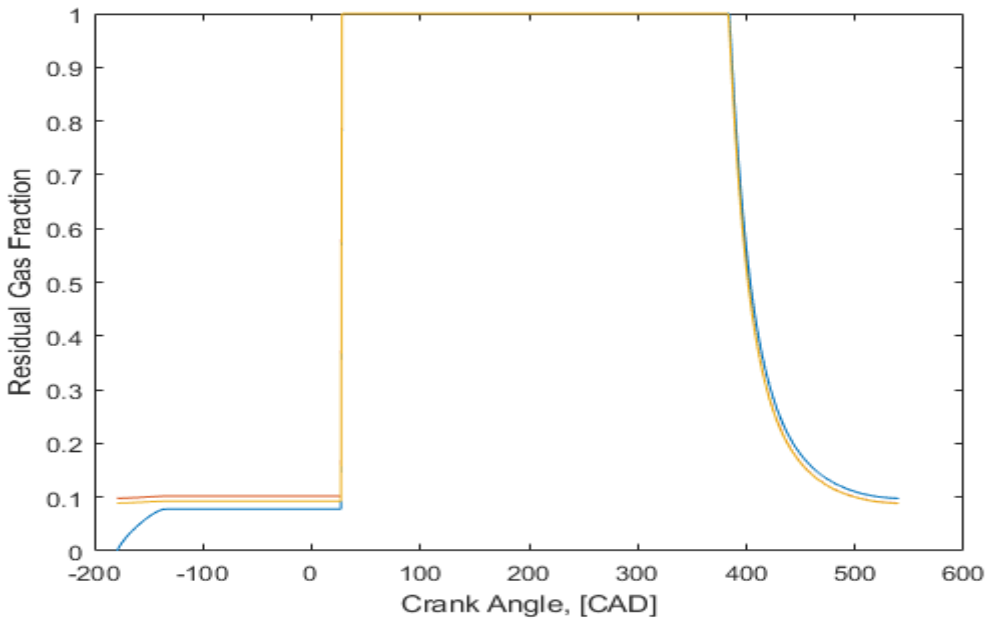
Residual Gas Fraction
Crank Angle, [CAD]
1
0.9
0.8
0.7
0.6
0.5
0.4
0.3
0.2
0.1
0
-200
-100
0
100
200
300
400
500
600

(b)

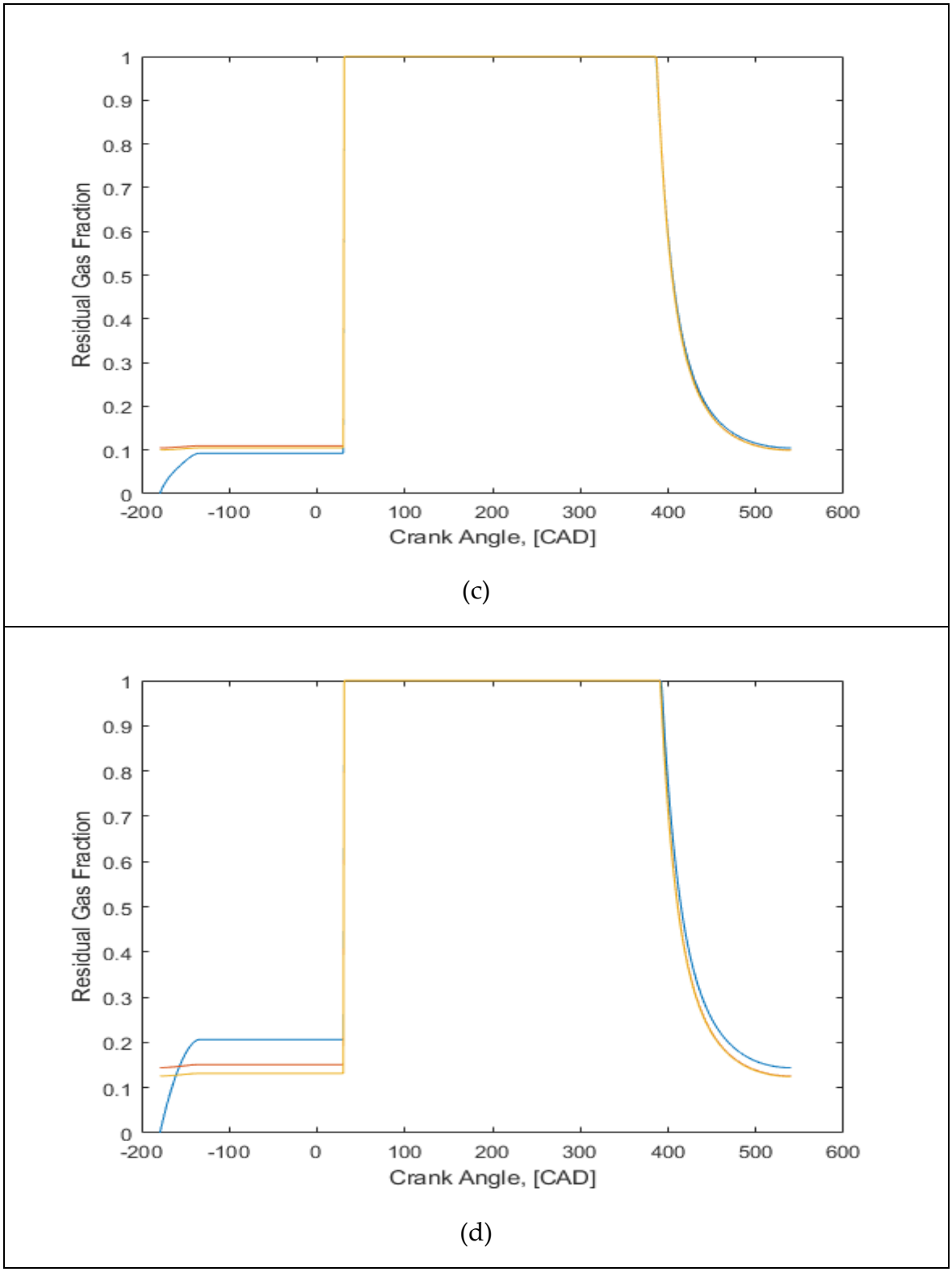

Figure 27 RESIDUAL GAS FRACTION AS FUNCTION OF CRANK ANGLE

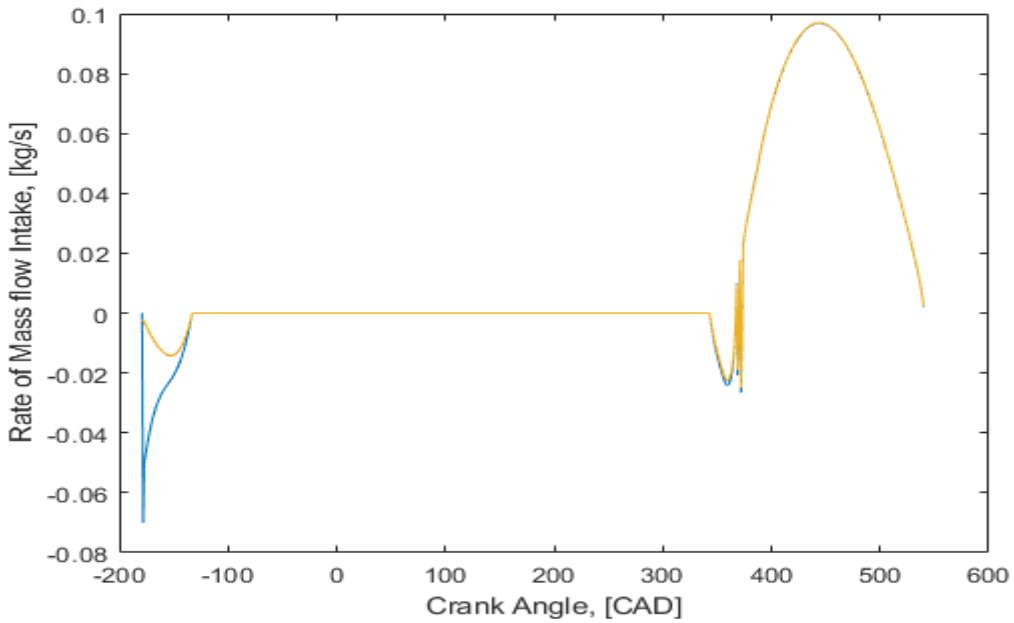
Rate of Mass flow Intake, [kg/s]
0.1
0.08
0.06
0.04
0.02
0
-0.02
-0.04
-0.06
-0.08
-200
-100
0
100
200
300
400
500
600
Crank Angle, [CAD]

(a)

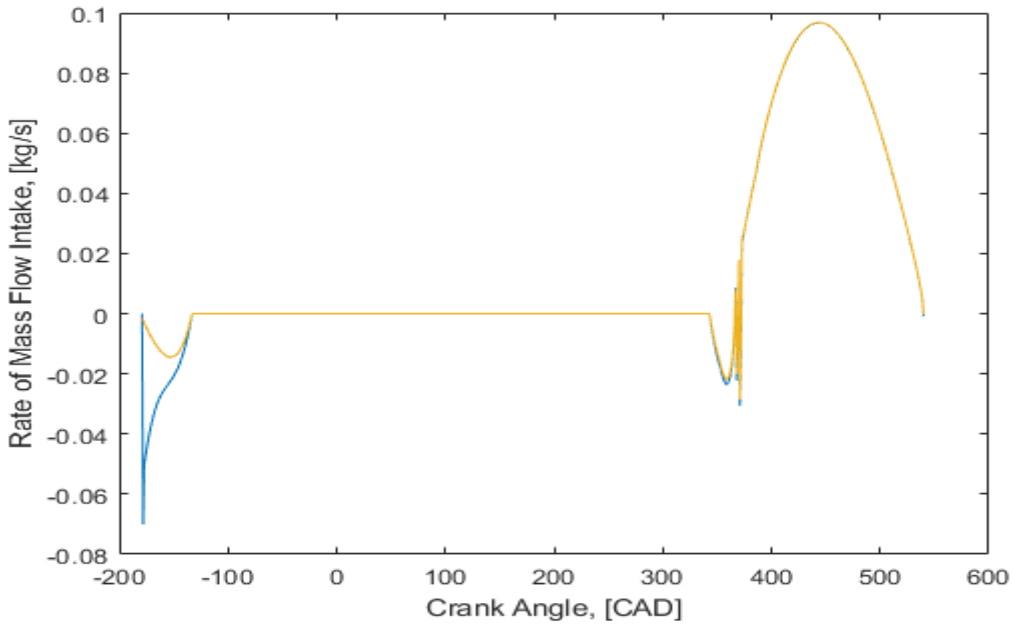
Rate of Mass Flow Intake, [kg/s]
0.1
0.08
0.06
0.04
0.02
0
-0.02
-0.04
-0.06
-0.08
-200
-100
0
100
200
300
400
500
600
Crank Angle, [CAD]

(b)

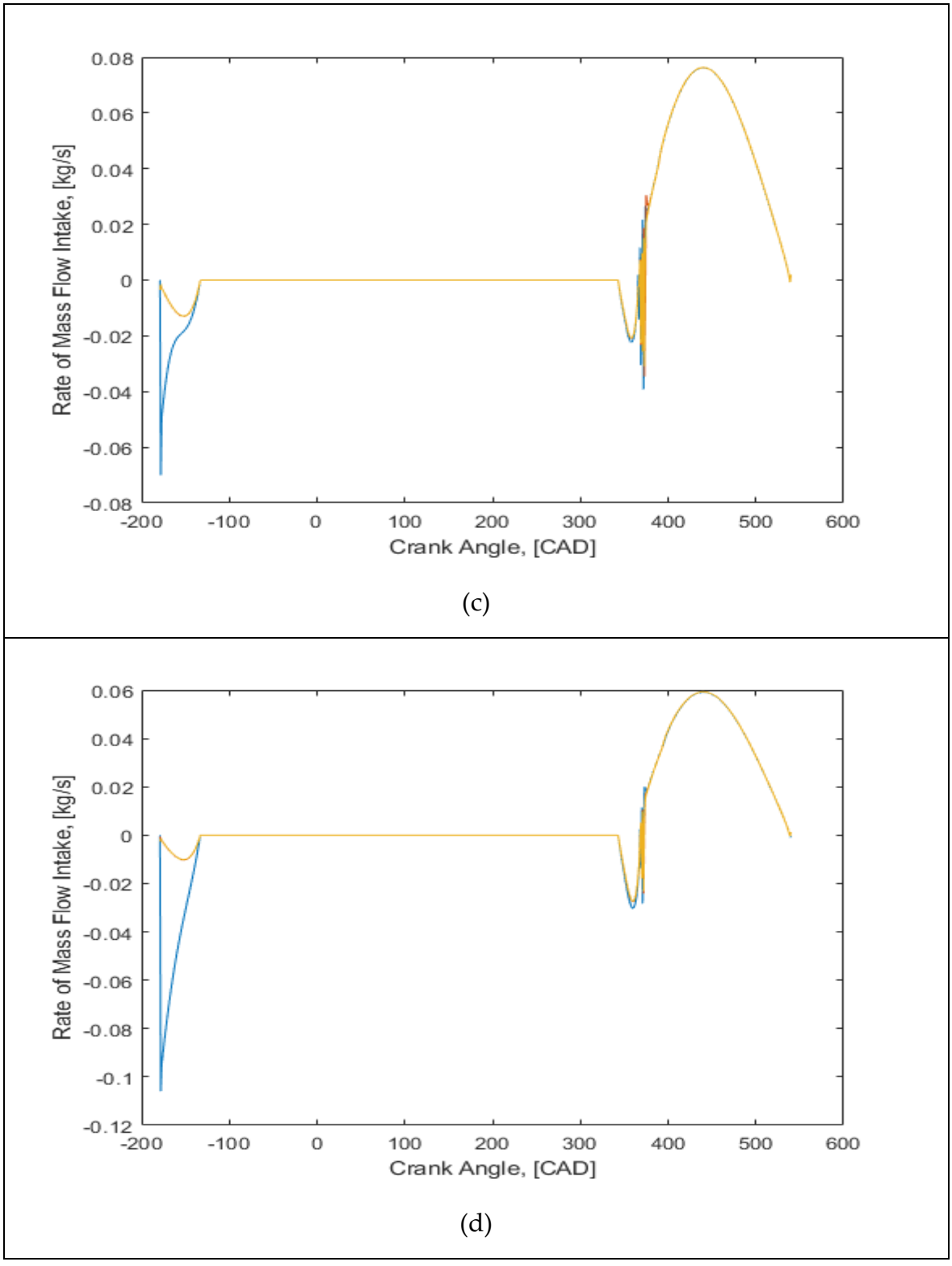

Figure 28 INTAKE MASS FLOW RATE AS FUNCTION OF CRANK ANGLE

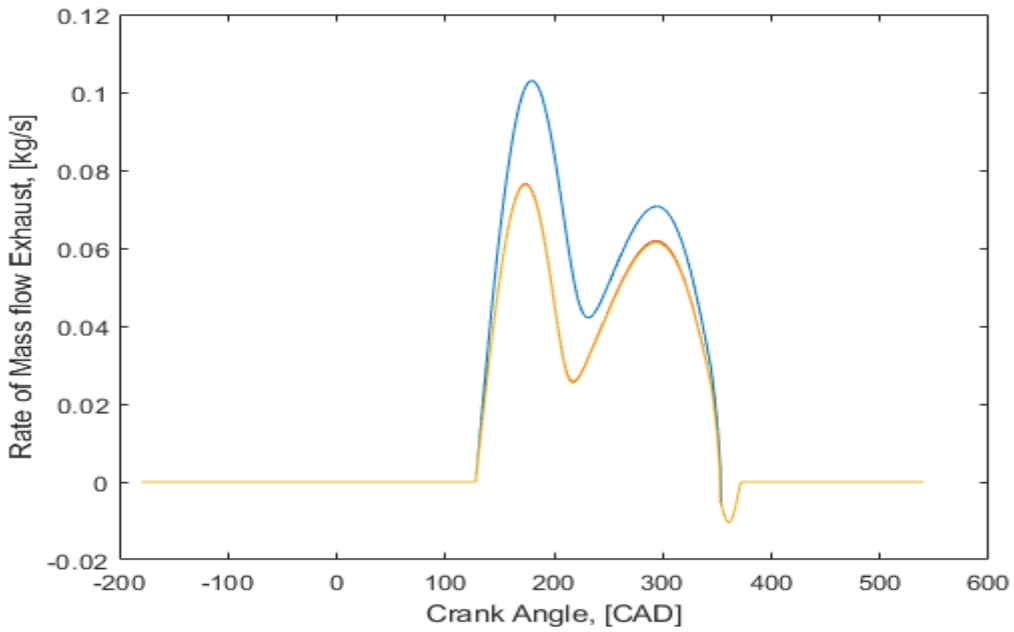
Rate of Mass flow Exhaust, [kg/s]
0.12
0.1
0.08
0.06
0.04
0.02
0
-0.02
-200
-100
0
100
200
300
400
500
600
Crank Angle, [CAD]

(a)

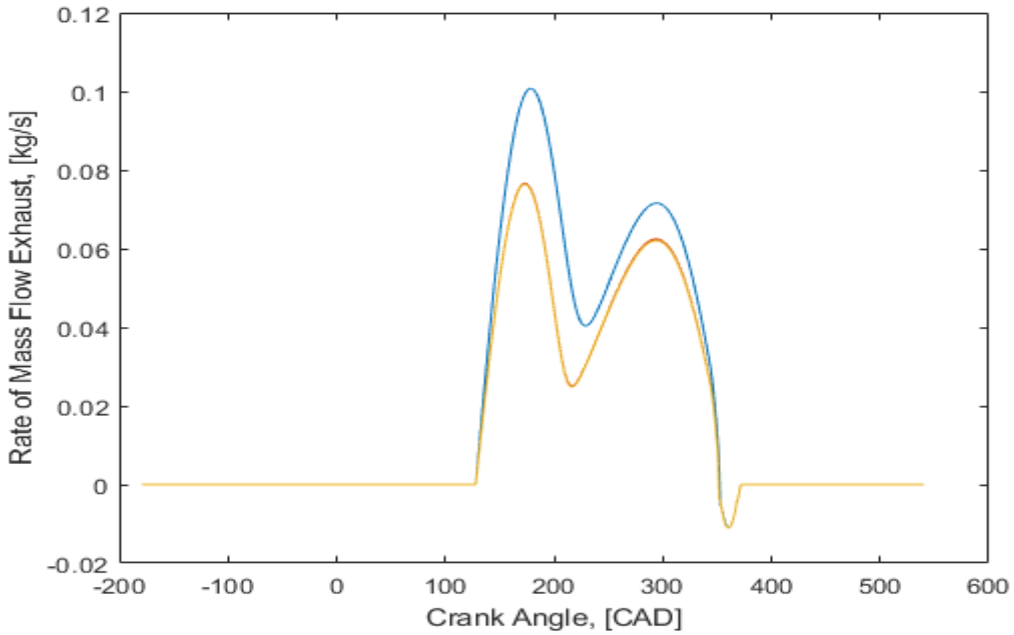
Rate of Mass Flow Exhaust, [kg/s]
0.12
0.1
0.08
0.06
0.04
0.02
0
-0.02
-200
-100
0
100
200
300
400
500
600
Crank Angle, [CAD]

(b)

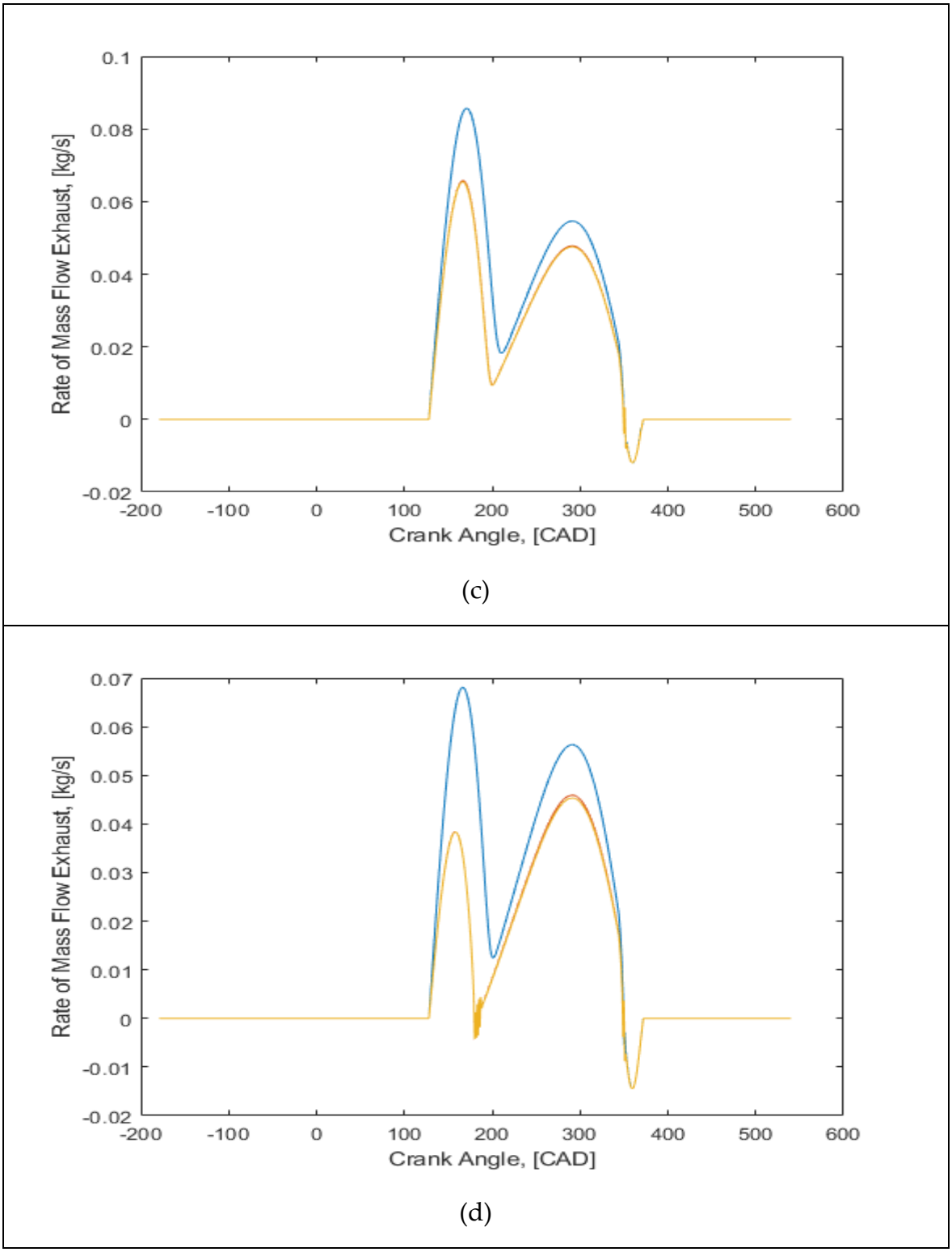

Figure 29 EXHAUST MASS FLOW RATE AS FUNCTION OF CRANK ANGLE

The positive flow rates are the flow rates in the natural directions, i.e. the intake flow is positive into the cylinder and the exhaust flow is positive out of the cylinder. The flow reverses into the cylinder for the exhaust valve flow, during the valve overlap period, the time between intake valve open and the exhaust valve close. [18]

When the intake valve first opens (IVO), the flow is into the intake manifold. The flow reverses shortly after the exhaust valve closes. The first mass into the cylinder is the mass that previously flowed into the intake manifold. Once that mass has returned, then the fresh air and fuel vapour mixture flows into the cylinder.

At the end of the intake valve open period, the flow reverses back into the manifold. The cylinder pressure is greater than the intake manifold pressure which causes the reverse flow.

Figures 26 and 27 show the mass flow rates during the intake and exhasut strokes, respectively. We can see from the figures the effect that various engine operating conditions have on gas exchange process, which then inturn affect the rest of the cycle.

Figure 28, show the specific enthalpy increase during compression which attains a maximum and then decrease during combustion and through expansion processes. After the reverse flow into the intake manifold, the fresh charge begins to enter the cylinder and the specific enthalpy begin to increase until they attain their original values at intake valve close. [18]

We can also see the effect of residual gas fraction on the specific enthalpy of the mixture in the combustion chamber at the end of intake stroke.

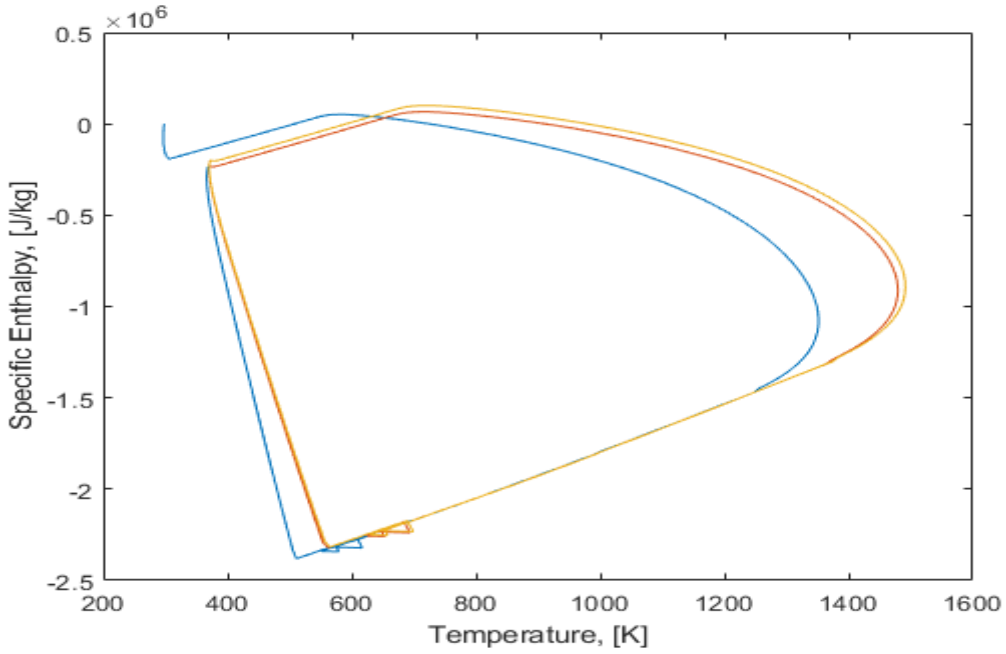
×10^6
0.5
0
-0.5
-1
-1.5
-2
-2.5
Specific Enthalpy, [J/kg]
200
400
600
800
1000
1200
1400
1600
Temperature, [K]

(a)

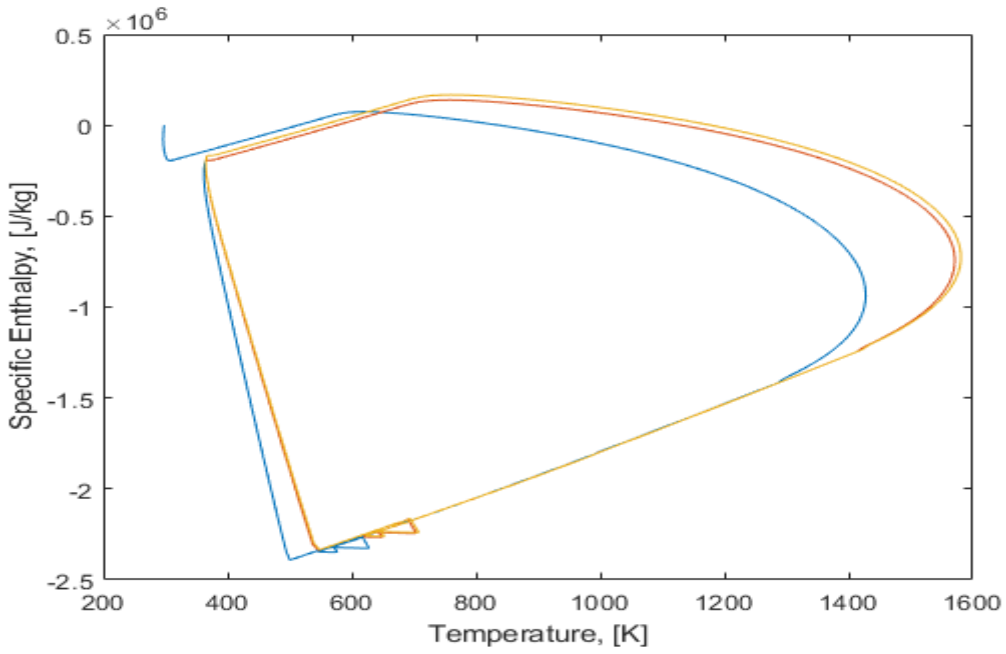
×10^6
0.5
0
-0.5
-1
-1.5
-2
-2.5
Specific Enthalpy, [J/kg]
200
400
600
800
1000
1200
1400
1600
Temperature, [K]

(b)

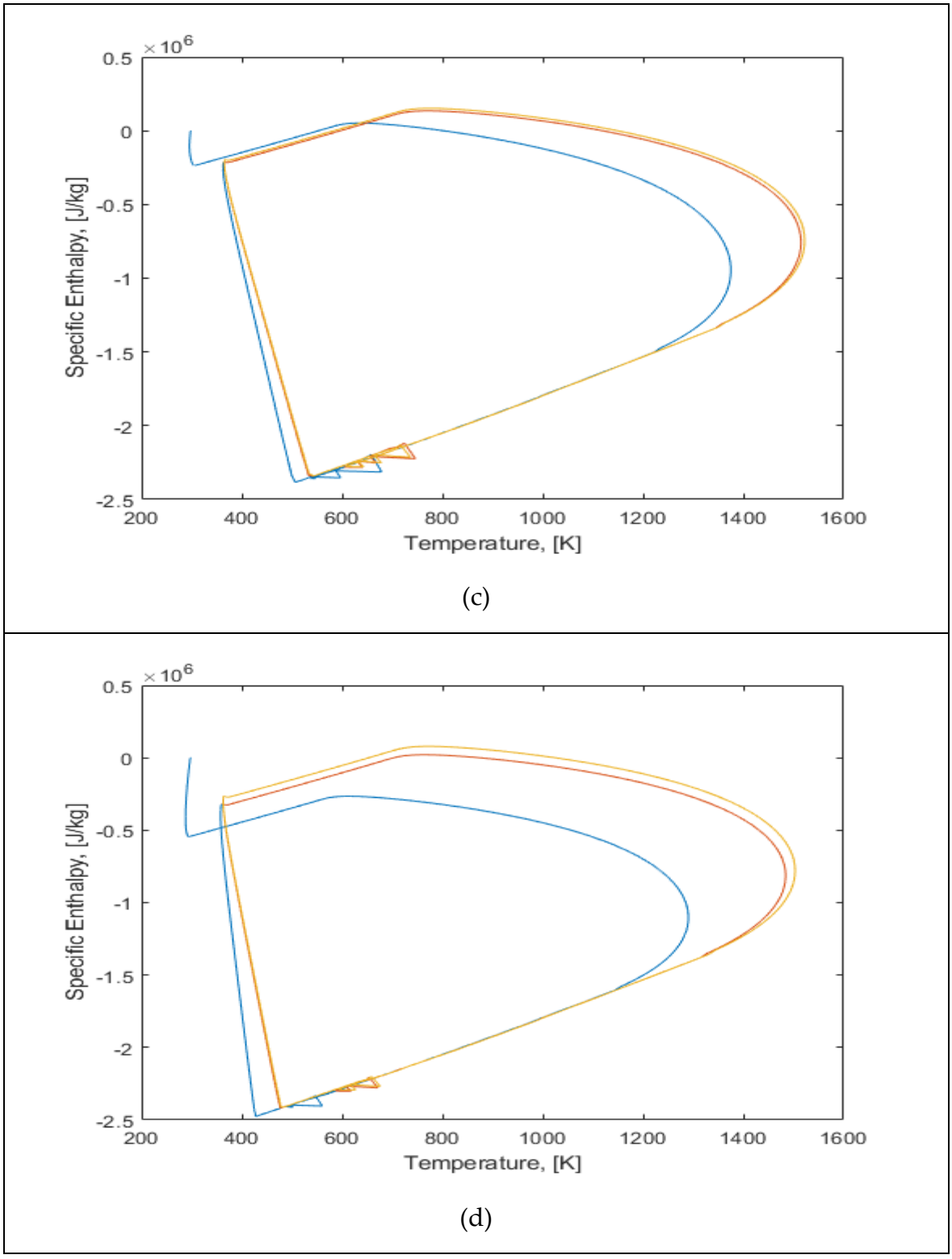

Figure 30 SPECIFIC ENTHALPY OF CYLINDER GASES AS A FUNCTION OF TEMPERATURE

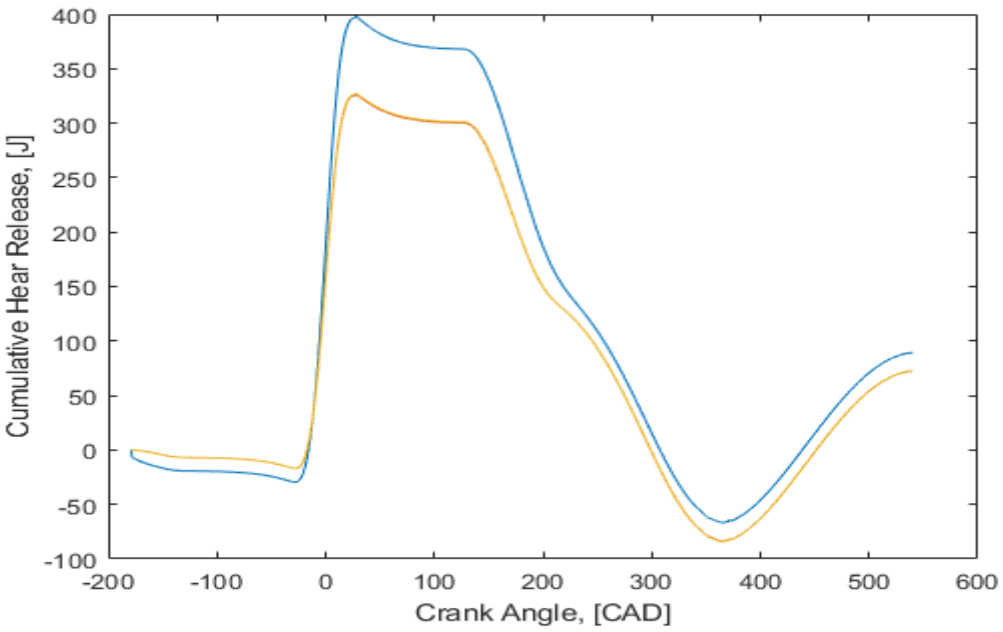
Cumulative Hear Release, [J]
400
350
300
250
200
150
100
50
0
-50
-100
-200
-100
0
100
200
300
400
500
600
Crank Angle, [CAD]

(a)

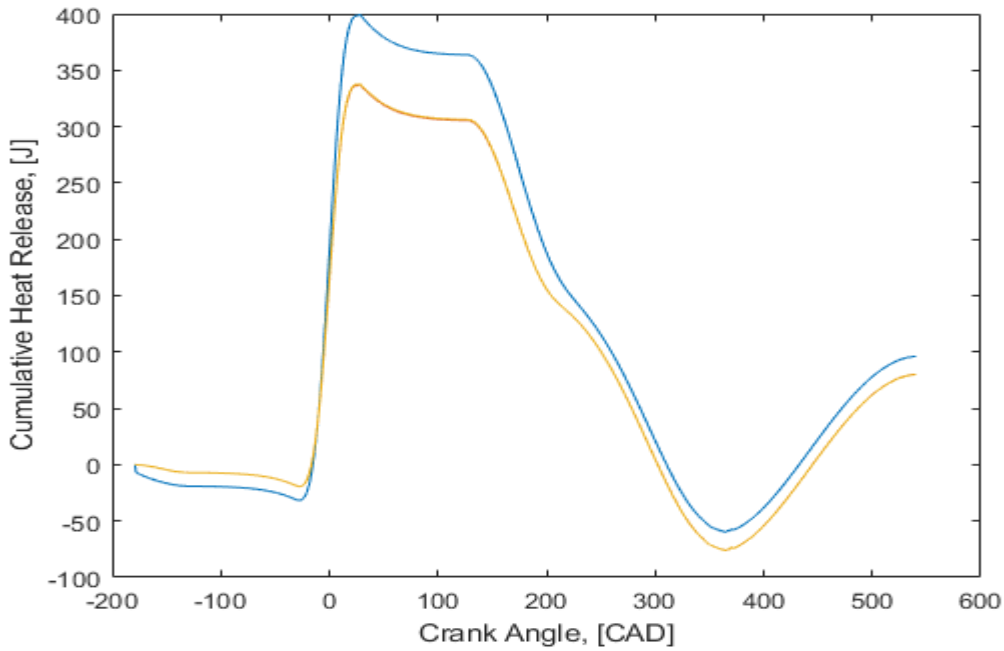
Cumulative Heat Release, [J]
400
350
300
250
200
150
100
50
0
-50
-100
-200
-100
0
100
200
300
400
500
600
Crank Angle, [CAD]

(b)

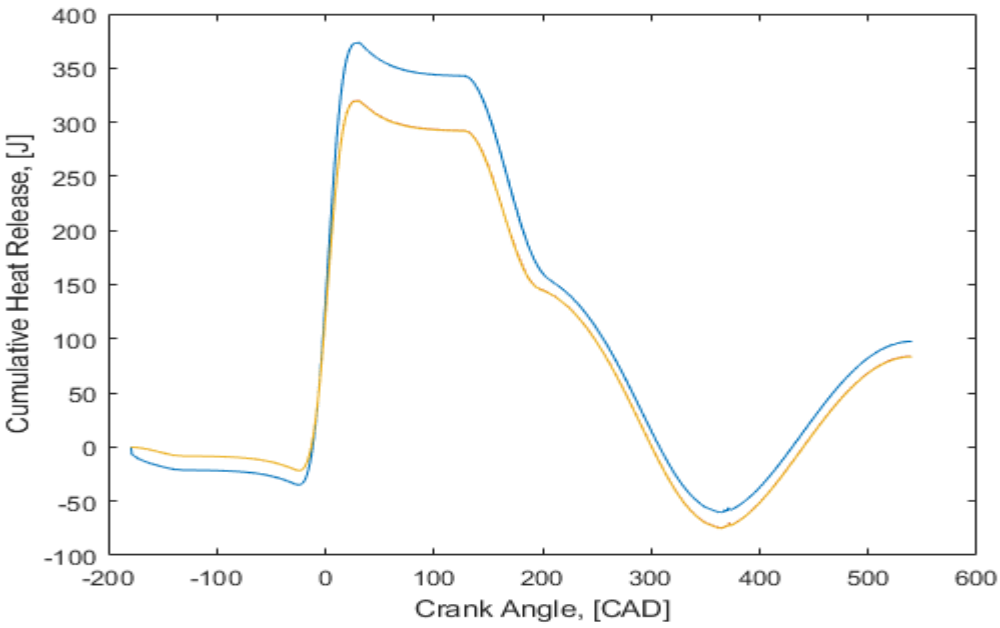

(c)

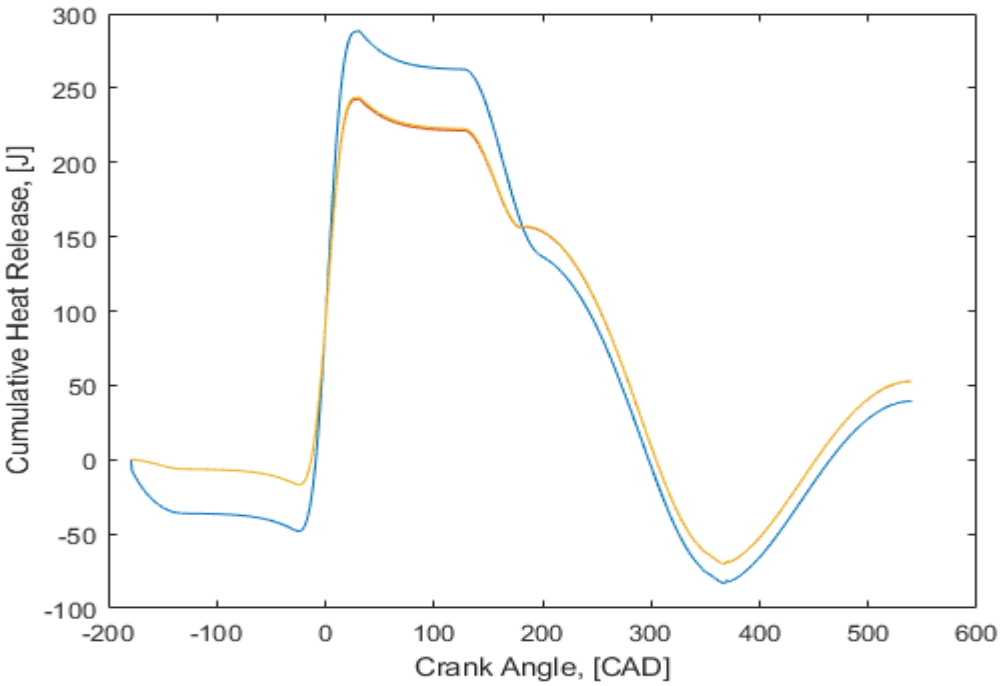

(d)

Figure 31 CUMULATIVE HEAT RELEASE RATE AS A FUNCTION OF CRANK ANGLE

3.2 Six-Stroke Dual-Fuel Engine Model Simulation

The six-stroke dual-fuel engine model is based on the four-stroke SI engine model. However, there are a few additional inputs required. We need to add the fuel used for the second combustion process and the heat supplied to the four-stroke cycle for comparison with the six-stroke engine cycle.

The engine specifications are same as that for four-stroke engine cycle. We update the duration for one cycle to include 3 revolutions of crankshaft, i.e. 1080 crank angle degrees.

The model created requires some additional inputs to simulate six-stroke engine cycle.

ITEM	VALUE (a)	VALUE (b)	VALUE (c)	VALUE (d)	VALUE (e)	VALUE (f)
Displaced Volume [litres]	2	2	2	2	2	2
Number of Cylinders	4	4	4	4	4	4
Bore to Stroke ratio	1.2	1.2	1.2	1.2	1.2	1.2
Con rod to Crank rad ratio	3.3	3.3	3.3	3.3	3.3	3.3

Compression Ratio	8	10	10	10	10	10
Engine speed [RPM]	4000	4000	3000	3000	4000	3000
Engine Load	0.9	0.9	0.9	0.7	0.85	0.85
Spark Advance	33	33	30	30	33	30
Equivalence Ratio	0.7	0.7	0.7	0.6	0.7	0.6
Fuel Used for the First Combustion Process	Iso-Octane	Iso-Octane	Iso-Octane	Iso-Octane	Iso-Octane	Iso-Octane
Fuel Used for the Second Combustion Process	Methanol	Methanol	Methanol	Methanol	Propane	Propane
Heat Supplied [J]	1087.3	1088.2	1070.4	810.30	1090	1090

Table 9 SIMULATION CONDITIONS

Presentation of results:

ITEM	**VALUE (a)**	**VALUE (b)**	**VALUE (c)**	**VALUE (d)**	**VALUE (e)**	**VALUE (f)**
Indicated Thermal Efficiency [%]	44.22	50.73	47.77	44.55	48.62	44.71

Indicated Power [kW]	16.11	18.50	12.85	9.06	17.75	12.23
Allocation ratio	0.21	0.215	0.215	0.323	0.267	0.372
Equivalence Ratio after First Combustion Process	1.26	1.262	1.254	1.201	1.473	1.40

Table 10 RESULTS FOR THE SIMULATION OF SIX-STROKE DUAL FUEL ENGINE

For the same heat supplied to the six-stroke cycle as that for four-stroke cycle we see an increase in thermal efficiency and indicted power.

For this particular simulation, we took equivalence ratio to be 0.7 for the first combustion process, which gave the mass of fuel to be 1.92e-05 kg of Isooctane giving out 851 Joules of combustion heat. Which we subtract from the reference heat supplied to the four-stroke cycle giving us the heat required for the second combustion process i.e. 236 Joules. Dividing this by the LHV of the second fuel (Methanol) gave us the mass of fuel required which comes out to be 1.18e-05 kg.

The equivalence ratio changes for the second combustion process to 1.26. The change in equivalence ratio is dependent on the fuel used for the second combustion process, here we use Methanol which contains Oxygen atoms therefore the rise is limited.

Total amount of fuel (Isooctane + Methanol) required for the dual fuel cycle is 3.10e-05 kg which is slightly more than that for four-stroke engine cycle at 2.33e-05 kg.

But we utilize more of the combustion heat as can be seen from the thermal efficiency.

The allocation ratio shows that the heat of combustion provided by the first combustion process is larger than that for the second combustion process, i.e we supply about 21% of the total heat of the four-stroke engine during the second combustion process.

Similar to what we saw in the results of the four-stroke engine simulation, we have here various figures depicting the change in different engine parameters with respect to the crank angle. However, for six-stroke engine simulation the crank angle ranges from -180 CAD (BDC) to 900 CAD (BDC) after the Intake stroke, completing three revolutions.

Figure 30 shows the change in cylinder volume at different compression ratios. Figure 31 shows the pressure in the cylinder at different volumes during the engine processes. From the Table 10 we can see that the engine condition (b) has the highest thermal efficiency and from Figure 31b we see the maximun peak pressure value.

The equivalence ratio after the addiditon of second combustion process fuel increases from the earlier value as we have already used up some oxygen in the first combustion process. From Table 10 we can see that the rise in equivalence ratio is lower for Methanol compared to Propane, since Methanol contains Oxygen atom in its molecule and therefore requires a lower Air to Fuel ratio for stoichiometric combustion.

The results show both the differences and similarities between four-stroke and six-stroke engine working.

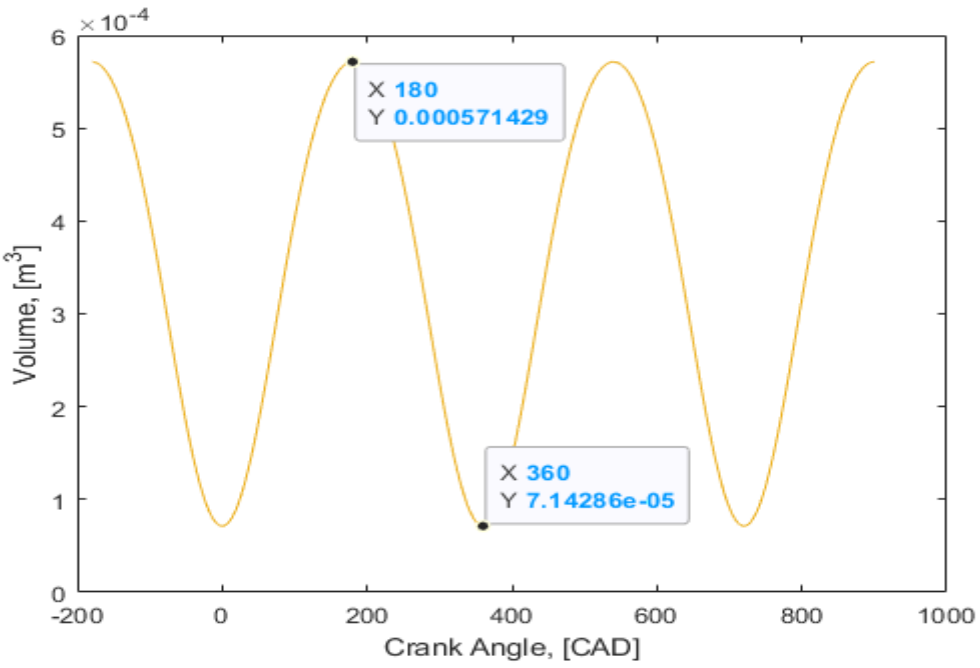

[Compression Ratio = 8]

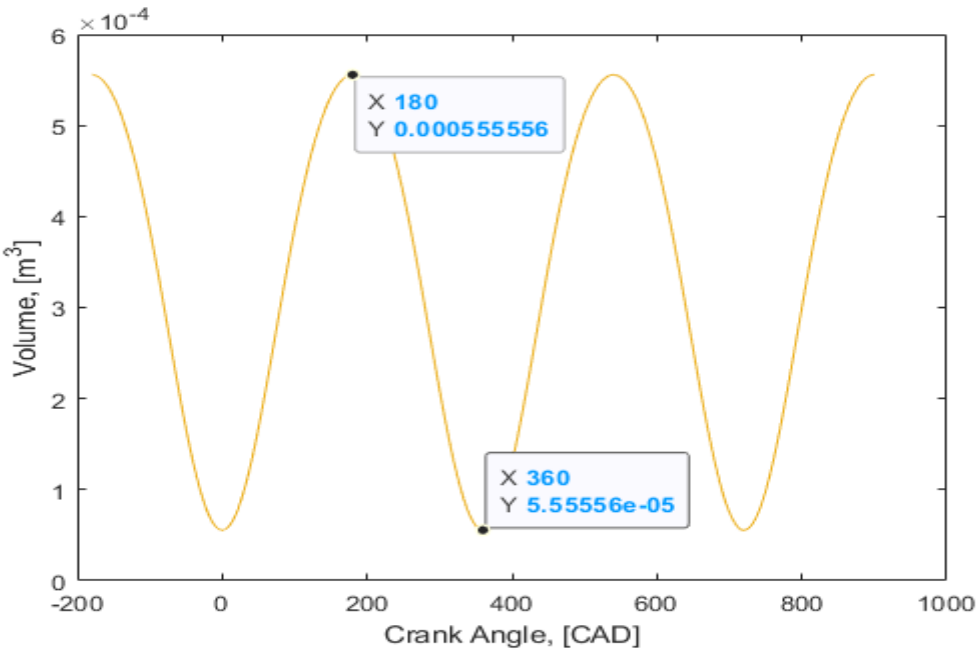

[Compression Ratio = 10]

Figure 32 CHANGE IN VOLUME AS A FUNCTION OF CRANK ANGLE

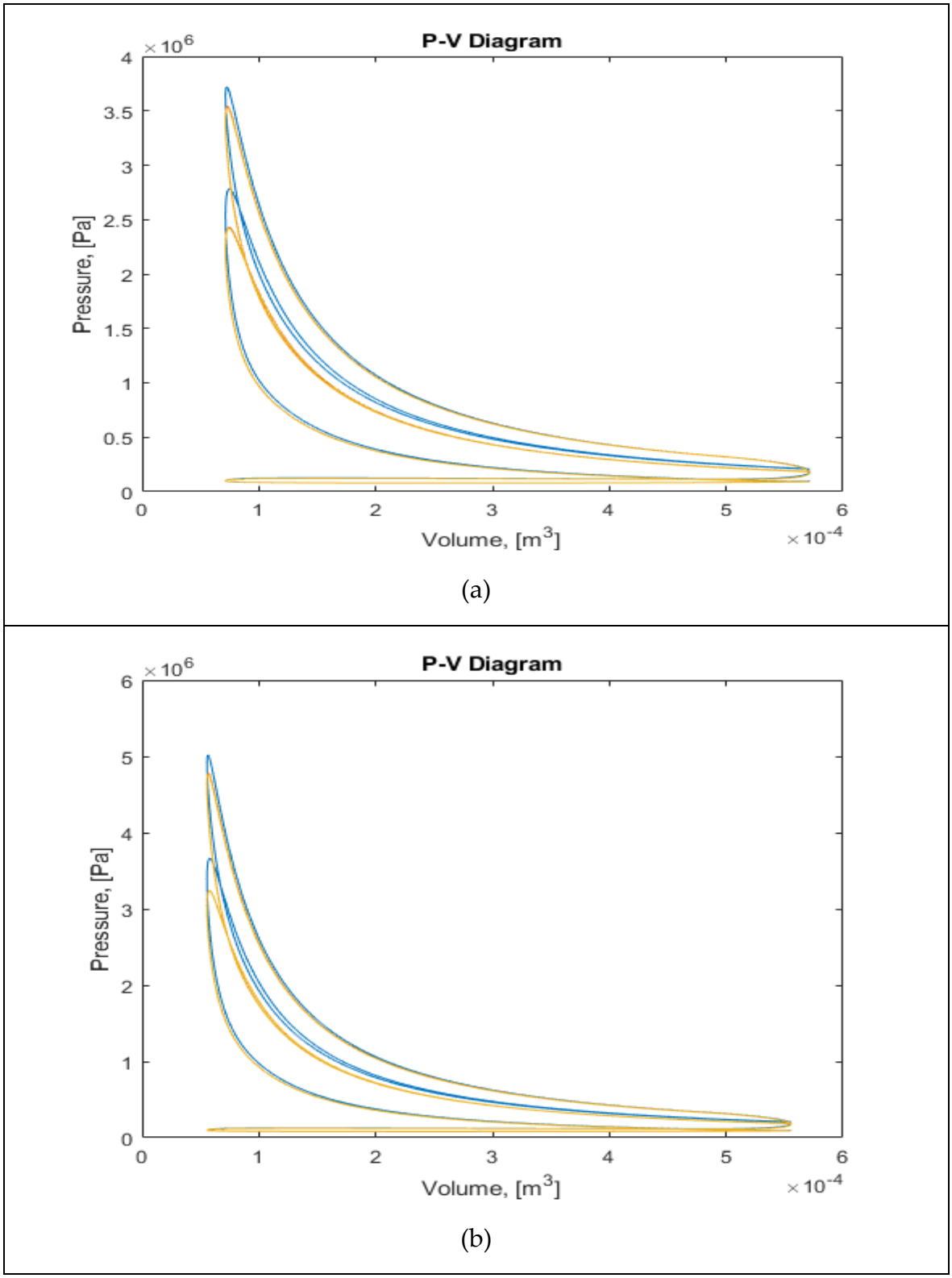
P-V Diagram
×10^6
4
3.5
3
2.5
2
1.5
1
0.5
0
Pressure, [Pa]
0
1
2
3
4
5
6
Volume, [m^3]
×10^-4

(a)

P-V Diagram
×10^6
6
5
4
3
2
1
0
Pressure, [Pa]
0
1
2
3
4
5
6
Volume, [m^3]
×10^-4

(b)

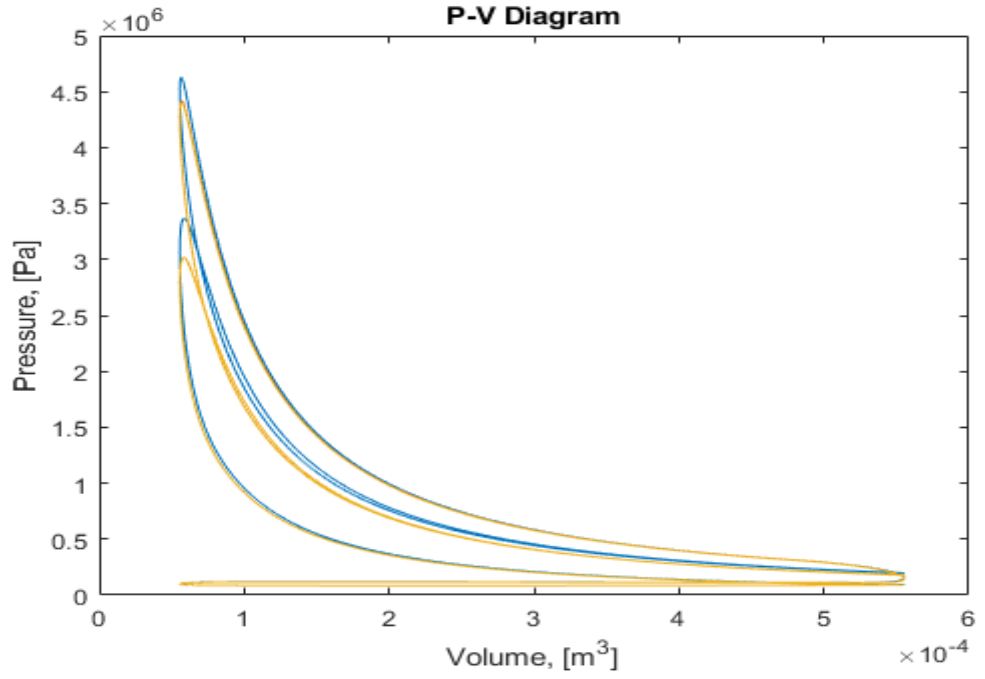
P-V Diagram
×10^6
5
4.5
4
3.5
3
2.5
2
1.5
1
0.5
0
Pressure, [Pa]
0
1
2
3
4
5
6
Volume, [m^3]
×10^-4

(c)

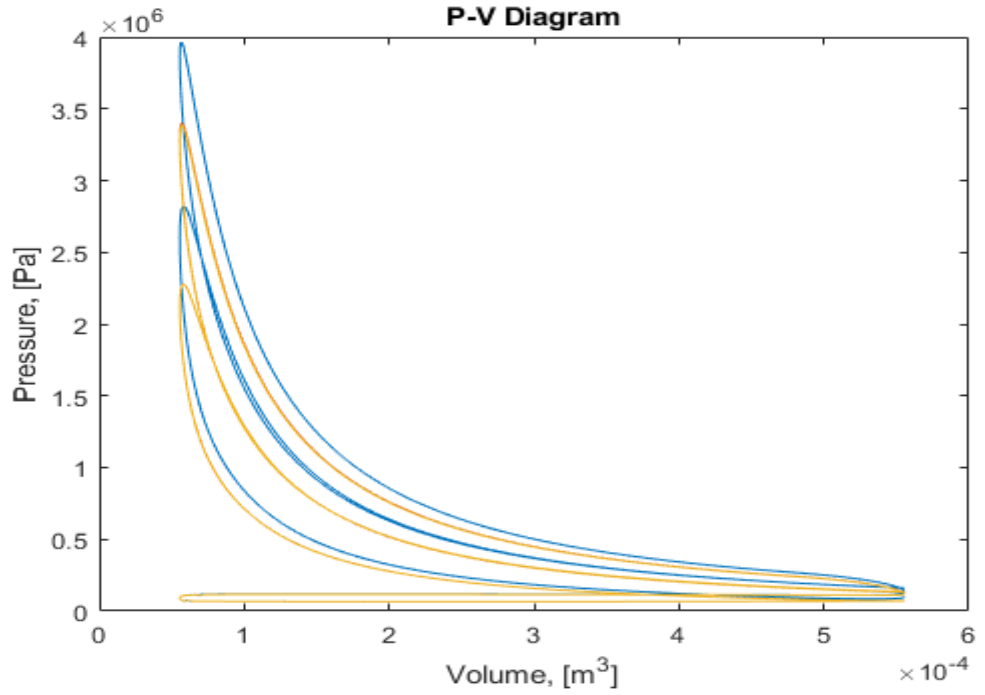
P-V Diagram
×10^6
4
3.5
3
2.5
2
1.5
1
0.5
0
Pressure, [Pa]
0
1
2
3
4
5
6
Volume, [m^3]
×10^-4

(d)

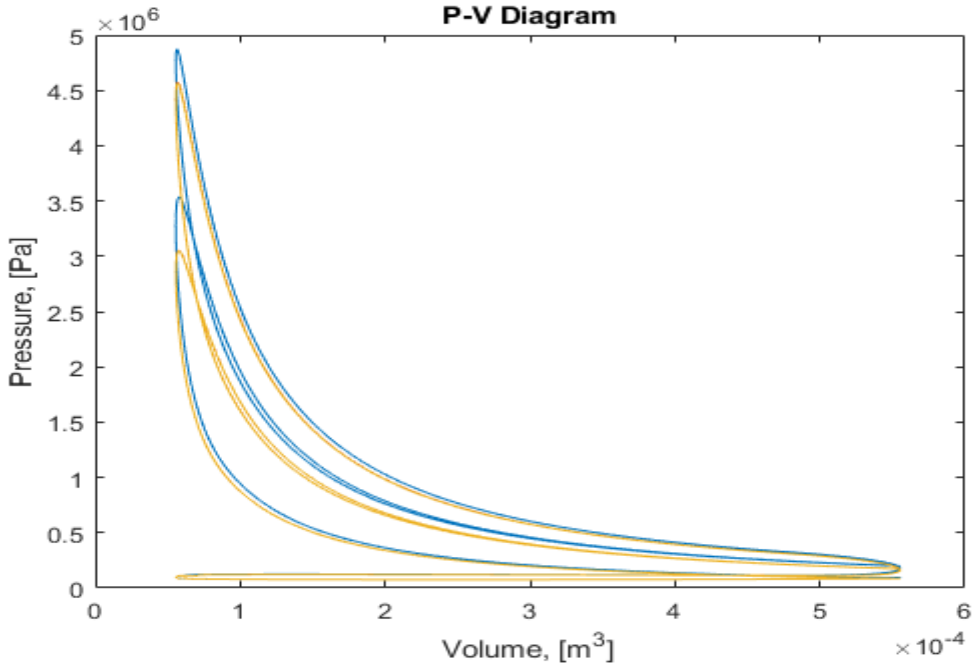

(e)

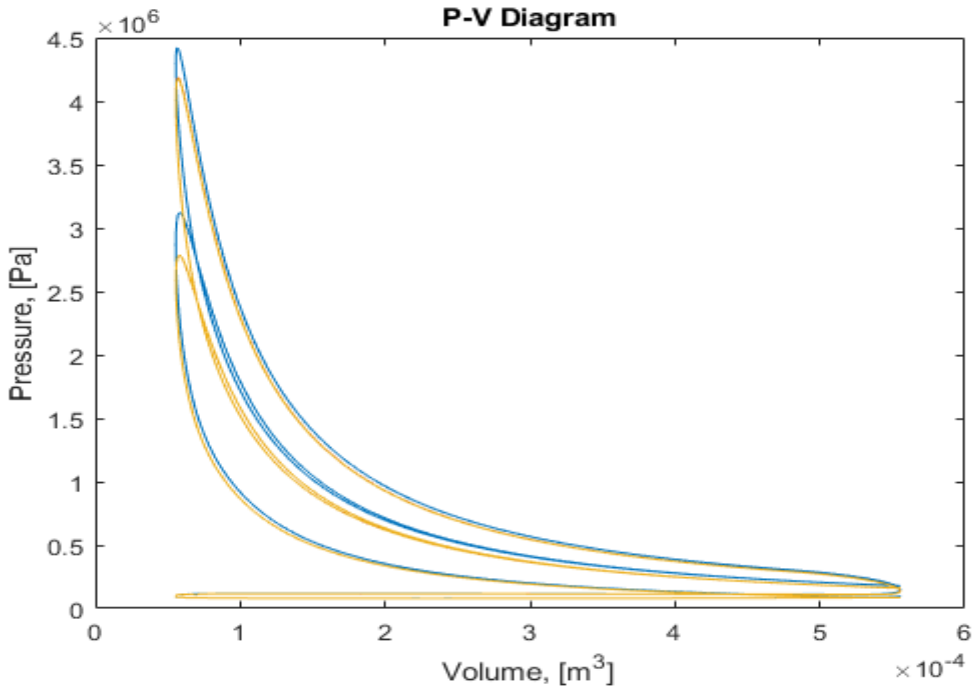

(f)

Figure 33 CHANGE IN PRESSURE IN THE CYLINDER AS A FUNCTION OF CYLINDER VOLUME

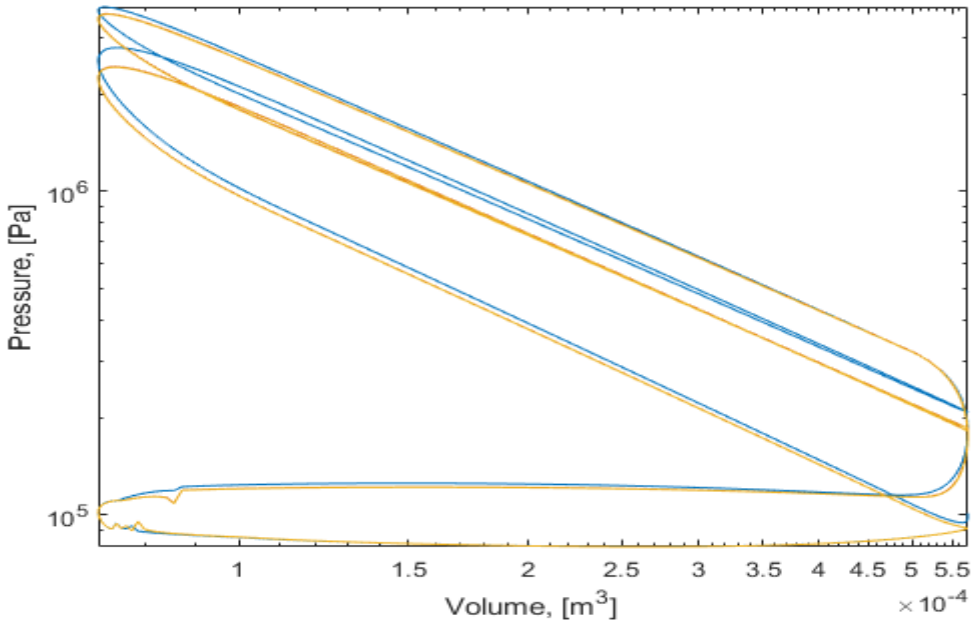
Pressure, [Pa]
10^6
10^5
1
1.5
2
2.5
3
3.5
4
4.5
5
5.5
Volume, [m^3]
×10^-4

(a)

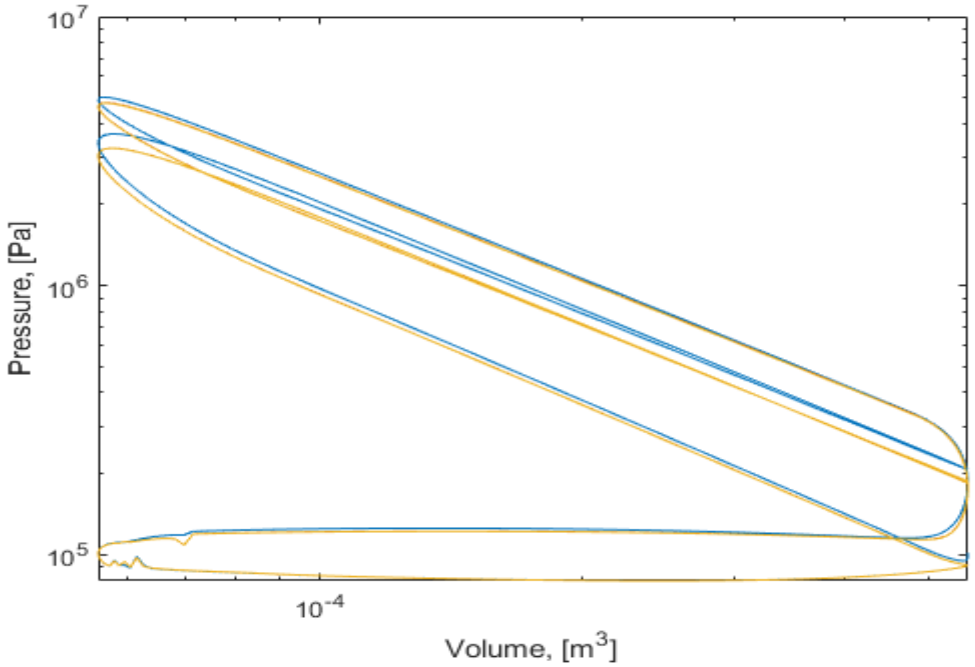
Pressure, [Pa]
10^7
10^6
10^5
10^-4
Volume, [m^3]

(b)

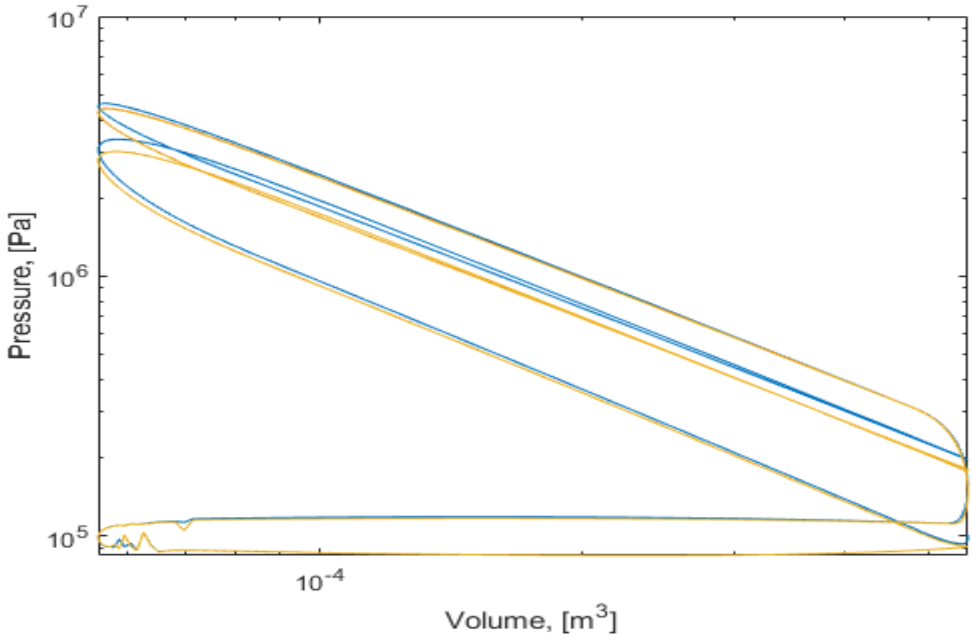
10^7
10^6
10^5
Pressure, [Pa]
10^{-4}
Volume, [m^3]

(c)

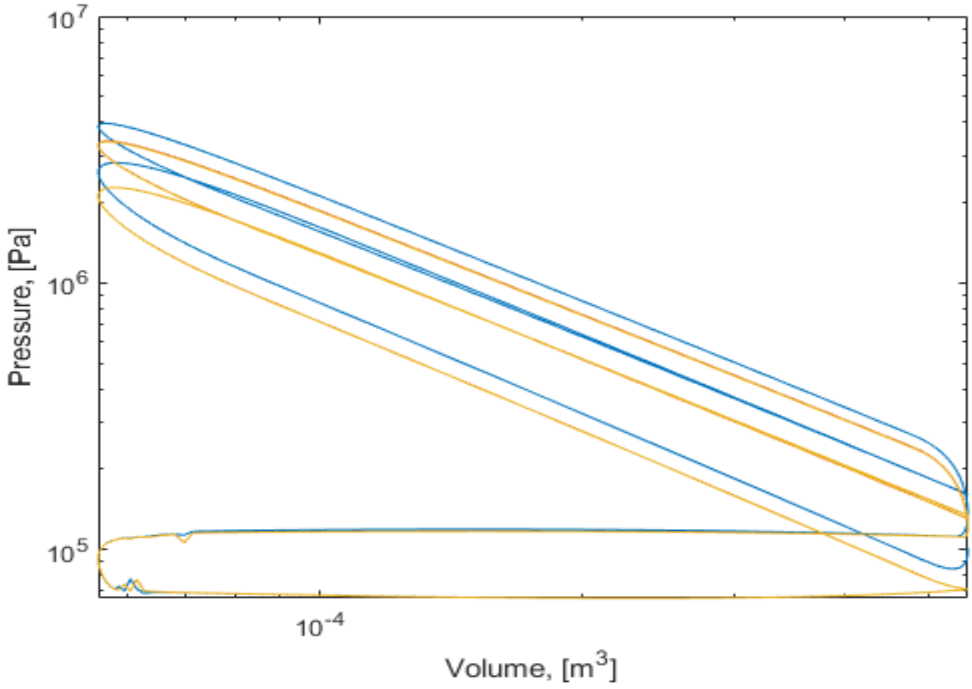
10^7
10^6
10^5
Pressure, [Pa]
10^{-4}
Volume, [m^3]

(d)

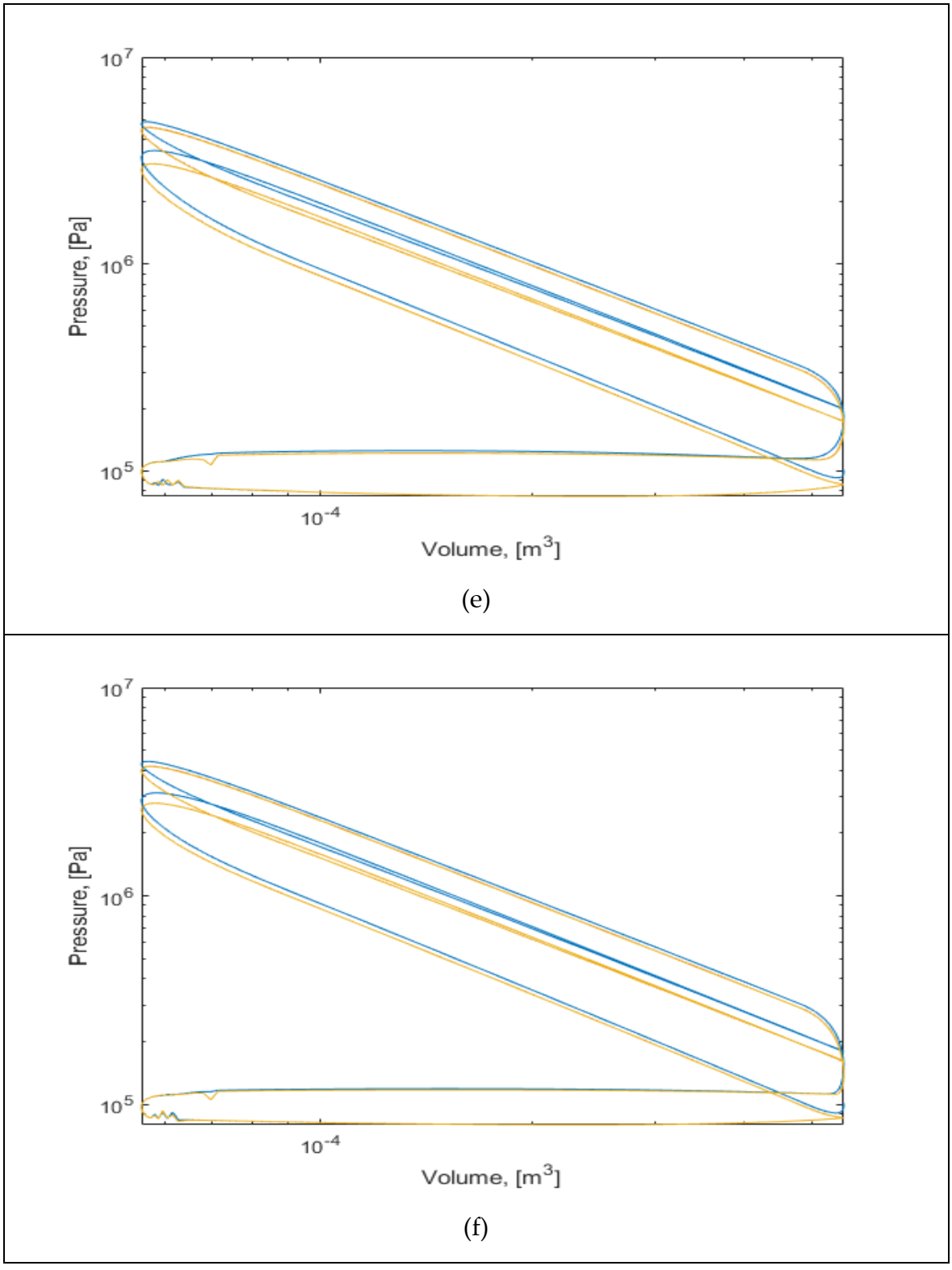

Figure 34 LOGLOG PLOT OF PRESSURE AS A FUNCTION OF VOLUME

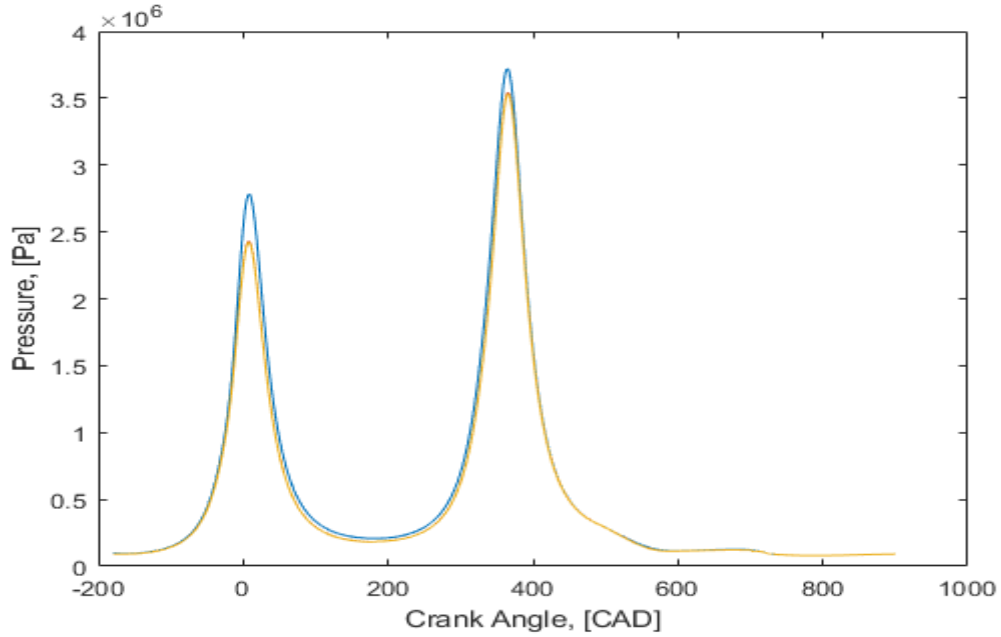
×10^6
4
3.5
3
2.5
2
1.5
1
0.5
0
Pressure, [Pa]
-200
0
200
400
600
800
1000
Crank Angle, [CAD]

(a)

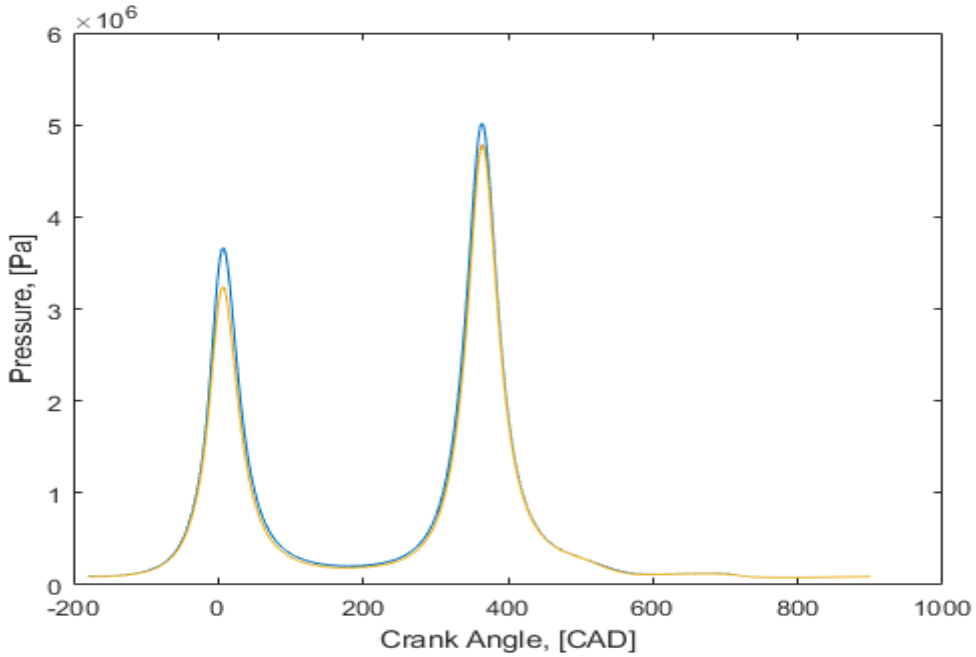
×10^6
6
5
4
3
2
1
0
Pressure, [Pa]
-200
0
200
400
600
800
1000
Crank Angle, [CAD]

(b)

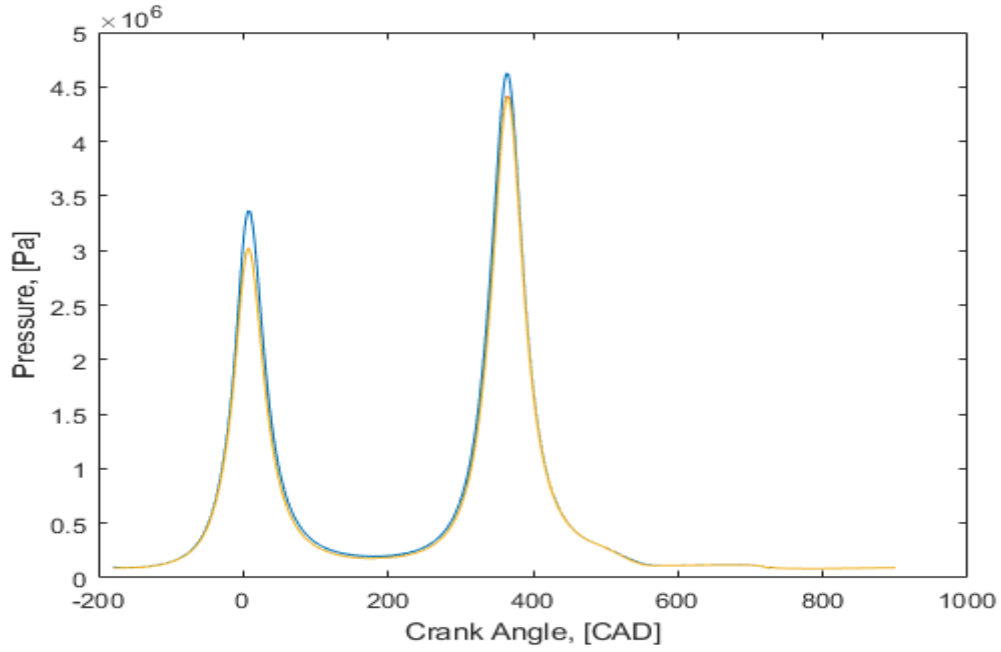
×10^6
5
4.5
4
3.5
3
2.5
2
1.5
1
0.5
0
Pressure, [Pa]
-200
0
200
400
600
800
1000
Crank Angle, [CAD]

(c)

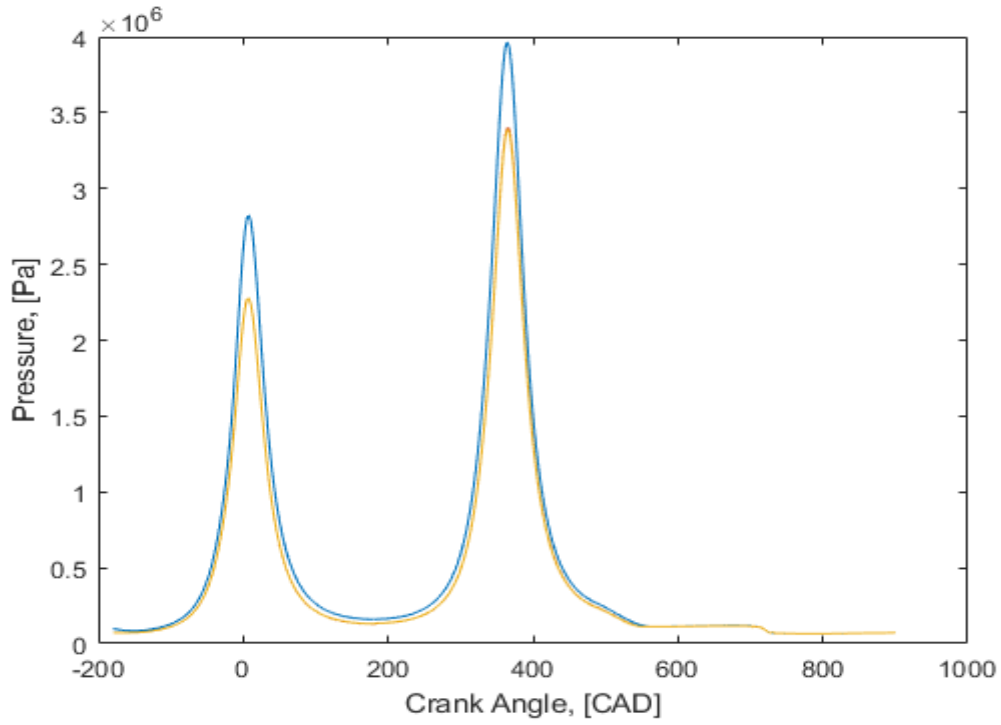
×10^6
4
3.5
3
2.5
2
1.5
1
0.5
0
Pressure, [Pa]
-200
0
200
400
600
800
1000
Crank Angle, [CAD]

(d)

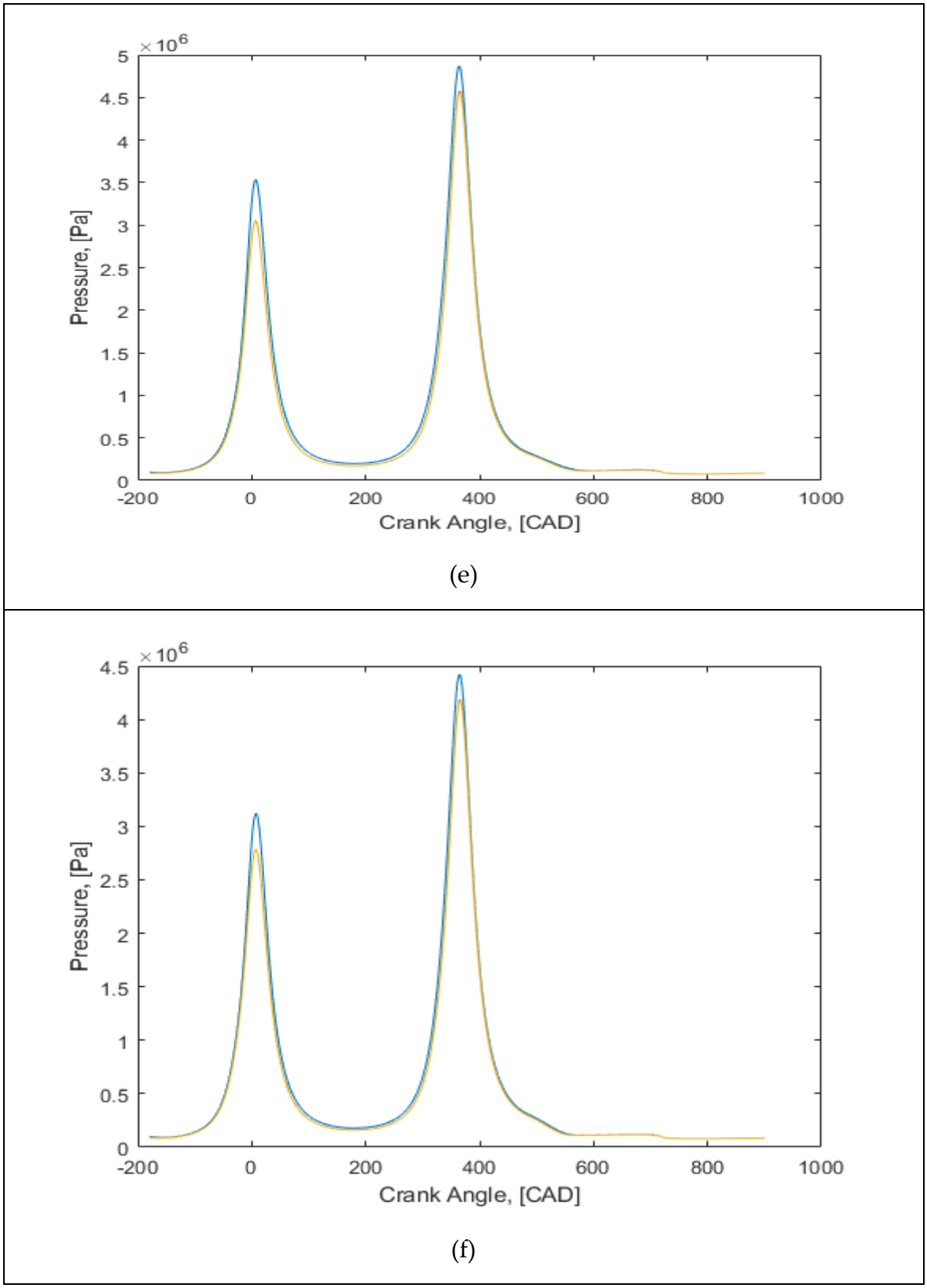

Figure 35 CYLINDER PRESSURE AS FUNCTION OF CRANK ANGLE

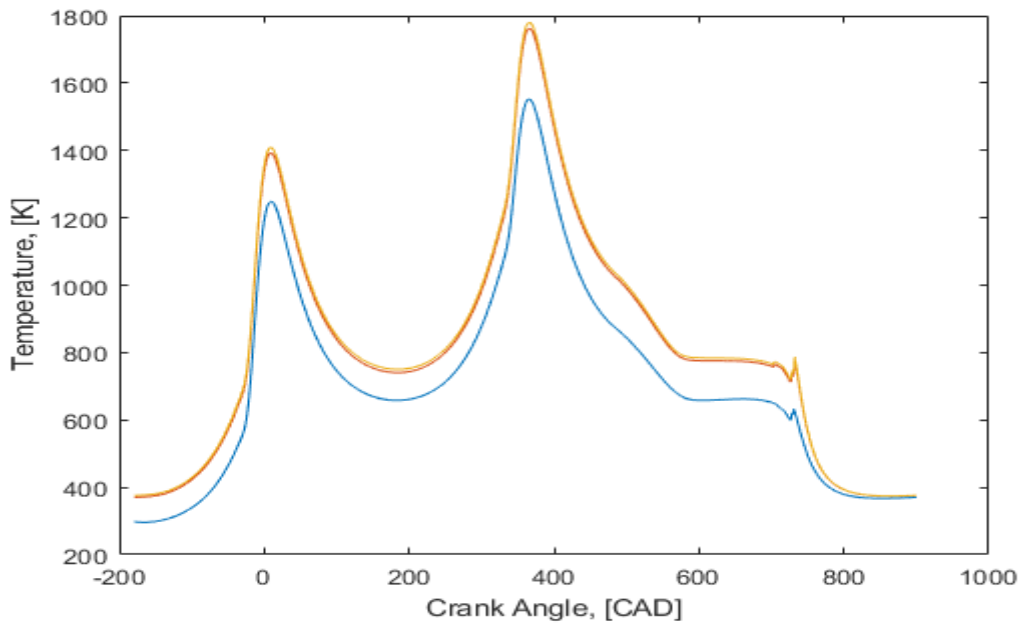
Temperature, [K]
Crank Angle, [CAD]
1800
1600
1400
1200
1000
800
600
400
200
-200
0
200
400
600
800
1000

(a)

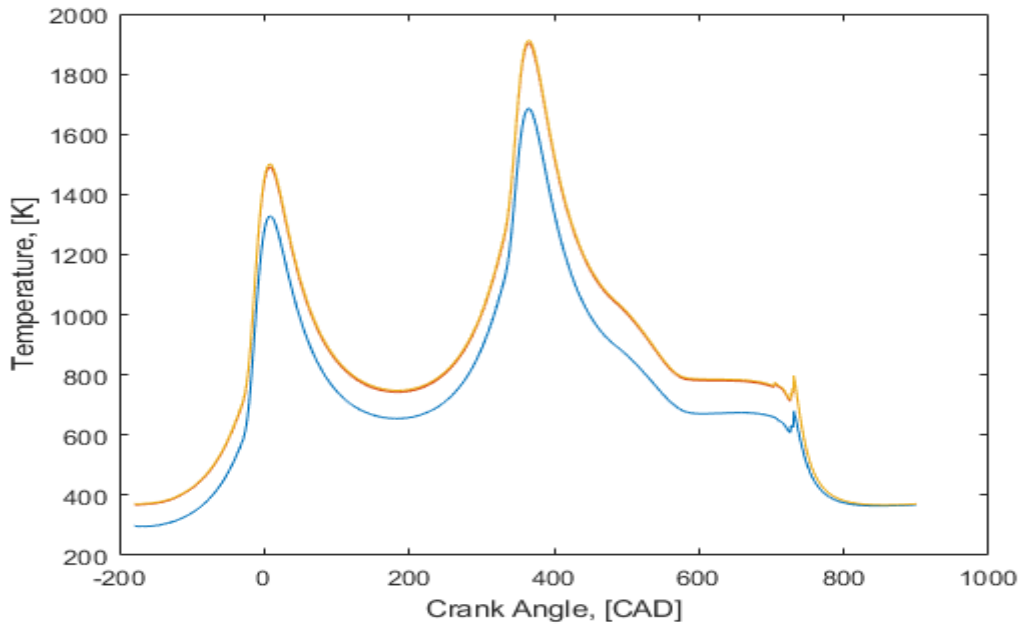
Temperature, [K]
Crank Angle, [CAD]
2000
1800
1600
1400
1200
1000
800
600
400
200
-200
0
200
400
600
800
1000

(b)

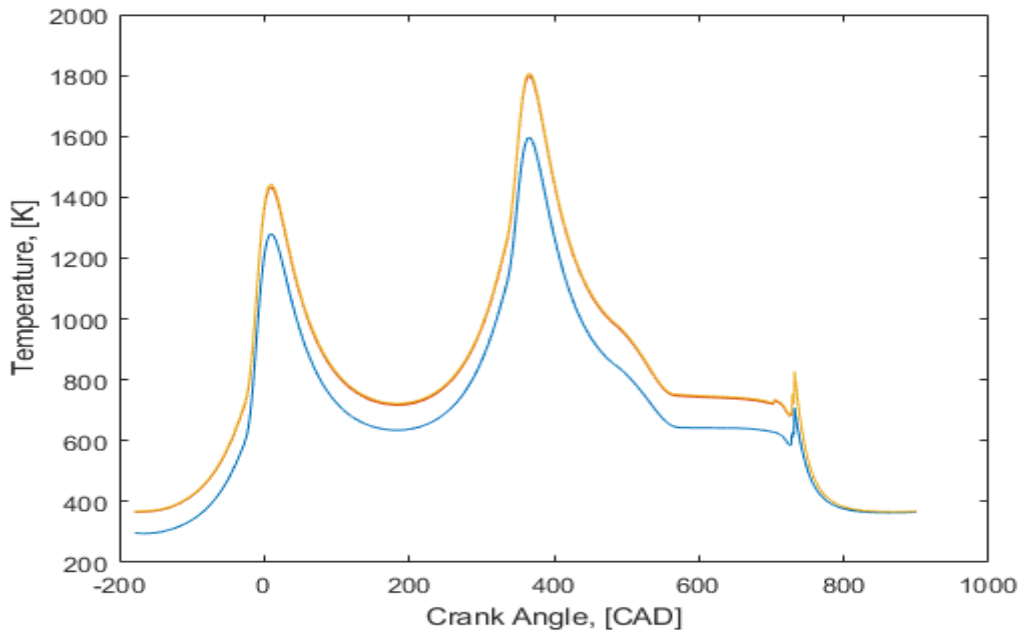
Temperature, [K]
Crank Angle, [CAD]
2000
1800
1600
1400
1200
1000
800
600
400
200
-200
0
200
400
600
800
1000

(c)

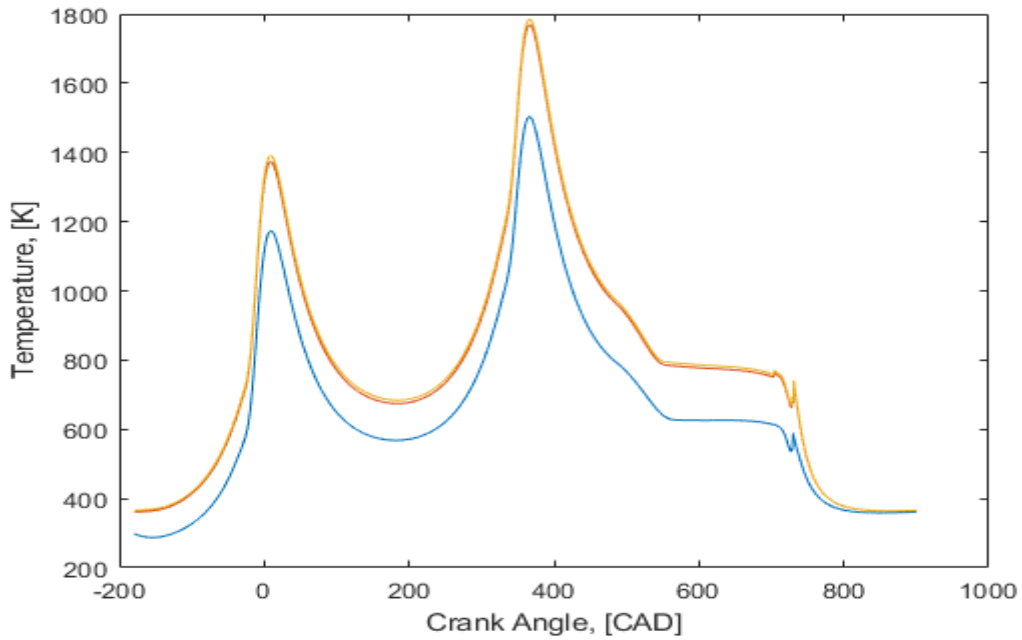
Temperature, [K]
Crank Angle, [CAD]
1800
1600
1400
1200
1000
800
600
400
200
-200
0
200
400
600
800
1000

(d)

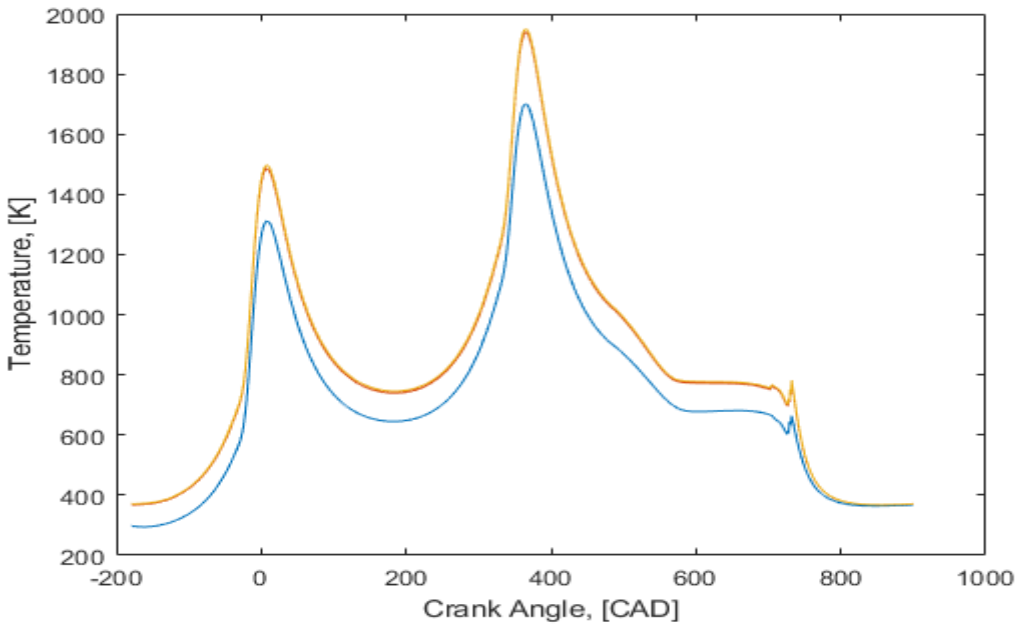

(e)

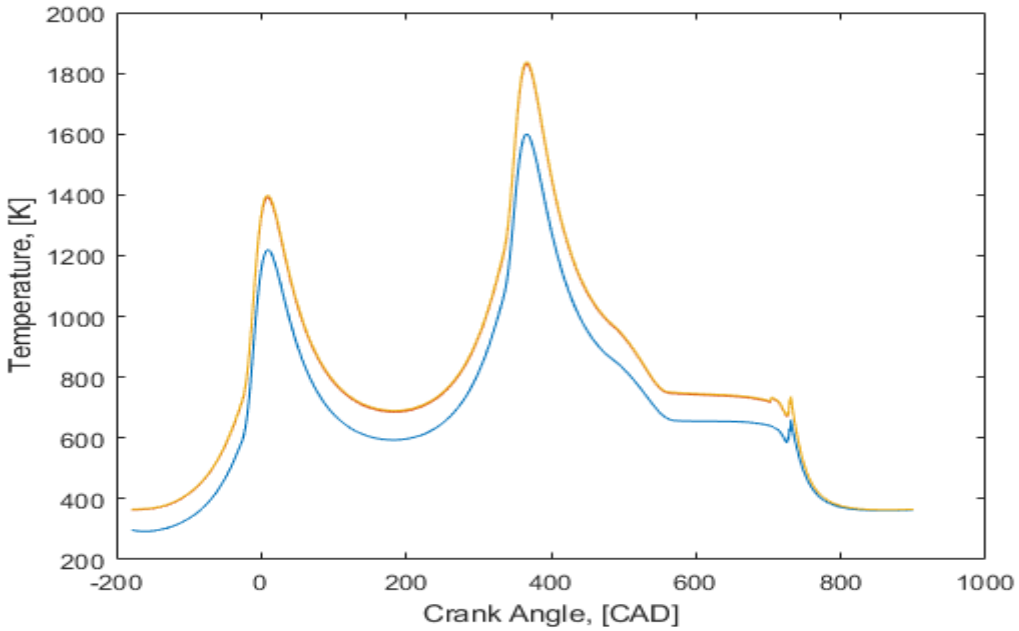

(f)

Figure 36 CYLINDER TEMPERATURE AS FUNCTION OF CRANK ANGLE

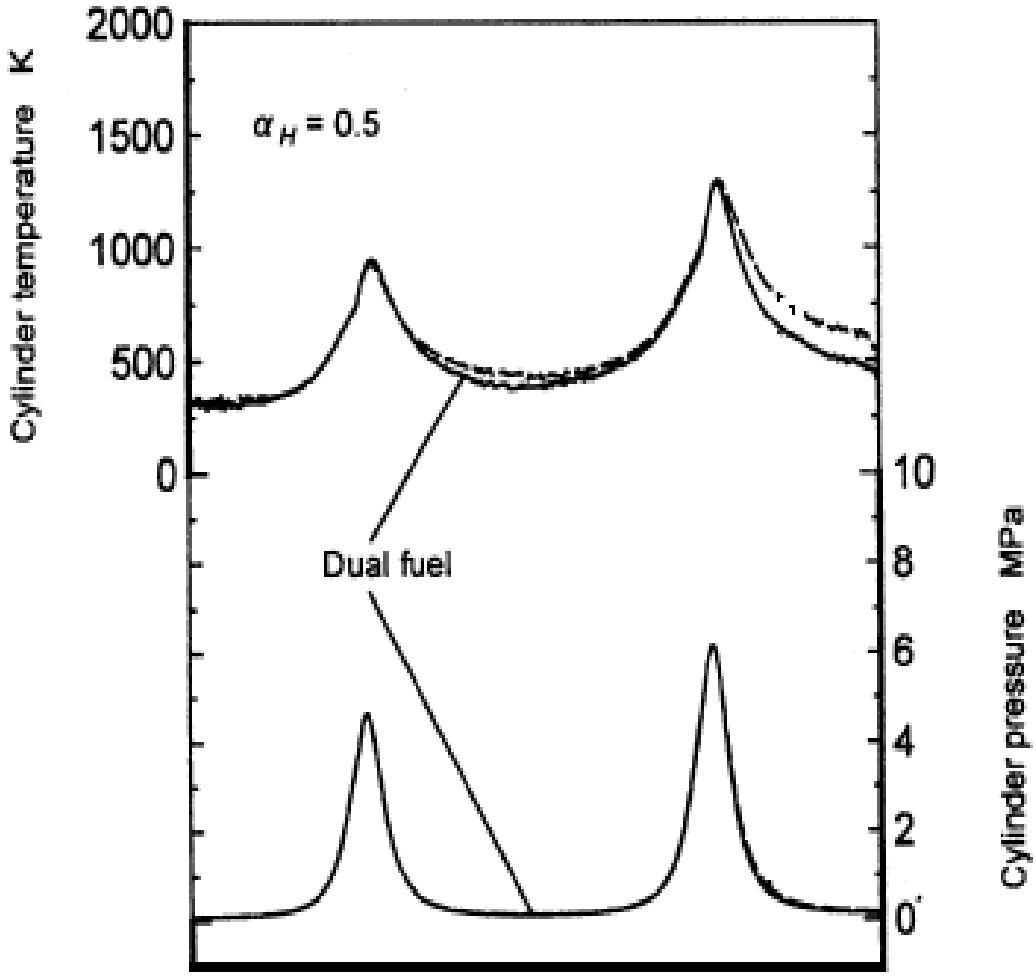

Figure 37 CYLINDER PRESSURE AND TEMPERATURE GRAPH [9]

We see similarities in the simulation calculations done here and the plots shown in the research paper for the dual fuel six-stroke engine cycle. The cylinder pressure for the second combustion process is higher compared to the first one due to higher temperature of gases at the end of first expansion process compared to temperature of gases at the end intake process.

We can see in Figure 36, a small uptick in the mass inside the cylinder at 180 CAD, this due to the addition of the second combustion process fuel.

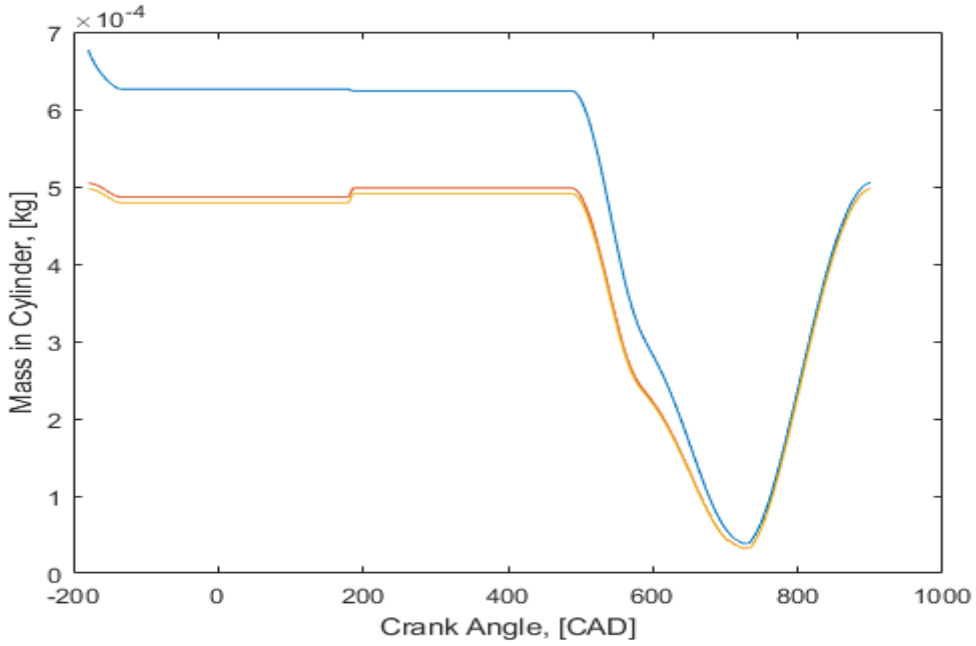
×10^-4
7
6
5
4
3
2
1
0
Mass in Cylinder, [kg]
-200
0
200
400
600
800
1000
Crank Angle, [CAD]

(a)

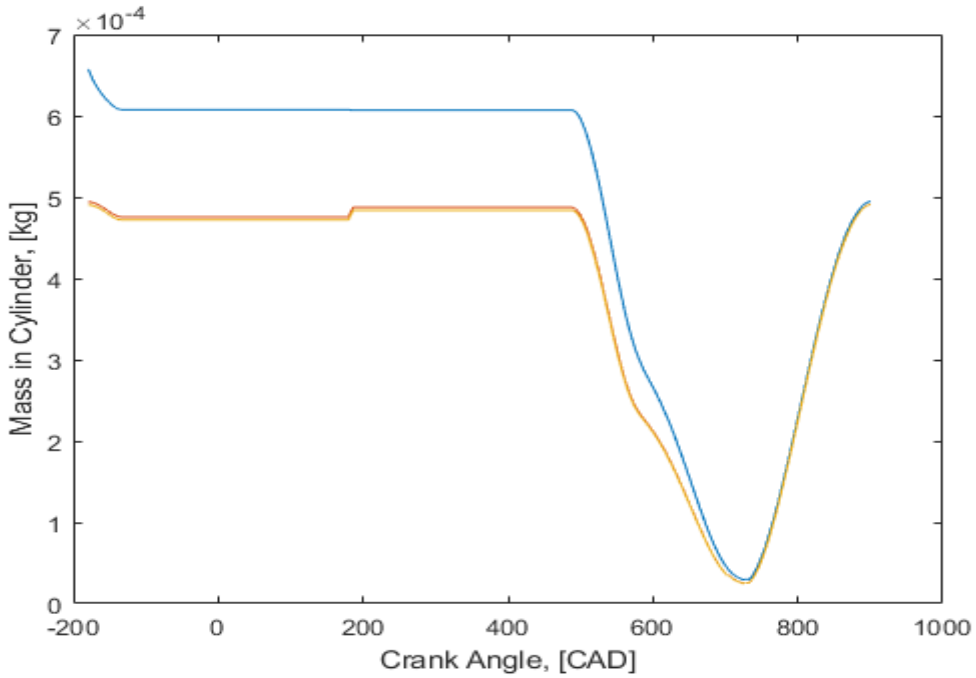
×10^-4
7
6
5
4
3
2
1
0
Mass in Cylinder, [kg]
-200
0
200
400
600
800
1000
Crank Angle, [CAD]

(b)

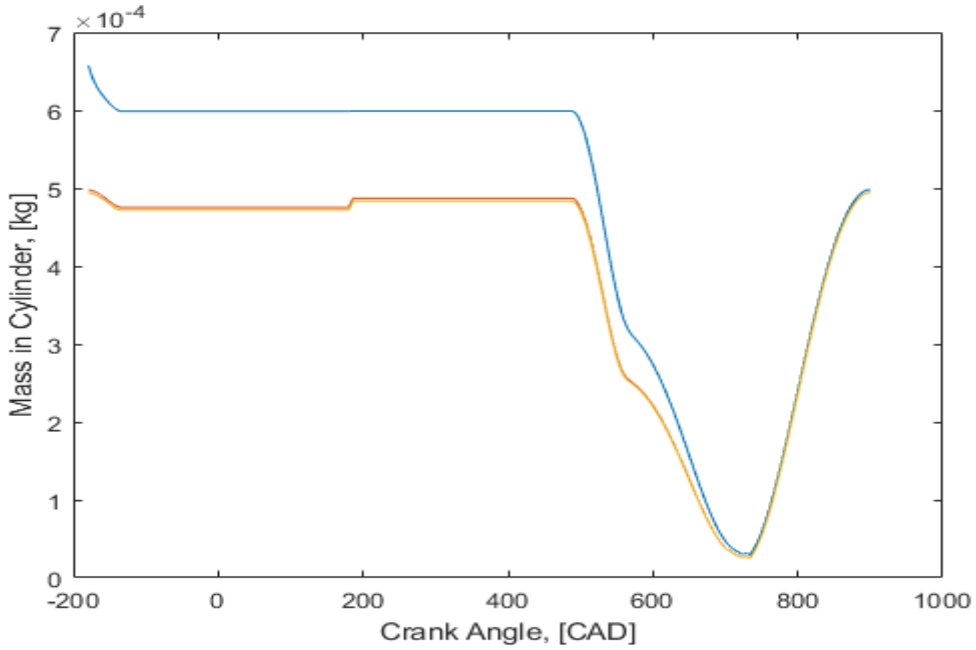
×10^-4
7
6
5
4
3
2
1
0
Mass in Cylinder, [kg]
-200
0
200
400
600
800
1000
Crank Angle, [CAD]

(c)

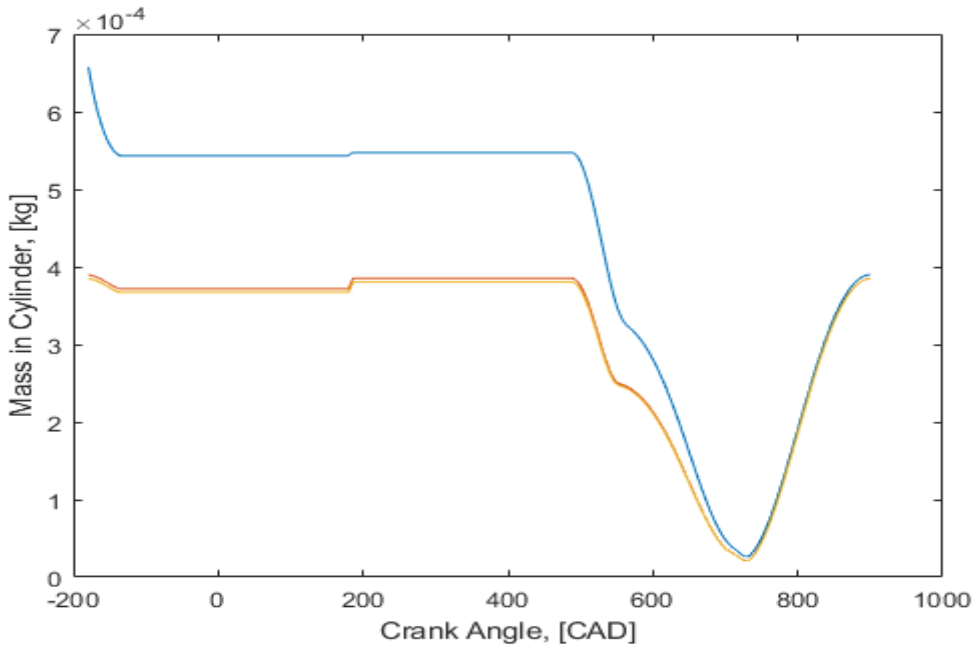
×10^-4
7
6
5
4
3
2
1
0
Mass in Cylinder, [kg]
-200
0
200
400
600
800
1000
Crank Angle, [CAD]

(d)

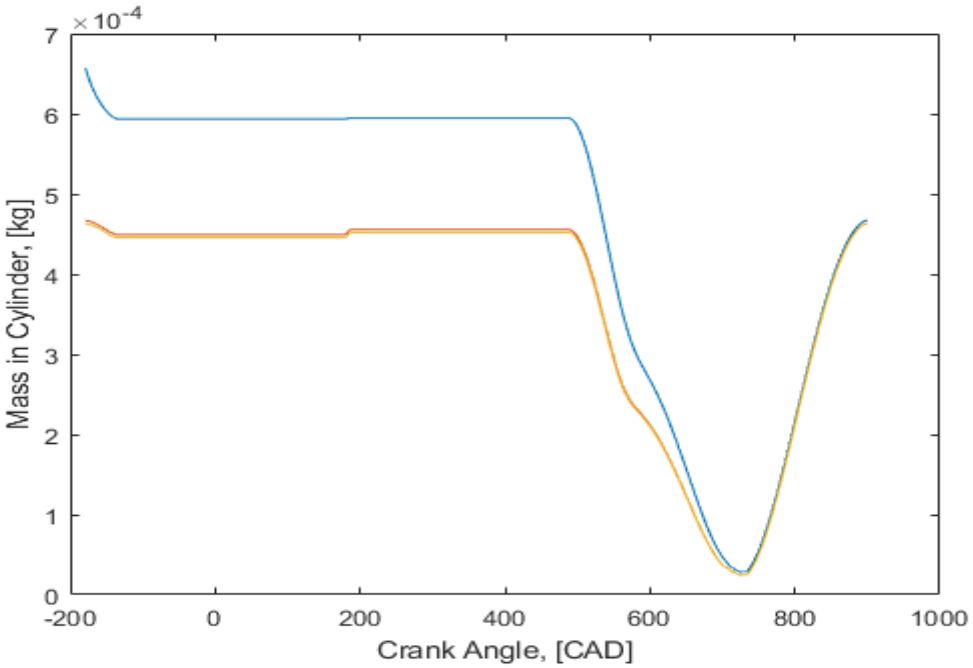

(e)

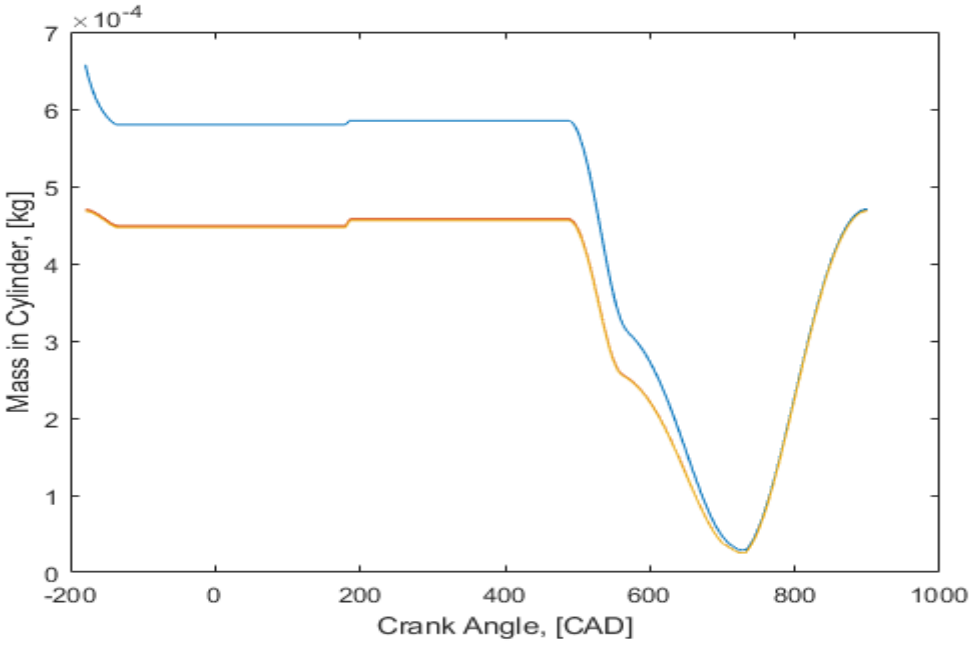

(f)

Figure 38 CYLINDER MASS AS FUNCTION OF CRANK ANGLE

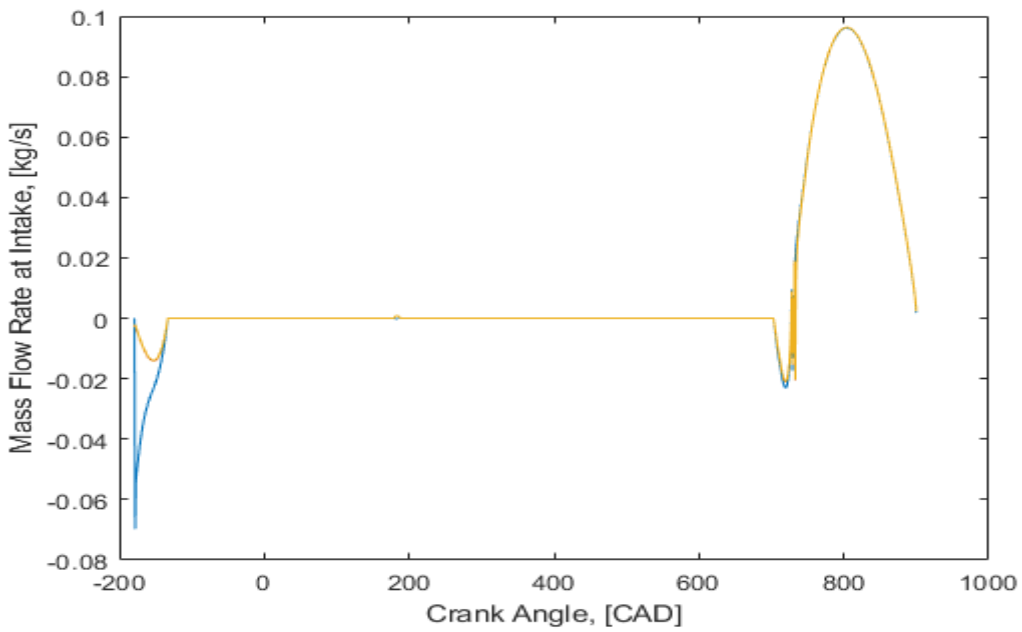
Mass Flow Rate at Intake, [kg/s]
0.1
0.08
0.06
0.04
0.02
0
-0.02
-0.04
-0.06
-0.08
-200
0
200
400
600
800
1000
Crank Angle, [CAD]

(a)

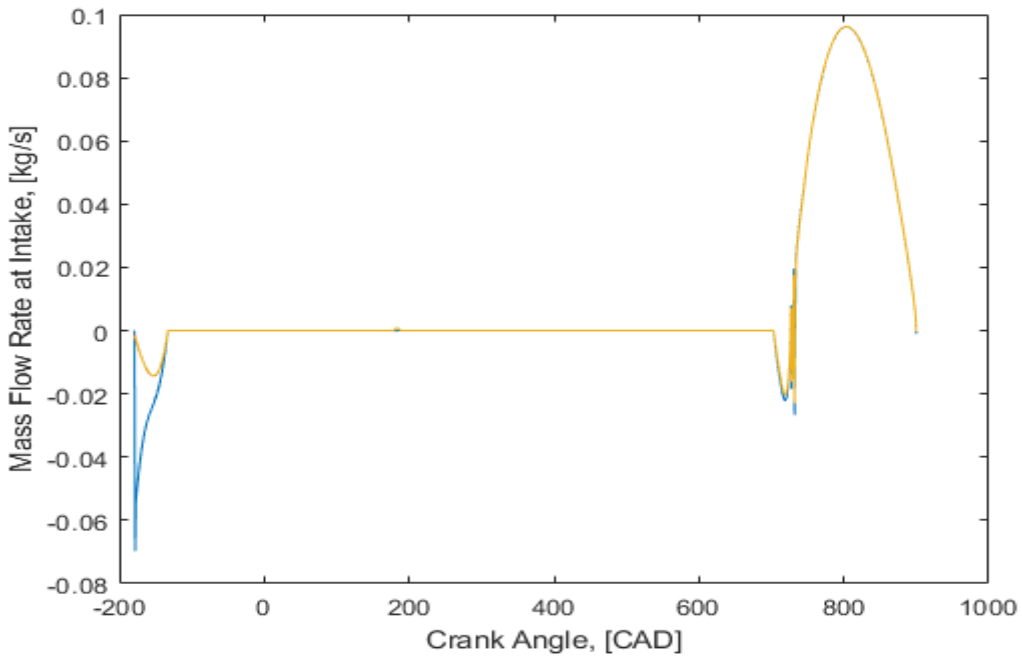
Mass Flow Rate at Intake, [kg/s]
0.1
0.08
0.06
0.04
0.02
0
-0.02
-0.04
-0.06
-0.08
-200
0
200
400
600
800
1000
Crank Angle, [CAD]

(b)

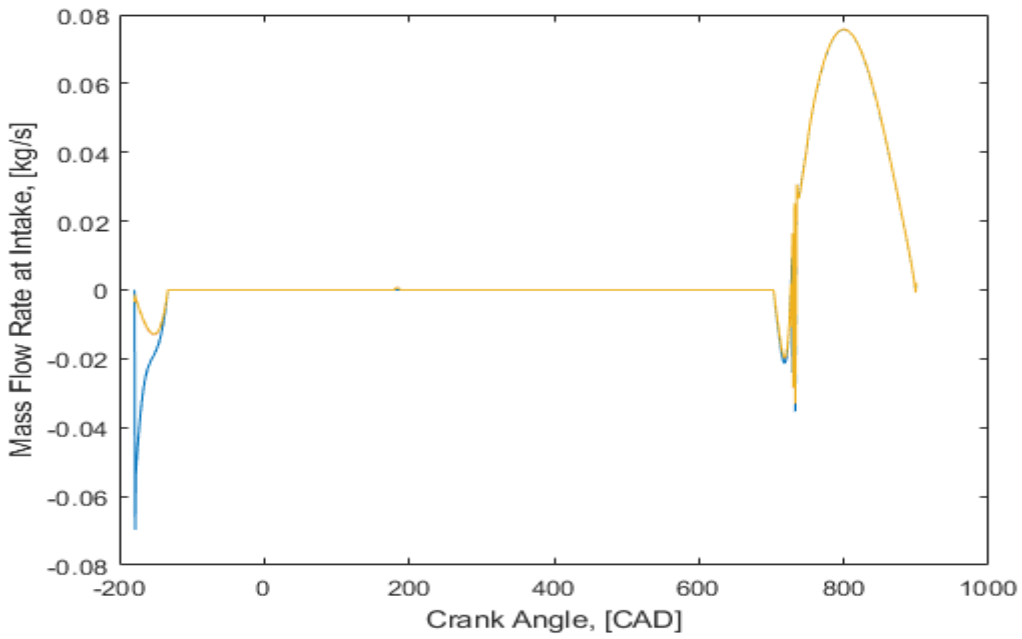
Mass Flow Rate at Intake, [kg/s]
0.08
0.06
0.04
0.02
0
-0.02
-0.04
-0.06
-0.08
-200
0
200
400
600
800
1000
Crank Angle, [CAD]

(c)

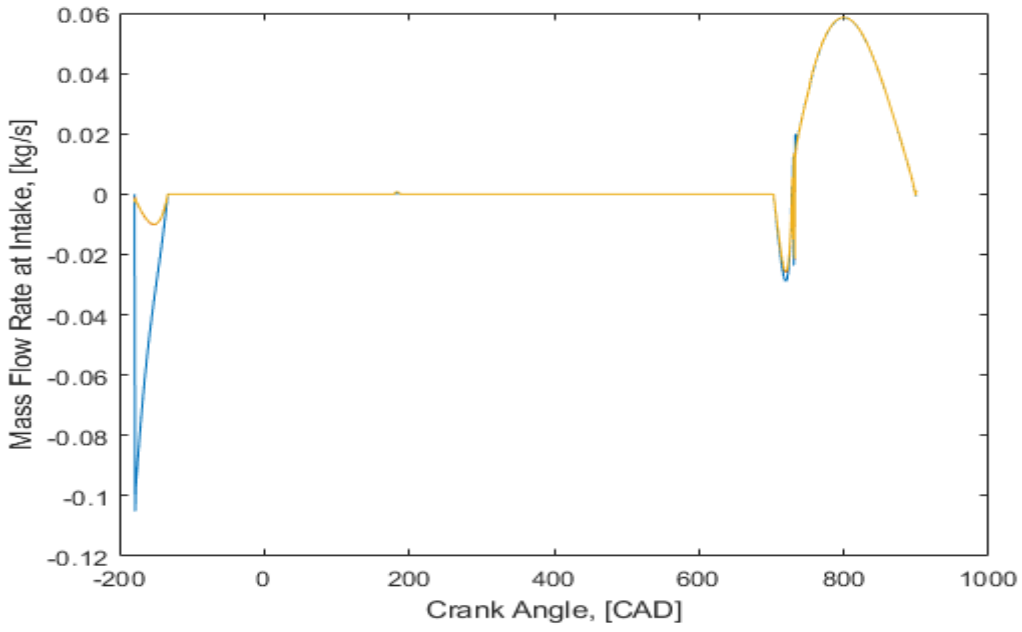
Mass Flow Rate at Intake, [kg/s]
0.06
0.04
0.02
0
-0.02
-0.04
-0.06
-0.08
-0.1
-0.12
-200
0
200
400
600
800
1000
Crank Angle, [CAD]

(d)

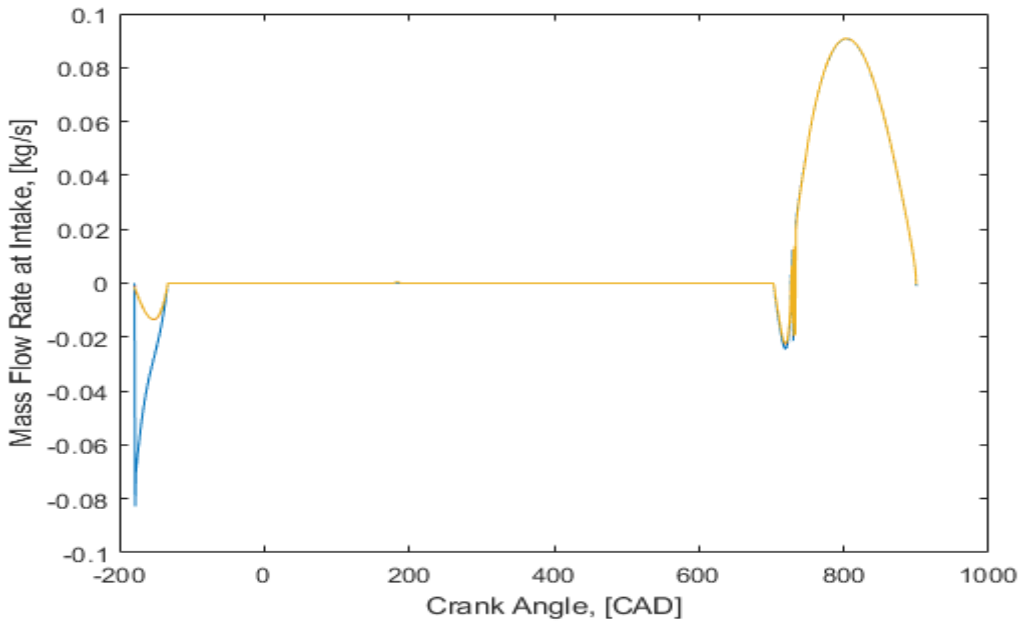

(e)

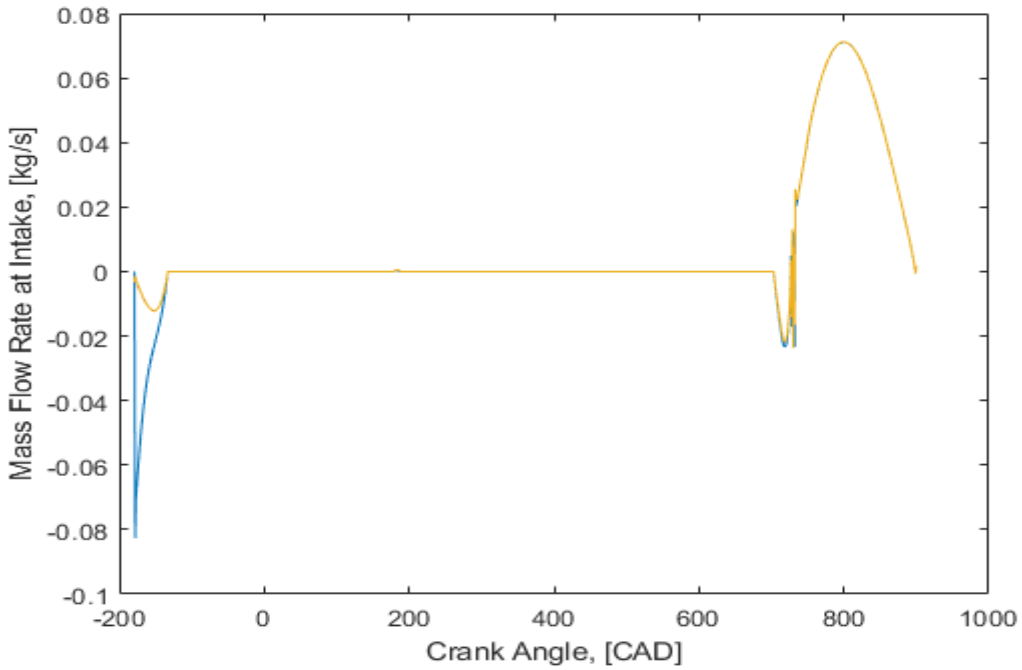

(f)

Figure 39 INTAKE MASS FLOW RATE AS FUNCTION OF CRANK ANGLE

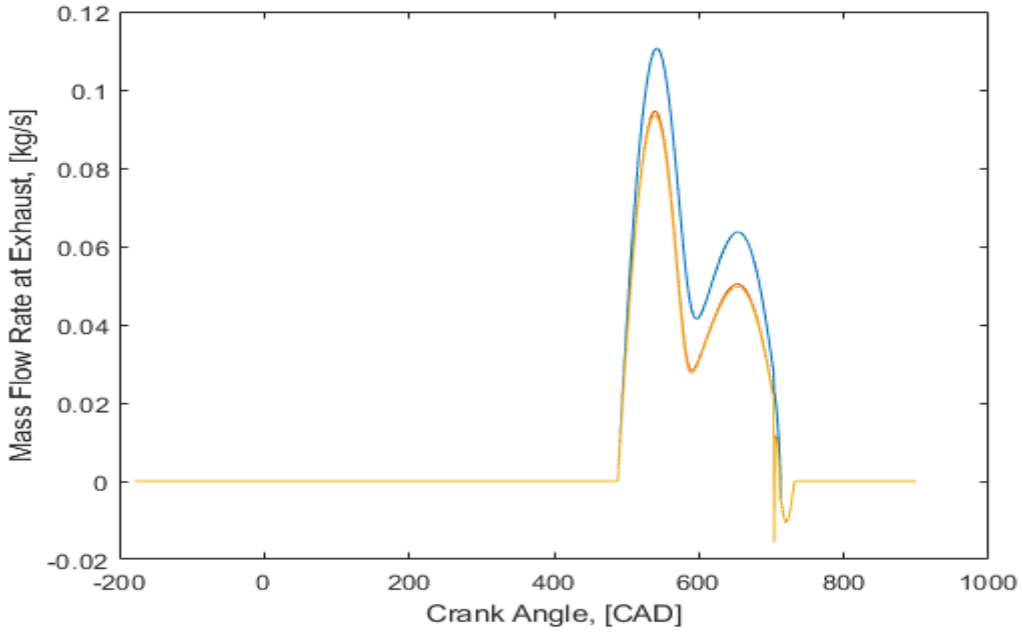
Mass Flow Rate at Exhaust, [kg/s]
0.12
0.1
0.08
0.06
0.04
0.02
0
-0.02
-200
0
200
400
600
800
1000
Crank Angle, [CAD]

(a)

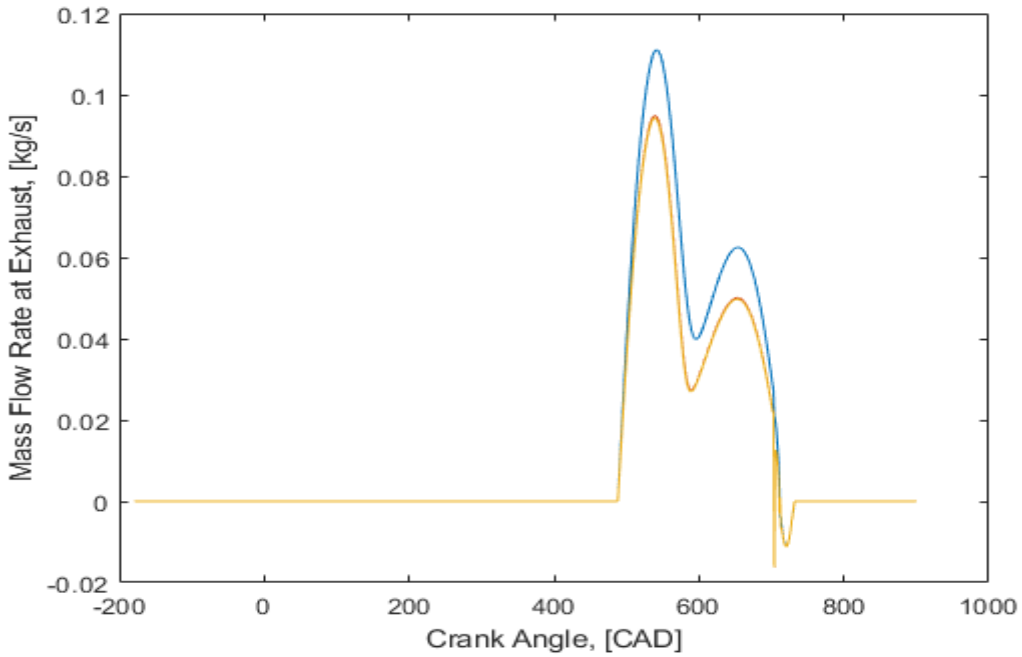
Mass Flow Rate at Exhaust, [kg/s]
0.12
0.1
0.08
0.06
0.04
0.02
0
-0.02
-200
0
200
400
600
800
1000
Crank Angle, [CAD]

(b)

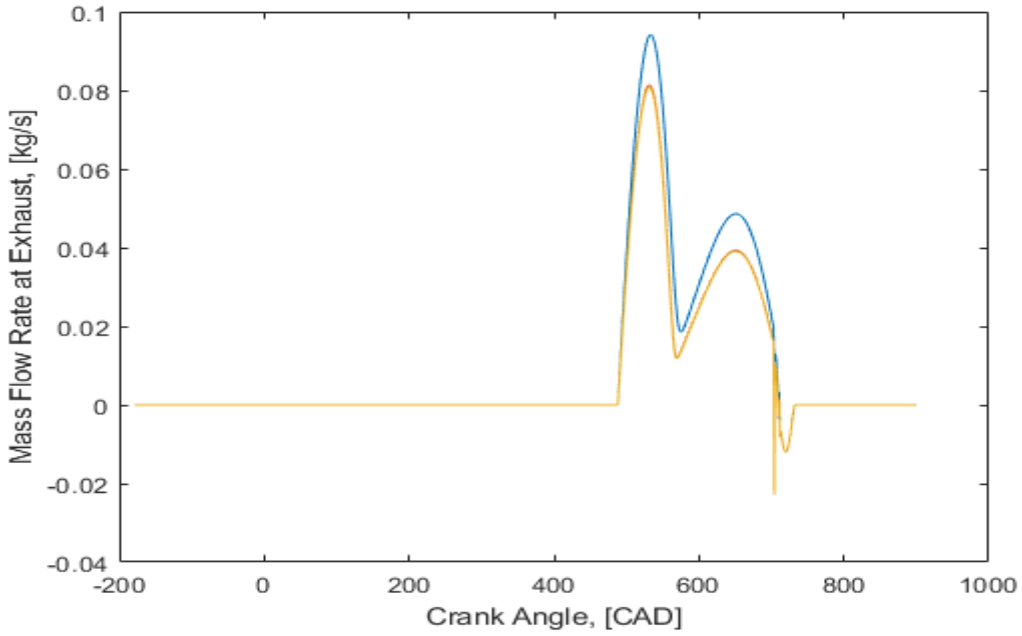
Mass Flow Rate at Exhaust, [kg/s]
0.1
0.08
0.06
0.04
0.02
0
-0.02
-0.04
-200
0
200
400
600
800
1000
Crank Angle, [CAD]

(c)

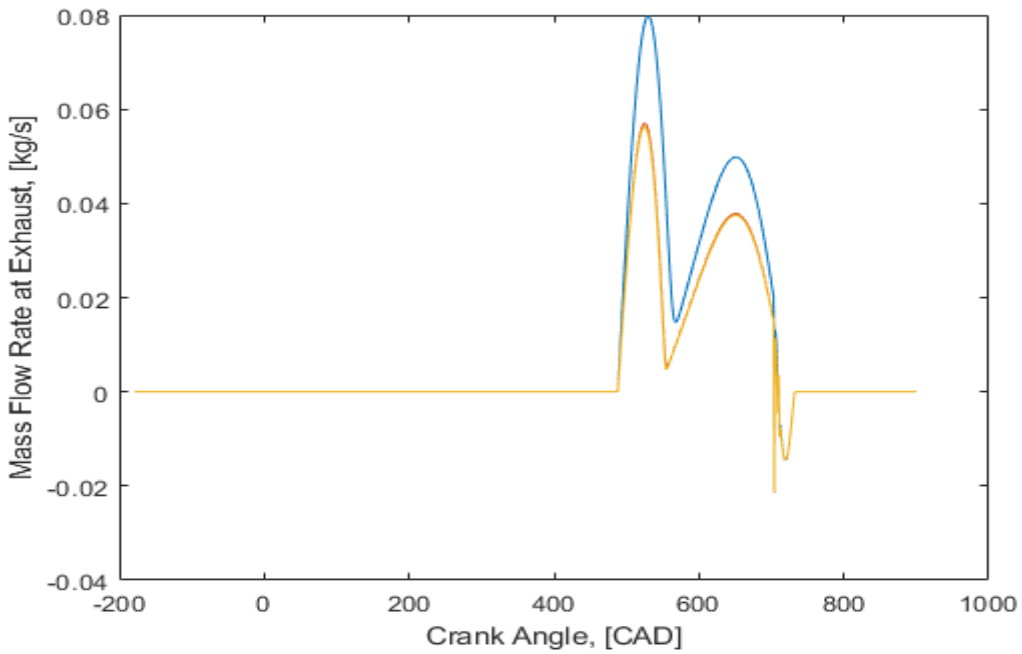
Mass Flow Rate at Exhaust, [kg/s]
0.08
0.06
0.04
0.02
0
-0.02
-0.04
-200
0
200
400
600
800
1000
Crank Angle, [CAD]

(d)

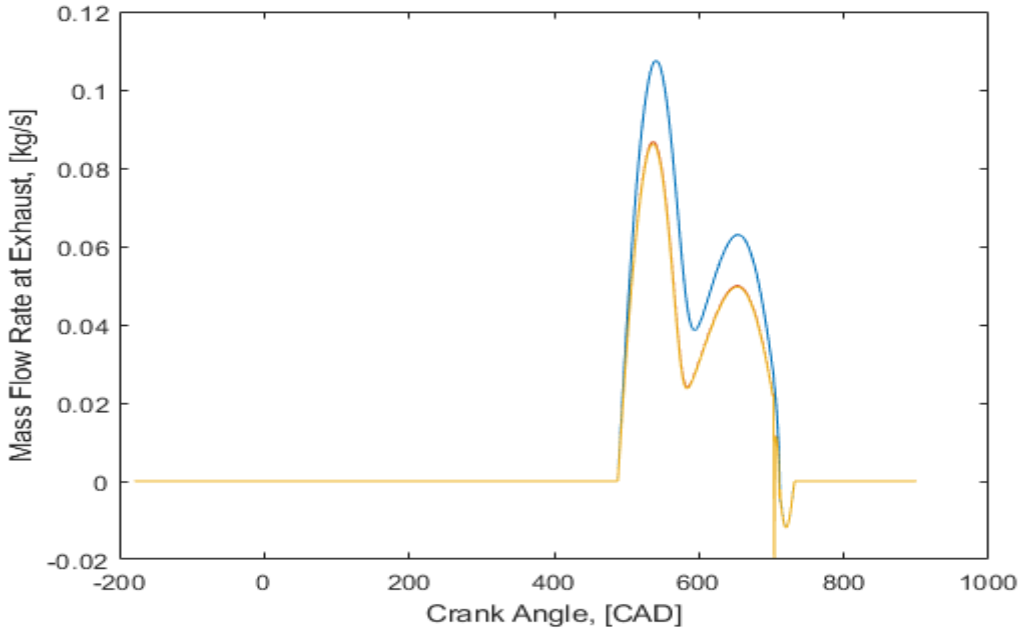

(e)

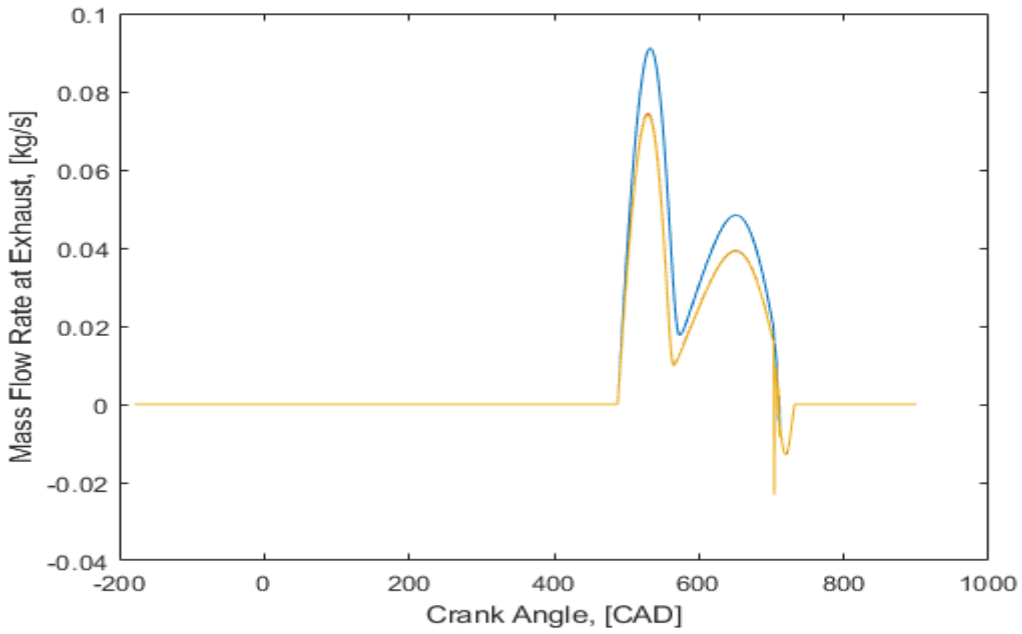

(f)

Figure 40 EXHAUST MASS FLOW RATE AS FUNCTION OF CRANK ANGLE

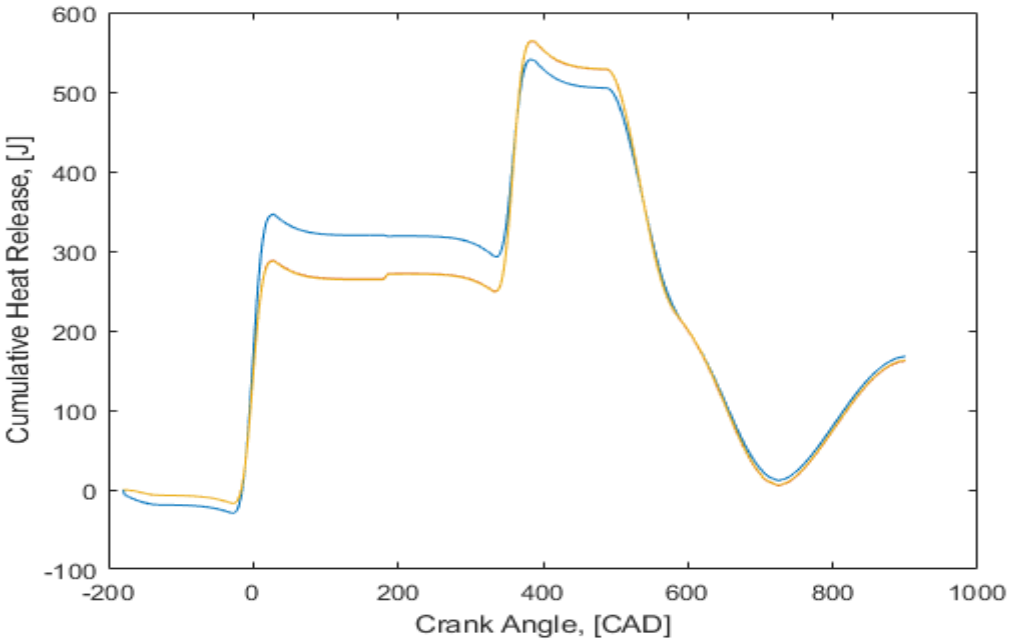
Cumulative Heat Release, [J]
600
500
400
300
200
100
0
-100
-200
0
200
400
600
800
1000
Crank Angle, [CAD]

(a)

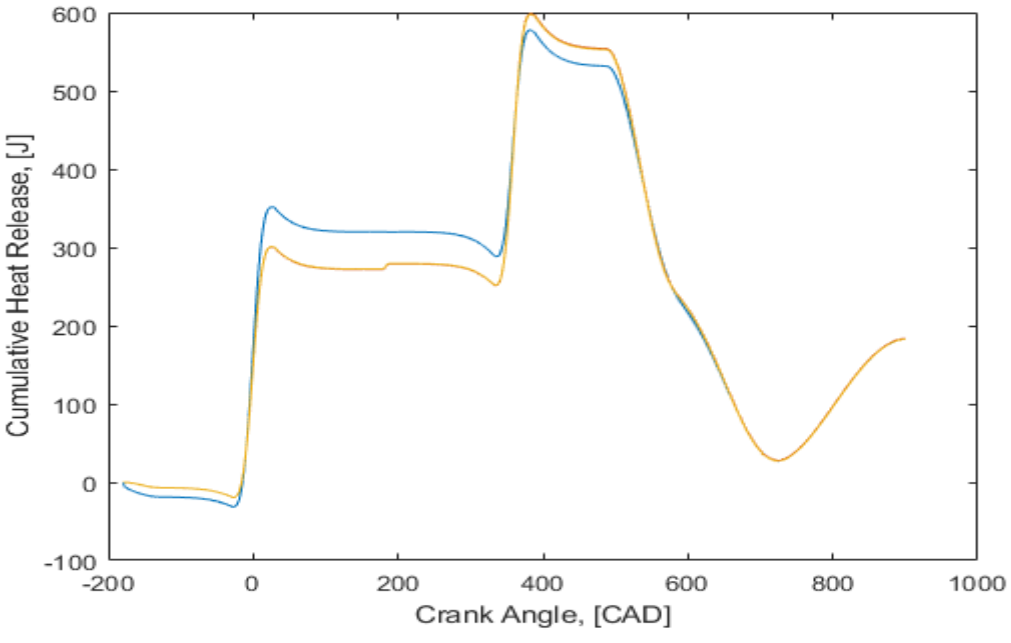
Cumulative Heat Release, [J]
600
500
400
300
200
100
0
-100
-200
0
200
400
600
800
1000
Crank Angle, [CAD]

(b)

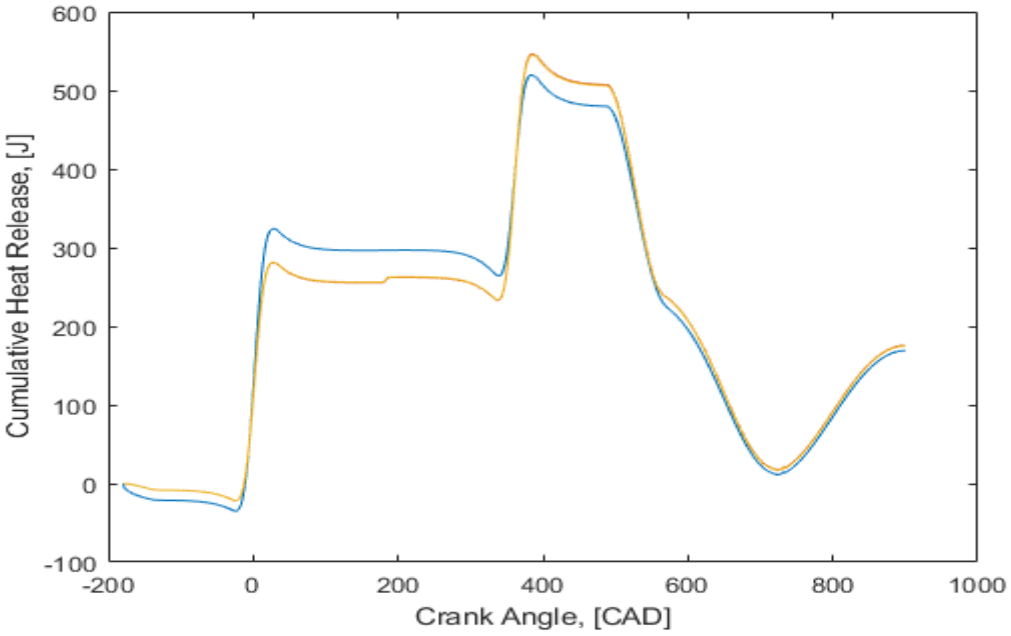
Cumulative Heat Release, [J]
600
500
400
300
200
100
0
-100
-200
0
200
400
600
800
1000
Crank Angle, [CAD]

(c)

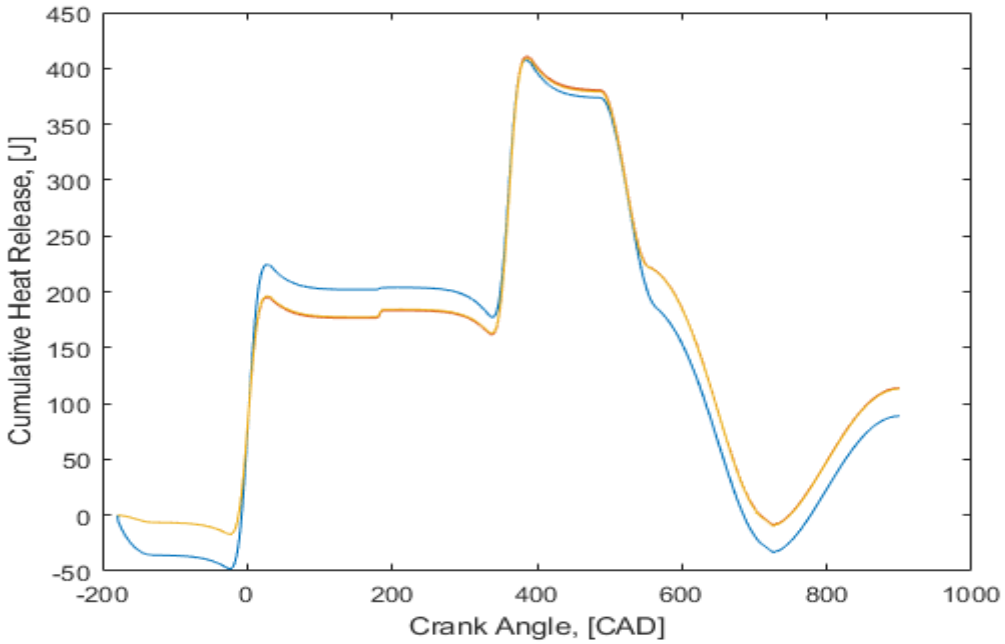
Cumulative Heat Release, [J]
450
400
350
300
250
200
150
100
50
0
-50
-200
0
200
400
600
800
1000
Crank Angle, [CAD]

(d)

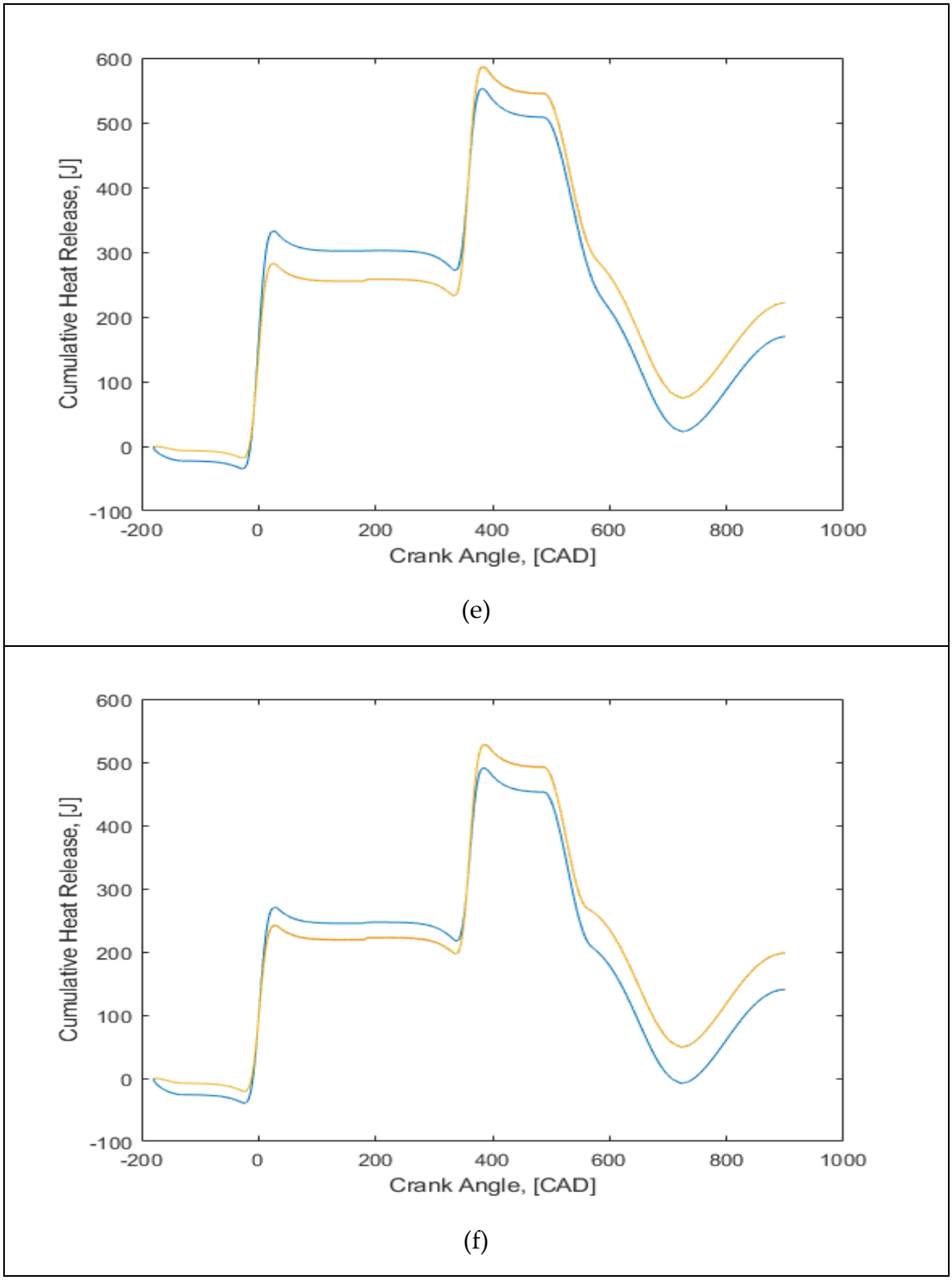

Figure 41 CUMULATIVE HEAT RELEASE

4 References

[1] Caudle, P.; Brain, Eric (September 2000). "The Griffin Engineering Company". staff.bath.ac.uk. Archived from the original on 2007-05-13.

[2] US Patent number 1,339,176 awarded to L.H. Dyer

[3] https://web.archive.org/web/20070515204554/http://www.bajulazsa.com/Site/sixstroke.html

[4] http://izoling.beep.pl/www.izoling.pl/badania/czytaj/engine.html

[5] http://www.sechstaktmotor.de/EN/infos.html

[6] Section 3-1 Air Standard Cycles – Engineering Fundamentals of Internal Combustion Engines by Willard W. Pulkrabek

[7] The Influence of Compression Ratio and Dissociation on Ideal Otto Cycle Engine Thermal Efficiency by Murray H. Edson

[8] A highly efficient six-stroke internal combustion engine cycle with water injection for in-cylinder exhaust heat recovery by James C. Conklin, James P. Szybist

[9] A Six-Stroke DI Diesel Engine Under Dual Fuel Operation by Tsunaki Hayasaki, Yuichirou Okamoto, Kenji Amagai and Masataka Arai

[10] Experimental investigation of the effects of direct water injection parameters on engine performance in a six-stroke engine by Emre Arabaci, Yakup Içingür, Hamit Solmaz, Ahmet Uyumaz, Emre Yilmaz

[11] Fundamentals of classical thermodynamics, 4th edition by Van Wylen, Gordon John

[12] Thermodynamic analysis of a six-stroke engine by Masataka Arai, Yuichi Ida and Kenji Amagai

[13] V. Ganesan, Internal Combustion Engines.

[14] Giancarlo Ferrari, Internal Combustion Engines.

[15] J.B. Heywood, Internal Combustion Engine Fundamentals.

[16] Sokratis Demesoukas. 0D/1D combustion modeling for the combustion systems optimization of spark ignition engines. Other. Université d'Orléans, 2015. English. NNT :2015ORLE2024. tel-02902187

[17] https://en.wikipedia.org/wiki/Six-stroke_engine

[18] Jerald A. Caton, An introduction to thermodynamic cycle simulations for internal combustion engines.

[19] https://www.afs.enea.it/project/neptunius/docs/fluent/html/ug/node337.htm

[20] Xu S and Filipi Z (2020) Quasi-Dimensional Multi-Zone Modeling of Methane-Diesel Dual-Fuel Combustion. Front. Mech. Eng. 6:46. doi: 10.3389/fmech.2020.00046

[21] S. Verhelst and C.G.W. Sheppard Multi-Zone Thermodynamic Modelling of Spark-Ignition Engine Combustion – an Overview

[22] G. Stiesch - Modeling Engine Spray and Combustion Processes

[23] Pulkrabek WW. Engineering Fundamentals of the Internal Combustion Engine. New Jersey: Pearson Prentice-Hall; 1997.

[24] A Study on Phenomenological Quasi-Dimensional Combustion Modeling of Spark-Ignited Engine by Namho Kim

[25] Four-Stroke, Internal Combustion Engine Performance Modeling by Richard C. Wagner

[26] Hoeven MVD. Energy and Climate Change International Energy Agency; 2015.

[27] https://theicct.org/wp-content/uploads/2021/08/plot_nedc_pc_SAFEGHG-aug2021.jpg

[28] Environmental and Economic Benefits of Car Exhaust Heat Recovery by Eleni Avaritsioti

[29] Parvate-Patil G, Hong H, Gordon B. An Assessment of Intake and Exhaust Philosophies for Variable Valve Timing SAE Technical Paper 2003-32-0078; 2003.

[30] Fontana G, Galloni E, Palmaccio R, Torella E. The influence of variable valve timing on the combustion process of a small spark-ignition engine. SAE Technical Paper 2006-01-0445; 2006.

[31] Fontana G, Galloni E. Variable valve timing for fuel economy improvement in a small spark-ignition engine. Applied Energy. 2009;86:96-105

[32] Sellnau M, Kunz T, Sinnamon J, Burkhard J. 2-step variable valve actuation: System optimization and integration on an SI engine. SAE Technical Paper 2006-01-0040; 2006.

[33] De Bellis V, Bozza F, Siano D, Gimelli A. Fuel consumption optimization and noise reduction in a spark-ignition turbocharged VVA engine. SAE International Journal of Engines. 2013;6:1262-74.

[34] Ha K. Development of Nu 2.0 L CVVL Engine. SAE Technical Paper 2014-01-1635; 2014.

[35] Hoffmann D, Widmann D, Kreusen D, Meehsen D. Cylinder deactivation for valve trains with roller finger follower. MTZ worldwide. 2009;70:26-30.

[36] Boretti A, Scalzo J. A Novel Mechanism for Piston Deactivation Improving the Part Load Performances of Multi Cylinder Engines. Proceedings of the FISITA 2012 World Automotive Congress: Springer; 2013. p. 3-17.

[37] Flierl R, Lauer F, Breuer M, Hannibal W. Cylinder deactivation with mechanically fully variable valve train. SAE International Journal of Engines. 2012;5:207-15.

[38] Cassiani MDB, Bittencourt ML, Galli LA, Villalva SG. Variable Compression Ratio Engines. SAE Technical Paper 2009-36-0245; 2009.

[39] Schwaderlapp M, Habermann K, Yapici KI. Variable compression ratio-A design solution for fuel economy concepts. SAE Technical Paper 2002-01-1103; 2002.

[40] Kim N, Cho S, Min K. A study on the combustion and emission characteristics of an SI engine under full load conditions with ethanol port injection and gasoline direct injection. Fuel. 2015;158:725-32.

[41] Koopmans L, Ogink R, Denbratt I. Direct gasoline injection in the negative valve overlap of a homogeneous charge compression ignition engine. SAE Transactions. 2003;112:1365-76.

[42] Sadakane S, Sugiyama M, Kishi H, Abe S, Harada J, Sonoda Y. Development of a new V-6 high performance stoichiometric gasoline direct injection engine. SAE Technical Paper 2005-01-1152; 2005.

[43] Castagné M, Cheve E, Dumas J, Henriot S. Advanced tools for analysis of gasoline direct injection engines. SAE Technical Paper 2000-01-1903; 2000.

[44] Han D, Han S-K, Han B-H, Kim W-T. Development of 2.0 L Turbocharged DISI engine for downsizing application. SAE Technical Paper 2007-01-0259; 2007.